Geology of the Weber Region, North Island East Coast, New Zealand.

A thesis presented in partial fulfilment of the requirements for the degree of

Master of Science

in Earth Science

School of Agriculture and Environment

Hannah Harvey

2019

MASSEY UNIVERSITY
TE KUNENGA KI PŪREHUROA
UNIVERSITY OF NEW ZEALAND

Abstract

Geological mapping of the East Coast Basin has tended to be at a broad scale with detailed mapping confined to a few specific areas of interest. The East Coast Basin is a petroliferous region and therefore of interest for petroleum exploration, however, further detailed mapping and sedimentological research is needed to have a better appreciation of the reservoir potential of the basin. Mapped geological boundaries are inferred based on broad tectonic features and structures, and little sedimentology has been undertaken. The current geological understanding is that this area contains a succession of Late Cretaceous (70 Ma) to Late Miocene (~5 Ma) sandstone, limestone, marl, flysch and mudstone facies. Few potential reservoir units are mapped or received detailed analysis and source rock has been an ongoing enigma due to known oil and gas seeps but low Total Organic Content results in most previously studied samples.

The purpose of this research is to produce a high- resolution 1:25 000 geological map and undertake biostratigraphical, petrological, structural and paleo-environmental studies to help differentiate the Miocene aged geology of the area.

Findings indicate the area is structurally complex with many faults, folds, including the Akitio Syncline, and local unconformities. Within the stratigraphic sequences identified both macro and micro fauna provide depositional environment and age control. Sedimentological and petrographic analysis of the major units also indicate variability in depositional environments from abyssal to shallow marine. Key areas have been located to provide accurate ages throughout the depositional sequence. This project will contribute to current research on the petroleum reservoir potential of the East Coast Basin.

Acknowledgements

Firstly, I would like to thank my supervisors, Jon Procter and Julie Palmer, for your guidance, encouragement, and patience throughout this project. Jon thank you for your 'just do it' attitude and Julie for always being there to talk about rocks with and being so supportive.

Thank you to Kyle Bland and Dominic Strogen for providing the opportunity and replying to my numerous emails. Hugh Morgans and Henry Gard, I cannot thank you enough for processing all 40 samples for microfossils. Matt Sagar, thank you for setting me up so I could understand the geochemical data and what it meant regarding provenance. Also thank you to Ben Durrant for the thin section preparation training, especially those pesky mudstones.

Thank you to Anja Moebis and Bob Toes for your assistance, advice and support in the lab. Matt Irwin thank you for saving this thesis document, for helping me with ArcGIS questions and for the drone footage of my area. Thank you to Callum Rees for taking me under your wing and always being there to talk about rocks and ideas. Thank you to all field assistants, you have been there when I could have easily injured myself, and I apologise for the Weber landscape being testing at times.

Thank you, property owners of the Weber district, especially the Hale family, Riddell family and all others for your support, for pointing out tracks to use, cliffs to avoid and if you have any fossils on your property. Hopefully, by pulling sheep out of mud-logged streams, it has made up for times of popping up on your property without notifying you. Thank you to Ernslaw Ltd. For letting me have full access to your forestry roads. Also, thank you to the owners of Herbertville Camp Ground and Pub for being so welcoming during my stay.

Thank you to my loving and supportive parents. You raised an independent, rugged, farm girl who still loves to be outside in the mud and that has caused me to be in my natural environment during the fieldwork of this project. Your encouragement had kept me going through times when I underestimated myself.

To my Aunties, cousins and GAM thank you for reminding me that I can do anything I set my mind to and being my cheerleaders throughout my university journey.

Thank you to Boglarka Nemeth and the other people I shared the office with. I have thoroughly enjoyed us encouraging each other to get work done and having a drink or few. Your help has been endless.

Thank you to Richie for the 3pm messages (3am London time for you) of support, for visiting when I was doing fieldwork and staying at Herbertville with me. I'm glad you are back in NZ and still enjoy listening to my rambles about rocks.

Lastly, thank you, other family-like friends, who supported and encouraged me and who pulled me out of the rabbit hole of my project to remind me to socialise.

Contents

Abstract i

Acknowledgements ii

List of Figures ix

Chapter 1 Introduction 1

1.1 Outline of the study 1

1.2 Location of the study area 3

Chapter 2 The East Coast Geological Setting 4

2.1 East Coast Tectonic History 4

2.2 Central East Coast Basin (ECB) 6

2.3 Akitio Sub-Basin Setting and Deposition 8

Chapter 3 Previous studies 9

3.1 Previous Mapping and Stratigraphy of the Akitio sub-basin 10

3.2 Zealandia and East Coast Structural Evolution 11

3.3 Stratigraphic Units and Deposition 14

3.4 Biostratigraphy and event/period deposition 16

3.5 Petroleum Potential 17

3.6 Provenance studies 18

Chapter 4 Methods 20

4.1 Akitio Sub-Basin Fieldwork and Mapping 20

4.2 Stratigraphy 20

4.3 Loss on Ignition (LOI) 20

4.4 X-ray fluorescence (XRF) 22

4.5 Petrography 23

4.6 Point Counting 23
4.7 Micropaleontology 23
4.8 Macropaleontology 24
Chapter 5 Stratigraphy 25
5.1 Introduction 25
5.2 Whangai Group 26
5.2.1 Whangai – Rakauroa Member 26
5.2.2 Whangai – Upper Calcareous Member (UCM) 27
5.2.3 Whangai - Te Uri Member 27
5.3 Wanstead Group 28
5.4 Weber Group 29
5.4.1 Weber – Glauconitic sandstone 29
5.4.3 Weber – Flysch Member 32
5.4.4 Weber – Mudstone Member 33
5.5 Ihungia Formation 34
5.6 Whakataki Formation 36
5.7 Tutamoe 37
5.8 Riddells Group 38
5.8.1 Mangato Mudstone 38
5.8.2 Lower Tahuokaretu 39
5.8.3 Middle Tahuokaretu 40
5.8.4 Upper Tahuokaretu 41
5.8.5 Riddells Mudstone 42
5.8.6 Riddells Culvert Member 43

5.9 Franklin Road 44
5.10 McCartie Group 45
5.10.1 McCartie Mudstone 45
5.10.2 McCartie Sandstone 46
5.11 Limestone units 47
5.11.1 Te Awaputahi Limestone 47
5.11.2 Scallop Limestone 47
5.11.3 Hillcap Limestone Conglomerate 48
5.12 Stratigraphy Summary 49
Chapter 6 Petrography and Geochemistry 51
6.1 Thin Sections 52
6.1.1 Introduction 52
6.1.2 Rakauroa Member 52
6.1.3 Upper Calcareous Member 52
6.1.4 Te Uri Member 52
6.1.5 Wanstead and Wanstead Glauconitic Sand 53
6.1.7 Weber Limestone 53
6.1.8 Weber Flysch 53
6.1.9 Ihungia 54
6.1.10 Whakataki 54
6.1.11 Tutamoe 55
6.1 12 Riddells Mudstone 55
6.1.13 Riddells Culvert 55
6.1.14 Franklin Road 56

6.1.15 McCartie Sandstone 56
6.2 Point Counting 57
6.2.1 Quartz, feldspar and lithics (QFL) 57
6.2.2 Basu Quartz Diagram 59
6.3 X-ray Fluorescence (XRF) and Provenance 60
6.3.1 Major Elements 60
6.3.2 Trace Elements 65
6.4 Petrology and Provenance Summary 73
Chapter 7 Evolution of the Akitio Sub-basin 74
Chapter 8 Discussion 79
Chapter 9 Conclusions 83
9.1 Key findings 83
9.3 Suggestions for further study 84
References 86
Appendices 92
Appendix One - Previous Maps 92
Appendix 1.1 – Geological Map of the Eketahuna Subdivision (Ongley, 1935) 92
Appendix 1.2 – Close up of the Weber Geology and Cross Section (Ongley, 1935) 93
Appendix 1.3 – Geological Legend of the Geology of the Eketahuna Subdivision (Ongley, 1935) . 94
Appendix 1.4 – Geological Map of the Mangatoro and Porangahau survey district (Lillie, 1953) . 95
Appendix 1.5 – Geology of the Waipatiki Syncline (Reid, 1998) 96
Appendix 1.6 – Partial Geology of the Wairarapa with the added Weber Region Boundary (Lee et al., 2002) 97
Appendix 1.7 – Legend and Stratigraphy of the Central and Eastern Wairarapa (Lee et al., 2002) .. 98

Appendix Two – Stratigraphic Columns 99

Appendix Three – Cross Section and Balanced Cross Section 103

Appendix Four - Microfossils 104

Appendix Five - Macrofossils 110

Appendix Six - Point Counting 113

Appendix Six - X-ray Fluorescence (XRF) 114

List of Figures

Figure 1.1 Tectonic setting for the Central and East Coast, North Island, New Zealand (Graham, 2008) .. 2

Figure 1.2 Rivers, roads and localities of the mapping area 3

Figure 2.1 Tectonic evolution of Zealandia and the East Coast Basin (ECB). Adapted from (Uruski, 2010)..... 5

Figure 2.2 Tectonic accretion of Late Cretaceous deposits of the East Coast from 24 Ma to present day. Note the development of thrust-faults and sub-basins which are filled with Miocene (orange) and younger (yellow) material. Basic regional stratigraphy is also shown in the top red square. Adapted from (Burgreen-Chan et al., 2016)..... 7

Figure 3.1 Geological studies from 1935 to 1998 near the mapping area. The Weber region is shaded, and the mapping boundary is outlined. Adapted from (Lee et al., 2002)..... 9

Figure 3.2 The East Coast at 16 Ma (Bailleul et al., 2013) 12

Figure 3.3 Provenance of the East Coast (Hines, 2018)..... 19

Figure 5.1 Chrono-stratigraphy of the Weber mapping area. Red lines indicate known unconformities and grey infill represents no deposition or erosion 25

Figure 5.2 Rakauroa Member of the Whangai. Note the red and black weathering 26

Figure 5.3 The Te Uri (left - light grey) and Upper Calcareous Member (right) of the Whangai Formation and the K/T boundary is the contact in between (red line)..... 27

Figure 5.4 Wanstead outcrop near Tawanui, Akitio River..... 28

Figure 5.5 Weber Glauconitic sand found in Akitio River..... 30

Figure 5.6 Bedded base of Weber Glauconitic sandstone 30

Figure 5.7 Weber Limestone (left) and Weber Flysch (right) found in the Akitio River..... 31

Figure 5.8 Weber Flysch at Tawanui from Bland et al. (2013)..... 32

Figure 5.9 Weber Flysch outcrop beside the Akitio River 33

Figure 5.10 Ihungia outcrop on Mangatoitoi Station, Tahuokaretu Road. Note thin sandstone bedding. . 35

Figure 5.11 Whakataki outcrop, Mangatoitoi Station, Tahuokaretu Road..... 36

Figure 5.12 Tutamoe overlying Ihungia, Akitio River. The red dashed line highlights the contact boundary..... 37

Figure 5.13 Colourful oil streaming down eroded Mangato Mudstone after recent rain 38
Figure 5.14 Mangato Mudstone with sandstone beds 38
Figure 5.15 Lower Tahuokaretu Mudstone found in Tahuokaretu Stream near the Riddells sheep yards 39
Figure 5.16 Middle Tahuokaretu Mudstone found in Tahuokaretu Stream. The exposed edges show the thin sandstone beds..... 40
Figure 5.17 Upper Tahuokaretu Mudstone found in Tahuokaretu Stream..... 41
Figure 5.18 Riddells Mudstone and chert beds found in Tahuokaretu Stream 42
Figure 5.19 Riddells Culvert 43
Figure 5.20 Franklin Road which is located on Franklin Road and Geologist Road. 44
Figure 5.21 McCartie Mudstone found at Mt McCartie cliff seen from Franklin Road. Note person in centre for scale. 45
Figure 5.22 McCartie Sandstone found on Franklin Road..... 46
Figure 5.24 Scallop Limestone block found in Tahuokaretu Stream and Akitio River 47
Figure 5.23 Te Awaputahi Limestone block found up Titoki Road..... 47
Figure 5.25 Hillcap Limestone which is found on Riddells property and Tahuokaretu Road as a loosely packed conglomerate..... 47
Figure 5.26 The Geology of the Weber area (1:25,000) 50
Figure 6.1 Rakauroa Member..... 52
Figure 6.2 Upper Calcareous Member 52
Figure 6.3 Te Uri Member 52
Figure 6.4Wanstead Glauconite 52
Figure 6.5 Wanstead..... 53
Figure 6.6 Weber Glauconitic Sand 53
Figure 6.7 Weber Limestone..... 53
Figure 6.8 Weber Flysch Sand (right) and Weber Flysch Mud (Left) 53
Figure 6.9 Ihungia 54
Figure 6.12 Whakataki Organic rich mudstone..... 54
Figure 6.11 Whakataki Sandstone..... 54
Figure 6.10 Whakataki mudstone..... 54

Figure 6.13 Tutamoe Mudstone (left) and Tutamoe fine sandstone (right) 55
Figure 6.14 Riddells mudstone..... 55
Figure 6.16 Riddells Culvert mudstone..... 55
Figure 6.15 Riddells Culvert sandstone..... 55
Figure 6.17 Franklin Road sandstone (left) and Franklin Road mudstone (right) 56
Figure 6.18 McCartie Sandstone with a central potassium feldspar 56
Figure 6.19 Weber QFL diagram regards to Folk classification (Folk, 1980). 58
Figure 6.20 Diagram showing this studies Quartz data applied to Basu et al. (1975)..... 59
Figure 6.21The major elements with time found in the Weber mapping area 61
Figure 6.22 ACNK/CIA weathering plot 63
Figure 6.23 Weber F1 and F2 plot results 64
Figure 6.24 Immobile trace elements with time. The impact of the K/T event is seen by a reduction of most element concentrations (towards the end of the Late Cretaceous) with a later decrease during the Oligocene (reduction of deposition) to a wavering increase until the Late Miocene where Immobile concentrations increase with increased deposition with the activation of the tectonic margin. 66
Figure 6.25 New Zealand terrane spidergram plot..... 67
Figure 6.26 Weber area Whangai and Waipawa spidergram 68
Figure 6.27 Weber and Wanstead spidergram 68
Figure 6.28 Weber flysch spidergram 69
Figure 6.29 Early Miocene spidergram..... 69
Figure 6.30 Middle to Late Miocene spidergram..... 70
Figure 6.31 Plio-Pleistocene spidergram..... 70
Figure 6.32Weber La/Th provenance plot..... 71
Figure 6.33 Weber Zr/Th provenance plot 71
Figure 6.34 Weber Ti/Zr-La/Sc plot..... 72
Figure 6.35 Weber Sc/Cr-La/Y plot 72

Table 1 Stratigraphic summary of the mapping area from previous studies. 16

Chapter 1 Introduction

1.1 Outline of the study

The geology of the East Coast of the North Island of New Zealand is structurally complicated by its location within the accretionary system formed by subduction of the Pacific oceanic plate beneath the Indo-Australian continental plate (Fig.1.1). Previous East Coast studies have highlighted the complexities of the geology with its unconformities and localised geological features such as faults and folds throughout the landscape. There remain areas of the East Coast that are not mapped in detail; the Weber region is one such part that lies within a forearc basin tectonic regime extending from Raukumara to Marlborough along the East Coast and the surrounding offshore. This forearc basin chain consists of a network of related sub-basins that have formed due to accretionary and tectonic mechanisms along and parallel to the plate subduction zone, in this case the East Coast. Mapping the local geology will provide more detail on the depositional environments and age of the geological units.

The purpose for this study is to gain more knowledge about the phases of evolution of the Central East Coast Basin by examining the geology of the Akitio sub-basin in detail that could contribute to better understanding the formation of potential petroleum systems. The onshore basins historically reflect the ongoing accretionary progression of offshore petroleum hosted basins.

The primary objective of this study is to map geological units and structures to a scale of 1:25,000. Historically, many of the plotted geological contacts are approximated, or are allocated by age correlation, generally at the group-level and not as members (Lee et al., 2002), from adjacent areas (Lillie, 1953); (Neef, 1992a, 1992b, 1995, 1997) or only cover a small part of the mapping area (Reid, 1998). In mapping the geology of the Akitio sub-basin we will also increase our knowledge of the biostratigraphy of the region by using both macro and microfossils. This will also aid in age control, paleo-water depth and additional paleoenvironmental information. The petrography, and whole rock geochemistry (XRF) of the lithologic units will also be examined to determine provenance.

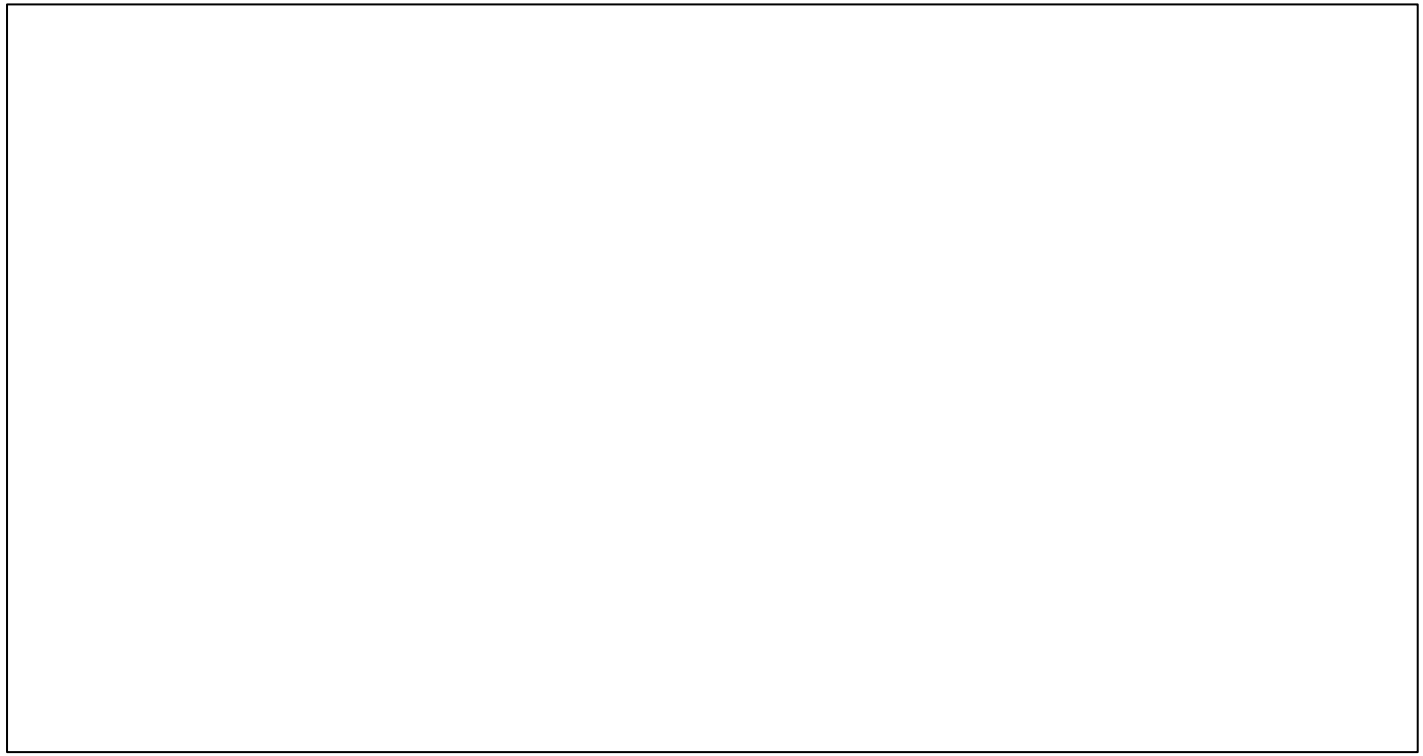

Figure 1.1 Tectonic setting for the Central and East Coast, North Island, New Zealand (Graham, 2008)

1.2 Location of the study area

The study area is located 95km east Palmerston North and 36km south-east of Dannevirke towards Herbertville. The mapping area is approximately 80 km² as outlined in (Fig.1.2); Waipatiki is the top-left corner and includes the Akitio River east to Mt McCartie. Weber road and Route 52 are used as the Southern limit. The mapping area is near the boundary of Northern Wairarapa or Southern Hawkes Bay. The highest elevations in the mapping area are Te Awaputahi (581m) and Mt McCartie (424m). Approximately 25 percent of the mapping area is owned by Ernslaw Forestry Ltd, and the rest is privately owned. The private land is used for extensive agriculture, such as sheep, beef and venison. Road access is by the sealed Weber/Route 52 road or unsealed secondary roads. Access to the Akitio River is limited but can be reached by Hales track off Speedy Road or by following Waipatiki Stream or from Tawanui landowners, with permission.

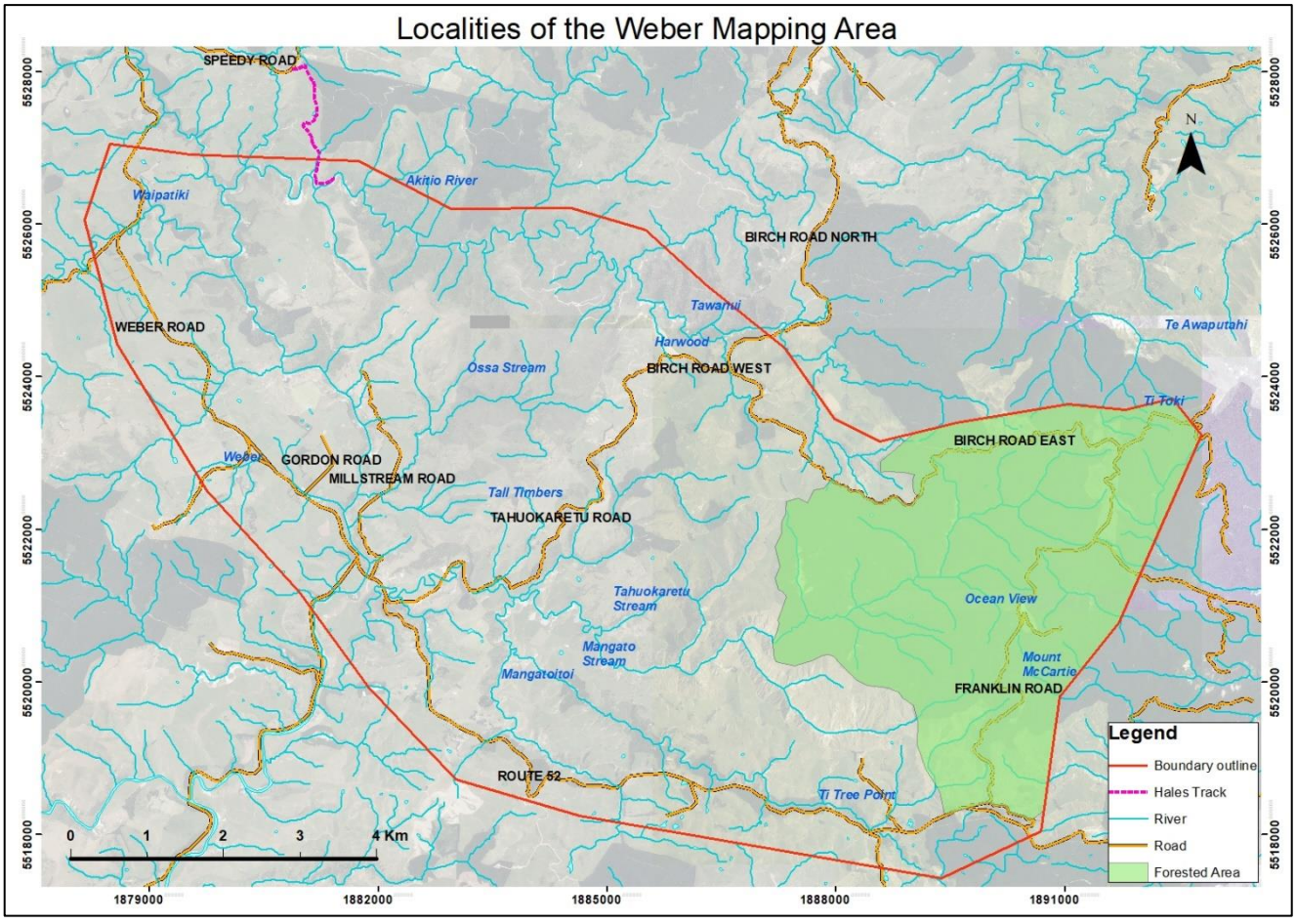

Figure 1.2 Rivers, roads and localities of the mapping area

Chapter 2 The East Coast Geological Setting

2.1 East Coast Tectonic History

During the Early-Mid Cretaceous, proto-Zealandia was a landmass that was forming by mass sediment accumulation on the edge of Gondwana (Fig. 2.1) (Uruski, 2010). There were a west-dipping subduction zone and rift system active along the inner Antarctic-Australian boundary during 100-83 Ma (Graham, 2008). This rifting motion was the start of the separation of Zealandia from Gondwana (Fig. 2.1). As sediment accumulated on the margin edge, the Torlesse Terrane formed and became accreted against the eastern edge of Gondwana (Lee et al., 2002) and formed a chain of ridges and slope basins (Rangitata Orogeny). The rifting inland of the accumulating margin caused complete isolation and drifting of a thinned continental crust and Zealandia eventually separated from the Antarctica-Australia portion of Gondwana. Rifting continued, isolating Zealandia as a blocky, low-lying landmass surround by the deep ocean. By 65 Ma separation of Zealandia was complete (Graham, 2008). Around 25Mya the Pacific and Australian plates began to converge which activated a new subduction zone in the North Island and transform boundary in the South Island (Bailleul et al., 2013). At this time Zealandia was somewhat submerged but later in the Miocene, tectonic uplift resumed and compressed the East Coast Basin (ECB) leading to the eventual emergence of land, including the more recent development of the Axial Ranges (Fig. 1.1). Subduction resulted in the development of the East Coast Forearc Basin. Forearc basins form in response to subduction. The forearc region includes the trench, accretionary complex, outer-arc ridge and the basin. The subduction boundary forms a trench, and in New Zealand's case, this is the Hikurangi Trough (Fig. 1.1). The Hikurangi Trough is up to 4km deep and is approximately 3500km long (Lewis et al., 2002)). As the Pacific Plate subducts under the Indo-Australian Plate, there is compression and the accretion of marine sediments onto the edge of the overlying tectonic plate. Shear friction of the plates causes an outer-arc ridge and an accretionary wedge to build up, as well as a basin to form (Fig. 1.1). In the accretionary complex, sub-basins can develop in response to faulting and folding (shortening) as has occurred for the ECB. The marine sediments have since been uplifted and exposed revealing deposition in "mini" basins similar to that occurring offshore in the East Coast Basin.

The Hikurangi Trough constrains the eastern margin of the East Coast Basin. The tectonic relationship changes from subduction in the north to the collision in the south and the geological regime varies along the margin. In the north (Raukumara Basin/ allochthon zone) deposition rates are very high. In the south

(Pegasus Basin zone), deposition is occurring at a significantly lower rate, and the accumulating deposits are laterally stretching by the transform tectonic system. The position of the Raukumara and Pegasus basins concerning the modern subduction system means they have experienced minimal deformation (New Zealand Petroleum & Minerals, 2014). In contrast, the central East Coast Basin (Wairarapa) is very deformed due to the influence of the Hikurangi deformation front/tectonic regimes. Therefore, the ECB is geologically complex with localised sub-basins formed and numerous unconformities.

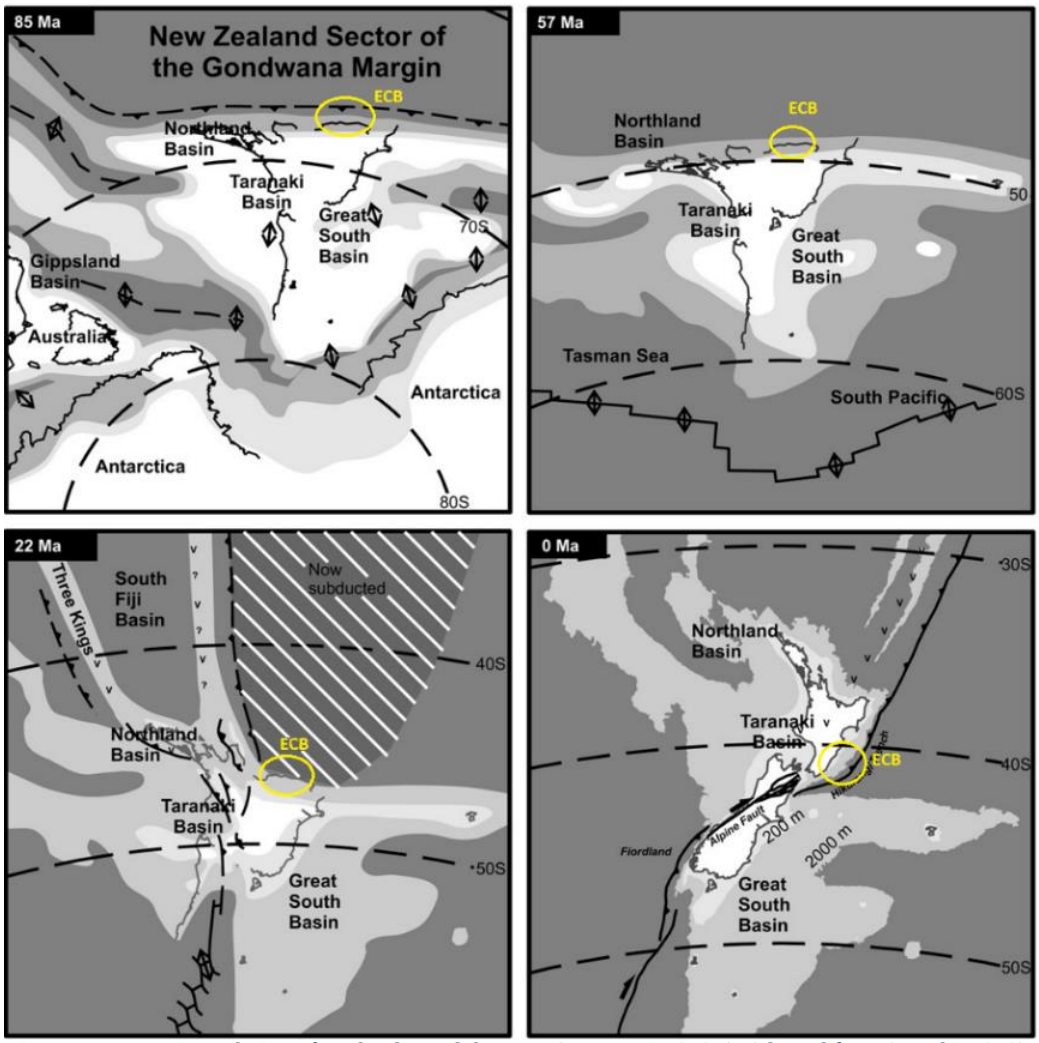

Figure 2.1 Tectonic evolution of Zealandia and the East Coast Basin (ECB). Adapted from (Uruski, 2010).

2.2 Central East Coast Basin (ECB)

During the Late Cretaceous, Whangai mudstone members and the Waipawa Formation were deposited then overlain by Paleocene and Eocene smectitic and calcareous mudstones (New Zealand Petroleum & Minerals, 2014). This evolution was continued by maximum subsidence in the Oligocene, which was then disrupted by Miocene uplift and sandstones were deposited. This coincides with the inception of the present-day plate boundary. The East Coast forearc basin was initiated approximately 25Mya, due to activity at the Hikurangi subduction (Barnes et al., 2010; Nicol et al., 2007; Reyners, 2013). Miocene sediments unconformably overlie Torlesse greywacke, and the subducting pressure of the Pacific Plate has caused the sequence to be imbricate by thrust faulting (Fig. 2.2). The subducting pressure, however, was not uniform along the plate margin and is nearly three times greater in the north than in the south of the ECB (Barnes et al., 2010; Wallace et al., 2004). The resultant higher relief in the north delivered sediments southwards into the axial channel of the basin (Wairarapa) producing thick (5km+) basin infill (Barnes et al., 2010; Davy et al., 1994; Lewis et al., 1998; Mountjoy et al., 2009; Wallace et al., 2004; Wood et al., 1994). There were many submarine canyons along the East Coast and, these also fed the axial channel basin, for example, the Madden Canyon (McArthur et al., 2019). Their interpretation of the Madden Canyon, which is perpendicular to the axial channel, is that it is feeding turbidite deposits into the trough system in a range of sedimentary styles, depending on slope, and sediment supply. Near the basin margin or on a shoal, marine sand facies are present whereas deeper in the basin mudstones usually predominate. The Miocene accretion resulted in the formation of a tectonic deformation front with the central East Coast Basin extensively folded, creating slope basins or sub-basins, e.g. the Akitio/Weber region.

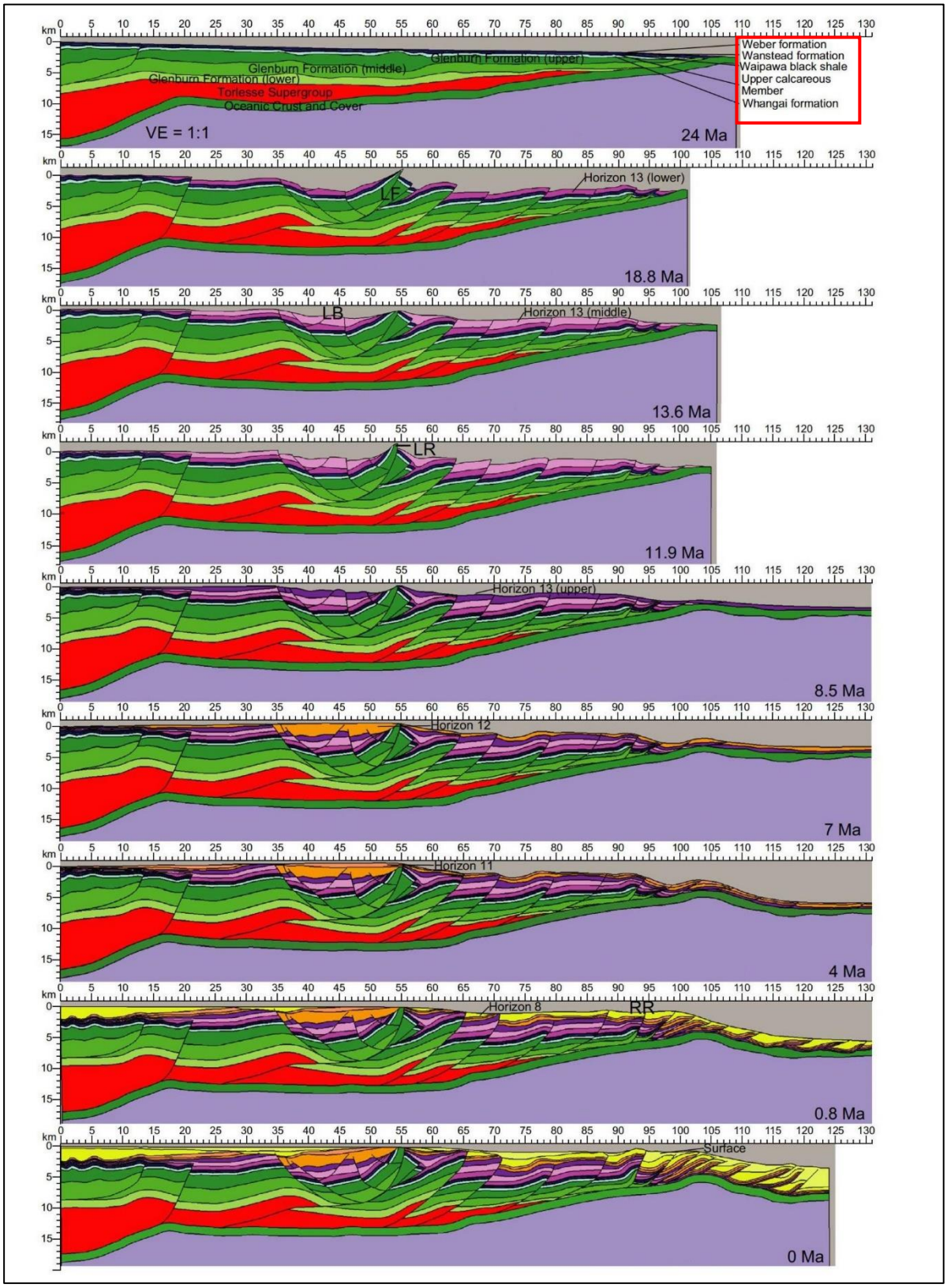

Figure 2.2 Tectonic accretion of Late Cretaceous deposits of the East Coast from 24 Ma to present day. Note the development of thrust-faults and sub-basins which are filled with Miocene (orange) and younger (yellow) material. Basic regional stratigraphy is also shown in the top red square. Adapted from (Burgreen-Chan et al., 2016)

2.3 Akitio Sub-Basin Setting and Deposition

With the activation and progression of the subduction margin of the East Coast, basement rock of the basin margin became folded and faulted which resulted in confined sub-basins. During the time Zealandia was attached or separating from Gondwana, the basement stratigraphy deposition consisted of Torlesse, Glenburn, and Whangai members were being deposited. As the shortening and uplift of the East Coast occurred, the Akitio sub-basin formed, along with other slope basins. On the outer periphery, the Adams-Tinui Fault and Pongaroa Fault confine the folded Akitio sub-basin (Appendix 1.6 - Lee et al. (2002)). Younger units, mostly of Miocene age, infill the basin. The basin also contains turbiditic deposits such as in the Whakataki Formation which is a product of the Miocene activated subduction zone. On the basin shelf edge, submarine canyons are formed by basin margin incisions and these direct the flow of turbidites across the basin. The Akitio sub-basin also received first tributary sediment from the north (the current Hikurangi Trough) until being separated from the main sediment contributory system. This change led to basin infill by more localised sources, while Miocene tectonism uplifted and shaped the landscape which encouraged extensive sedimentation farther into the lower trough system .

Basin infill reflects the source influence of tectonics on the sub-basin**.** With the Akitio sub-basin being approximately 15km wide and shaped by anticlines and synclines, the pathway for Miocene deposition, especially turbidites, is confined and is dependent on the regional erosion tributaries (Broome, 2015). This confinement causes rapid changes on facies and thicknesses as observed in the Tutamoe and Mapiri formations, and this variability makes the correlation in the field problematic (Kingma, 1958). Slope basins reflect processes which occur in offshore basins and sub-basins which is as shown by McArthur et al. (2019) comparing facies of the Akitio sub-basin with the morphology of the Madden Canyon. They suggest that the Akitio sub-basin is a detached deep-water submarine canyon (detached from direct terrestrial sediment supply) which has sporadic and limited sediment input. The portion of the Akitio sub-basin of the mapping area has two shelf/margin areas, Waipatiki and Mt McCartie with anticlinal exposure of Late Cretaceous Whangai in the centre.

Chapter 3 Previous studies

Many studies have focused on the East Coast Basin and have led to regional structural evolution interpretations (Fig. 3.1), regional stratigraphy and for specific rock groups or members, rock chemistry, petroleum source rock studies, and biostratigraphy. Three zones divide the East Coast Basin, the northern East Coast (Hawkes Bay/Raukumara), central East Coast, and southern East Coast (Cook Strait and South Island). The differences between each of these zones reflect the differing tectonic and depositional regimes. In response to the tectonic evolution of Zealandia, the northern and southern zones have accreted as whole terrane blocks (Graham, 2008), whereas the intensely faulting and folding occur the central zone. The present study is on the Akitio Sub-basin which is wholly onshore. This literature review summarises previous studies in and around the Akitio Sub-basin.

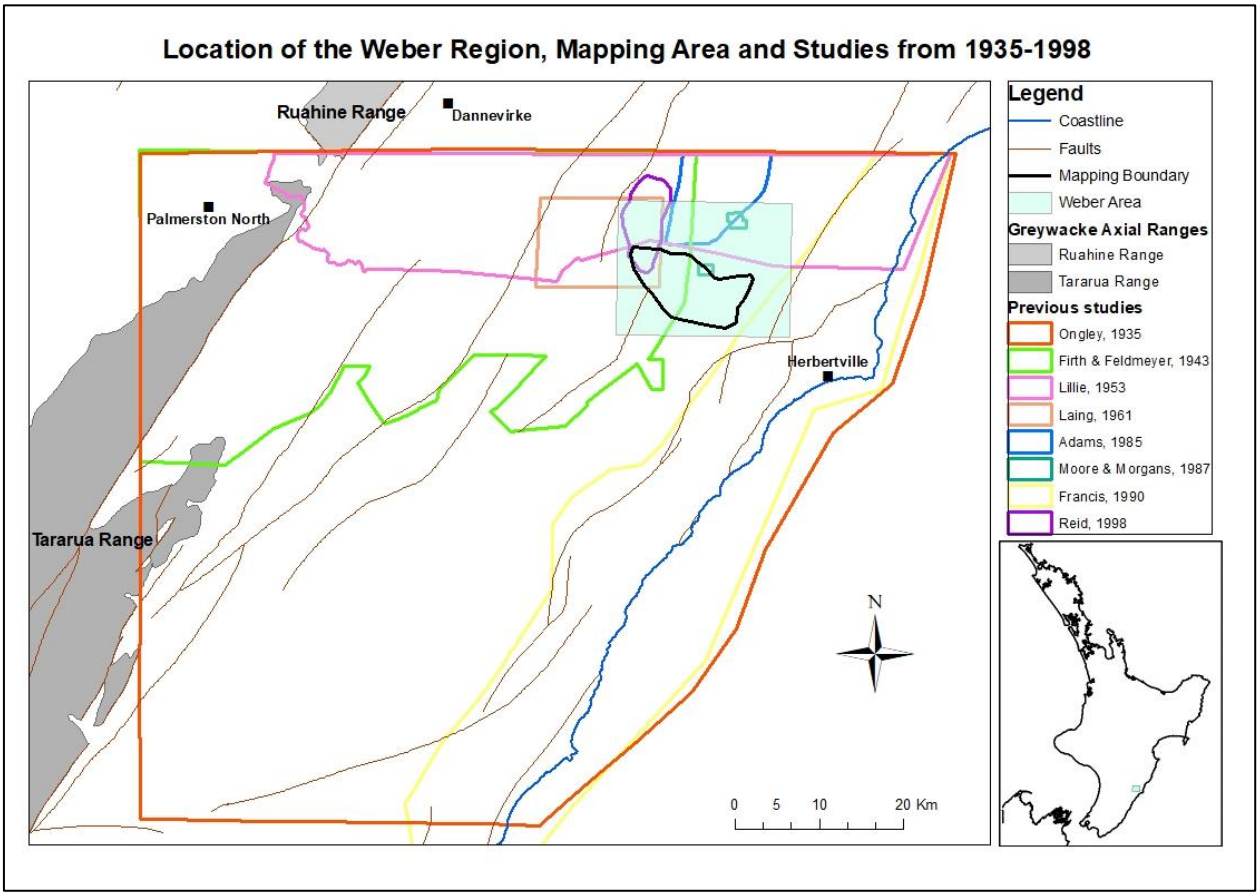

Figure 3.1 Geological studies from 1935 to 1998 near the mapping area. The Weber region is shaded, and the mapping boundary is outlined. Adapted from (Lee et al., 2002)

3.1 Previous Mapping and Stratigraphy of the Akitio sub-basin

One of the first geological maps of the south-eastern North Island was Ongley (1935) (Appendix 1.1, 1.2 & 1.3). Ongley mapped a large part of the Wairarapa region at a 1: 253,440 scale. North to Weber and the Akitio River at its northern limit. The map shows a broad scale resolution of structural features and stratigraphy, but, some stratigraphic units are grouped, i.e. Weber and Ihungia formations, and some are not mentioned, e.g. Mapiri mud near the Titree Anticline and McCartie Syncline. This grouping may be a reflection of the map's resolution. The presence of the Mapiri mudstone is unknown due to the maps limited resolution. Ongley's map includes a cross-section which shows a fold dominated landscape. The report accompanying this map is an oil and gas-based review of the geology and includes sections about the topography, structure and stratigraphy of the Eketahuna Subdivision.

A significant study of rocks within the ECB by Lillie (1953) (Appendix 1.4), provided a detailed map at approximately 1:62500 scale of the region from Norsewood/ Woodville to the coast, but did not cover the study area. Lillie reviewed Cretaceous petroliferous beds and potential natural resources (i.e. lignite, bentonite and limestone). This study describes the strata and proportions of sand and mud. The maps units can be extrapolated into the research area, and strong paleontological material is presented.

Reid (1998) mapped a small portion (approx. 4km²) of the upper-left north-west limit near Waipatiki to the north-west of the study area (Appendix 1.5). The map was redrawn from NZMS 260 metric 1:25,000 scale and differentiates the Early Miocene into three units: called Tunakore Mudstone, Westcott Sandstone and Mangapuku Mudstone. The distribution of these three units within the mapping area is unknown but are useful for biostratigraphic and early Miocene stratigraphic correlation.

Lee et al. (2002) (Appendix 1.6 & 1.7) described the geological members and produced a map at a 1:250,000 scale (also known as Qmap). This scale means the map and geological boundaries are helpful as an overview. There are some geological boundaries which have been mapped and the names Mapiri, Tutamoe and Ihungia are not used.

Morgans (1977) covers 24km² including the western portion of the Akitio River. This publication reviews the foraminiferal and lithological sequence from the Whangai Formation to the Ihungia Formation, with a focus on the Weber Formation. It also includes a detailed stratigraphic column, and structural cross sections, and discusses the evolving depositional environments as the East Coast is accreted. Like previous maps, it does not cover the entire given mapping area and analyses only the older portion of the stratigraphy (Weber, Wanstead and Whangai Formations).

The more recently Morgans (2016) focuses on the Weber region showing the distribution of the Weber Formation in the ECB defining type sections for the mudstone, flysch, limestone and glauconite members (which builds upon his 1977 Honours project) and providing stratigraphic correlations for Late Cretaceous – Paleogene units together with bio-stratigraphy and sedimentology.

3.2 Zealandia and East Coast Structural Evolution

The tectonic evolution of Zealandia and the eastern coast is significant in the context of petroleum potential. Sedimentary processes which form and preserve source reservoir rocks, as well as the tectonic regime, provide insight into the basin's attributes and petroleum potential. Kingma (1958) has reviewed the range of tectonic and sedimentary basin processes of the East Coast Basin. He showed tectonic movement caused older horst-like blocks to "pierce" through younger deposits, creating horst and graben structures punctuated by unconformities. This is exemplified in the Weber area where the Whangai Group appear to push through younger Miocene units as shown in Qmap (Appendix 1.6 & 1.7). Kingma goes onto state that local basins had very rapid and thick infill which is visible by the Mapiri, Tutamoe and Ihungia formations. Kingma (1959) examined the tectonic history of New Zealand, in particular, the formation and significance of the troughs and mountain ranges in various New Zealand regions. This publication has had a powerful impact on Zealandia reconstruction studies and states that the East Coast Basin lithologies are traceable to the very north of the eastern terranes of the North Island and as far south as Canterbury. In Kingma (1960) the sedimentation and lithologies of the East Coast Basin are reviewed in terms of New Zealand Geological series and stages. This provided an overall timeline of the sequence and succession deposition and integrated the timing of tectonic phases using local and regional unconformities, Kingma's interpretations are generalisations but, the concepts are applied to the Weber region.

Chanier et al. (1991) review the initiation of the subduction margin and the onset of tectonic processes in the southern Wairarapa region. Chanier et al. used facies observation, stratigraphy and onshore structures (field studies) to identify deformation features and conclude that the margin activation was quick which led to high sedimentation rates. Major, seaward-facing, thrust sheets developed in less than 6Myrs and recognised a close correspondence between compaction of deposits and amount of deformation visible. Rait et al. (1991) discusses the timing of activation of the subduction margin and put it at the start of the Early Miocene. He suggests the presence of ophiolites and the uplifting of older rock by large thrust faults

of the mid to outer slope caused the iconic deformation that is primarily seen today. Folding and the accompanying shortening occurred as the subduction progressed; the same processes are still occurring today. Lewis et al. (1993) also highlight that deformation of the East coast occurred during the past 25Myrs due to oblique subduction of the Pacific Plate. He divides the subduction wedge into six parts, the frontal ridge, the forearc basin, the transform basins, the structural trench and the northern, central and southern wedge. Lewis compares the basin system to other imbricated-thrust wedges around the world compares the deformation and deposition styles. Geographical differences of the deformation are related to the variation of tectonic movement along the Hikurangi Trough and Lewis rules out the term accretionary prism for the inner frontal wedge, due to not all features being strictly accretionary. The development of new terms and classifications of the East coast continued to develop further. Field et al. (1997) discuss the three phases of tectonic movement of the East Coast, Cretaceous accretion, Paleogene subduction and extension, and Miocene compression and uplift. The different regions of the East coast are discussed in detail for both onshore and offshore. For the onshore Wairarapa, which includes the Weber region, significant faults and folds are highlighted such as the Adams-Tinui fault and Akitio Syncline which have formed the structural highs (Late Cretaceous exposures) and lows (Miocene infill). Basin formation mechanisms (extensional rift, thrust-bounded and strike-slip) which occur in different regions have caused the East Coast structure to be complicated with, in places, rapid stratigraphic and structural changes. Chanier et al. (1999) noted two major extensional deformation events (Mid to Late Miocene subsidence and Quaternary uplift) in the past 25 Ma. This relates to the Weber region by providing times or stages of deformation which is likely to be reflected in the stratigraphy and sedimentology.

Figure 3.2 The East Coast at 16 Ma (Bailleul et al., 2013)

Nicol et al. (2007) present paleogeographic reconstructions of New Zealand for the past 24Myrs. Nicol et al. noted that reconstructions like this could be invalid if the depositional environment and the deformation changes are not considered. By incorporating all available data into the reconstruction, Nicol concluded that the south-east coast has rotated on its axis and shortened significantly. The calculated rate of upper plate convergence and rotation rates in the past 10Myrs have decreased with collision, but motion parallel to the plate margin has increased.

Uruski (2010) presents an overview of New Zealand's sedimentary basins, when and how they are formed, their Neogene structures and how their gentle deep water basin structure means it is more probable to find large intact hydrocarbon reservoirs. The proposed theories of the tectonic evolution of Zealandia all conclude that the basins formed on the mostly submerged continent are prospective petroleum basins. Deposition patterns and sediments change as tectonic settings develop and Bailleul et al. (2013) reviews this in detail. The Neogene trench-slope basins of the East Coast can be classified into four different categories: flysch filled basins, narrow turbidite rich basins, wider basins (30-40km) associated with shelf widening and lastly, basins that reflect uplift and infill of the previously widened shelf basins. At the start of the Miocene (25 Ma), subduction was deepening the forearc basin. This was followed by an extension from 13.2 Ma to 5.3 Ma which lead to today's contraction and uplift. The Akitio sub-basin mapping area can be seen as a two-part basin, flysch filled basin in the west and farther east a basin associated with uplift and infill, including turbidite deposition. Offshore Multichannel Seismic Reflection Profiles (MSRP) and foraminifera biostratigraphy studies in the central East Coast has greatly assisted onshore mapping, structural analysis and stratigraphic succession (Bailleul et al., 2013). Depositional sequences are defined together with their bounding unconformities and deformation. MSRP divides the depositional packages into three main stages; stage one is the Acoustic Basement (S1) to Middle Miocene (15.5-14.2 Ma) and older deformed strata which contain west-dipping thrust faults; stage two is Middle-Late Miocene Narrow Trench-Slope Basins (S2) which is separated from S1 by an undulating major angular unconformity. It represents Mid to Late Miocene (14.2 – 6.2 Ma) syntectonic deposition which is folded (anticlinal) in response to movement on the underlying thrust faults. Stage three (S3) which is Plio-Quaternary Turnagain Wide Slope Basin and Shelf Deposits (6.2 Ma and younger). These also have an undulating major angular unconformable base and represents rapidly shallowing depositional environment (Morgans et al., 1995). Uruski (2010) also correlates the offshore stages to the onshore stratigraphy and paleocurrent measurements. The onshore stages are further

subdivided into three stages making a total of eleven phases. During the Early Miocene flysch basins were prominent transitioning into trench-slope basins, followed by broad slope basins which are today's current shelf environment. He states that from 25-18 Ma there was the change from pelagic to distal turbiditic deposition. These deposits were subsequently formed by the thrust faults. Later during 17.5-15 Ma rapid facies changes locally and structural ridges formed due to compression (Fig. 3.2). From 15-6.5 Ma the Cape Turnagain structural high separated two domains, one of subsidence (local basin infill) and one of extension (ridge and shelf development). From 6.5 Ma onwards contraction and uplift has continued to deform the margin. Lastly, Noda et al. (2017) correlate growing accretionary wedge styles shown around the world with deposition, deformation and overall basin formation. Three deformation models are presented, the single wedge, two-wedge and strike slip and from the presented models, it is clear that the Hikurangi Trough is clasified as a single-wedge model. Noda furthermore divides the Hikurangi Trough into four domains which highlights the lower-eastern North Island is more subjected to frontal accretion (thrust faulting and ridge uplift) than other three domains. Noda also uses the Motu-o-Kura basin (Hawkes Bay) as an example and shows that because of the East Coast basins have been largely affected by sea level, sediement deposition and unconformities are highly variable throughout the accretion front.

3.3 Stratigraphic Units and Deposition

Moore (1988a) examined the Whangai, Waipawa and Weber formations at numerous locations of the East Coast of the North Island. From key sections, distributional differences and relationships have been made by using the stratigraphy and petrology. Sedimentary textures such as paleocurrent textures, bioturbation, and bedding type and thickness were correlated to provide a paleoenvironmental interpretation for the East Coast at a particular time. Moore correlated the petrology to show geographic variation within the region. For example, the carbonate content of the Whangai Formation increases toward the west, and there are significant differences comparing samples taken from various localities set within the East Coast Allochthon. Moore also included X-ray fluorescence data and clay mineralogy and discussed the petroleum potential of the region.

Field et al. (1997) presented the lithological and structural progression from the Cretaceous to Cenozoic for the East Coast region. Field et al. incorporated onshore and offshore seismic data to provide

stratigraphic correlations, structural interpretations, and an assessment of the petroleum system of the region.

Francis (1990a) highlights the notable features of three East Coast Miocene synclines in the Akitio, Fingerpost and Turnagain areas. This was the first mention of the informal unit, McCartie sandstone, the upper sand unit of the McCartie Formation. Francis (1990b) provides a useful overview of key localities in the East Coast and looks at rock formations, their distributions and their petroleum potential.

In 1992 Neef published three East Coast studies, firstly about Miocene turbidite deposition (Neef, 1992a), secondly about the geology of the Akitio region (Neef, 1992b) and Gisborne geology (Neef et al., 1992c). Neef (1992a) describes five units, their distribution, and depositional environment. He concludes the Whakataki Formation deposition is consistent with fan modelling and low angle gradients along the East Coast. Neef (1992b) details the stratigraphy, maps, and cross sections that show the area is structurally complex.

Unpublished reports provide descriptions of type sections in the Tahuokaretu Stream, Akitio River and Tawanui areas (Bland et al., 2013; Bland et al., 2014; Clowes et al., 2016). All these reports focused on multiple sites and undertook biostratigraphy for depositional environment and age control. Bland, Morgans, & Strogen (2013) provides a regional overview whereas Bland et al. (2014) focus on two well-exposed sites, the Tahuokaretu/Mangato streams (TK) near Weber and Taylor-White section (TW) near Wimbledon. Bland et al. also discuss the stratigraphy from the Whangai members to Whakataki Formation in detail. Clowes et al. (2016) expanded on the previous work at Tahuokaretu/Mangato streams and Akitio River, with the objective of defining the base of the Kaiatan Stage, and "a reference section for the base of the Runangan Stage".

Rogers et al. (2001) investigate localities where the Waipawa Formation equivalent is found in the East Coast, including Tawanui. Rogers et al. concluded that the Waipawa Formation accumulated very slowly and was often associated with wide-spread glauconite production during the Early Paleocene. This was demonstrated by using biomarkers and Total Organic Carbon (TOC) data. Hollis et al. (2014) expand on the climate, and the Waipawa equivalent found at Tawanui. The Waipawa Formation is a popular topic due to its petroleum potential, however, due to its absence in the mapping area, it will not be a primary focus of this project.

More recently Clare et al. (2017) presented a model of Miocene sedimentation patterns in the Akitio sub-basin. Their study covers the 120km length of the basin, and compared past basin, deposition, the

sediments of which are now onshore, to present day offshore deposition. Clare et al. present a canyon and tributary depositional model to explain the observed features.

McArthur et al. (2019) studied marine littoral feeders of the East Coast Basin, more specifically the Madden Canyon. Their fieldwork consisted of onshore paleocurrent measurements, developing a lithofacies scheme which was supported by previous micropaleontological data. Bathymetric data were also used to compare with offshore depositional systems. This publication looks at varying canyon systems and Miocene deposition as an analogue for what is likely to be occurring in the modern-day Hikurangi margin.

		Ongley (1935)	Lille (1953)	Lee et al. (2002)	Bland et al. (2014)
Pleistocene		Mangahao	Mangatarata		?
Pliocene	**Late**	Petane	Kumeroa	Totaranui Limestone	?
		Te Aute	Te Aute	Te Onepu Limestone	?
	Early			Rongomai Limestone	?
		Waihoki	Mangatoro	Kairakau Limestone	?
Miocene	**Late**		Mapiri	Late Miocene Palliser Group	Whakataki
	Mid	Mapiri	Tutamoe	Middle Miocene Palliser Group	Ihungia
	Early	Tutamoe	Ihungia	Early Miocene Palliser Group	Weber
Oligocene	**Late**	Ihungia	Weber	Weber	Mud / Flysch / Lime stone / Glauc
	Early				
Eocene	**Late**	Weber			
	Mid		Wanstead	Wanstead	Wanstead
	Early				
Paleocene	**Late**	Tinui	Te Uri Member	Whangai	Te Uri Member
	Early		Upper Calcareous Member		Upper Calcareous Member
Late Cretaceous			Rakauroa		Rakauroa

Table 1 Stratigraphic summary of the mapping area from previous studies.

3.4 Biostratigraphy and event/period deposition

Kaiho et al. (1996) investigated foraminiferal extinction behaviour near Tawanui during the Paleocene. Results show that at 55.3Myrs there was a decrease in benthic foraminifera productivity causing 9% of species to become extinct and at 55.5Myrs (a major event) 25% of species became extinct at due to changes in climate, ocean salinity and sediment supply. For the following 40kyr low oxygen conditions continued causing high TOC levels and low terrestrial organic carbon.

Crouch et al. (2005) present marine environmental changes during the Paleocene-Eocene (61-49 Ma) transition. At this time the climate was warmer and ocean circulation altered which caused typically warm

environment organisms to be found living in polar regions. This publication uses Kaiho et al. (1996)and the Tawanui section as an example as well as Moeraki-Hampden beach to gain age control of the event and substages. From this study, local phases were identified which show changes in sea surface temperature and organism abundance curves. The article contributes to this project by giving a known biostratigraphic age to a location before collecting and analysing any samples as well as providing a known location of a geological contact boundary. It also shows that Tawanui is a significant site for many structural and biostratigraphical reasons.

3.5 Petroleum Potential

Studying the geology and stratigraphy of the ECB indicates different source rocks, hydrocarbon generation, expulsion and petroleum potential. Leckie (1992) preliminarily investigated the source rock potential of the Late Cretaceous and Paleogene. Leckie logged a ~50m section at the Tawanui and through geochemical analysis found that the Whangai members have Total Organic Carbon (TOC) contents of 0.2 to 1.55% (Rakauroa Member, Upper Calcareous Member and Te Uri Member). The hydrocarbons generated within the Waipawa Formation indicate oil and gas (Leckie, 1992), however, the abundance is uncertain due to hydrocarbons being able to travel through the oil window and from outcrops. An oil and gas window is the area at depth (and temperature) where oil and gas are produced and ejected. For the case of the East Coast, seeps are prevalent, but reservoirs and sources are not well established..

Rogers et al. (1999) examined samples from ten different oil and gas seeps from the central East Coast and Raukumara Peninsula and used biomarkers to compare oil sources. Elgar (1997) analysed the geochemistry of oil and gas seeps, and their sources in the region south of Napier. Elgar also undertook X-ray fluorescence (XRF) analyses of the Late Cretaceous to Paleogene units. Results show that the Whangai Formation and Waipawa indicate good source rock potential whereas Early Cretaceous and Neogene rock shows poor source rock potential.

Francis et al. (2004) reviews petroleum potential of the ECB and presents the distribution, thickness and source rock potential of the Late Cretaceous-Paleocene (Whangai Formation and Waipawa Black Shale) as well as Miocene and Pliocene rocks and their structural relationship within the East Coast. Francis et al. (2004) like Leckie (1992) and Elgar (1997), discuss the potential of the Whangai and Waipawa Formation. Francis et al. (2004) furthermore discusses the timing of expulsion of hydrocarbons for the

ECB. Miocene paleo-seep limestones found on the East Coast indicate generation and expulsion, and the Whangai is unlikely the source due to the Miocene strata being overlying. This additionally indicates an older source which would now be over-mature and that the Whangai and Waipawa hydrocarbons matured during the Pliocene. These studies highlight importance of understanding the stratigraphic relationships of the units at higher resolution. Investigating the petroleum potential of source rock furthers knowledge about other potential petroleum hosting basins which are currently forming offshore.

3.6 Provenance studies

Few provenance studies have been undertaken in the ECB therefore restricted detail is available. Lillie (1953) suggests that the Whangai was derived from a very low elevation landmass which at that time would have been the Torlesse Terrane. He also suggests that the Wanstead Formation was wash formed in shallow water which was derived from the Whangai Formation. This is not proven with any data but does initiate the idea of a reworked terrane provenance setting.

Van der Lingen et al. (1980) studied the Makara Basin, north of the East Coast Basin and its structural and geological setting, including provenance and basin development. Because the Makara Basin is geographically near the Akitio sub-basin, provenance and basin development are likely closely aligned.

Roser et al. (1986) and Roser et al. (1988) identify four petrographic Terranes with different major element provenance signatures. As previously mentioned, Moore (1988a) uses geochemistry to rule out unlikely provenance sources and suggest the likelihood of others.

Smale (1993) used heavy mineral analysis of Cretaceous-aged rock from the North Island East coast and Marlborough to show indurated and low-grade metamorphic Torlesse derived provenance.

Lastly, Hines (2018) studied the provenance of the East Coast and affirms that by 86Myrs all sediments were derived from basement strata and during the break up of Gondwana (110-83Ma) the Western Province Terranes, and Median Batholith were depositing sediment in to the ECB and other regions of the North Island of New Zealand (Fig. 3.3).

Figure 3.3 Provenance of the East Coast (Hines, 2018)

Chapter 4 Methods

4.1 Akitio Sub-Basin Fieldwork and Mapping

Fieldwork took place during the summer of 2017-2018 with the occasional reconnaissance day trip earlier 2017 to become familiar with the landscape. Hazards such as steep cliffs, landslides, animals, flash floods and forestry trucks were identified, and precautions such as a personal locator beacon, satellite radio, forestry traffic radio and high visual clothing were used. The mapping area is approximately 80sqkm, and access to private property was enabled by landowners' permission. Access to the river is restricted in places, and landowners pointed out tracks and access points. A quarter of the mapping area was covered by Ernslaw Ltd. Forestry and a master key were obtained, so forestry roads were available to use. During fieldwork, notes were recorded along with samples and structural measurements where possible. Fieldwork was done on foot due to the steepness of the terrain. A 1:5000 scale topographic map was used in the field on which structural data and facies boundaries were recorded.

4.2 Stratigraphy

Originally, an objective of this project was to focus on type sections and collating stratigraphic columns; however, due to erosion and lack of exposure, this was not always possible. There are previous type sections that have been illustrated and described, but there are two sections that had not been presented that were exposed, Mt McCartie Cliff and a waterfall cliff site near Waipatiki which is informally called Reid Waterfall after Reid (1998). Both sites contain Mid to Late Miocene aged rocks which proved helpful differentiating the Miocene stratigraphy. The Miocene-aged stratigraphy was differentiated by the lithology seen in the field. Each lithology was sampled, described and stratigraphically correlated up the Tahuokaretu Stream. Repeating lithologies were noted and mapped. Biostratigraphy also confirmed age and depositional environment similarities of the repeating lithologies.

4.3 Loss on Ignition (LOI)

Firstly, samples from each unit (either one from homogeneous or two or three from bedded units) are broken up to small gravel size (2mm to 5mm) and dried at 50 degrees Celsius until very dry. Once dry, the samples are ground in the Tungsten mill which is cleaned thoroughly with alcohol between samples. Then approximately 2 grams of the sample is weighed into a previously weighed ceramic crucible, and

the total weight is recorded. The crucibles have previously been washed with alcohol and dried in a 100-degree Celsius oven to remove any moisture. The samples are then stored in a desiccator or 50-degree oven until weight reduction from water loss stops.

The proportion of organic carbon is calculated by burning off the organic matter (OM) and calcium carbonate in a rock sample at the temperatures of 550ºC and 900ºC. Typically, the temperature of up to 375ºC are used to calculate the proportion of OM and 375 ºC to 550 ºC measures structural water lost from clays, however OM is often still present above the temperature of 550 ºC, therefore for this study only the temperatures of 550 ºC and 900 ºC will be used, and the structural water lost from clays was not determined due to it often being a minor proportion and OM being a more important factor. The result of the LOI calculation is used when performing X-ray fluorescence (XRF) in order to account for the carbonate loss.

The crucibles containing 2grams of the sample are placed in the furnace from room temperature and is set to heat to 550ºC. Once the furnace and samples have heated at 550ºC for 2 hours (removes OM), the samples are weighed and then put back in the furnace to further heat to 900ºC for 2 hours (removes carbonate) and are later reweighed. The LOI is then calculated using the formula below:

%LOI = 100* (weight change during ignition) / (fresh sample weight)

Or L.O.I. (weight %) = 100 x ((n_2-n_3) / (n_2-n_1)) where

n1= empty crucible, n2= crucible +sample powder, n3= weight of crucible + sample after furnace

Campos et al. (2002) justified using this technique by comparing their results by using the same samples in a CHNS automatic elemental analyser. This article highlights how sample size, ignition temperature and time all have a significant influence on LOI results. Other studies have suggested different sample weights and ignition temperatures, but Campos et al. have systematically tested the variables to optimise most consistent results. Campos et al. show that for their black shale samples, an optimum ignition time of six hours at 550 ºC to burn off OM and three hours at 1000 ºC to burn off the carbonate. This duration of time was not used for this study as the samples knowingly have low OM Campos et al. (2002) and some samples have higher carbonate content.

4.4 X-ray fluorescence (XRF)

Thirty-five samples were selected for XRF (either one from homogeneous or two or three from bedded units). XRF measures major and minor trace elements. For accurate results both fused beads (major trace elements) and Pressed Powder Pellets (PPP) (minor trace elements) are made. The reason for analysing major elements with fused beads is to overcome the micro-mineralogical effect on the PPP. The micro-mineral effect is caused by platy or flat minerals covering more area when using PPP, giving an impression of a higher proportion compared to other minerals. Using both PPP and fused beads provides very accurate results. The pellets contain a mixture of different crystals, and when the x-rays hit the sample, the composition of the individual crystals is measured, in which can vary considerably over the surface area. This results in different chemical analysis depending upon the surface area of the mineral measured. The fused beads, however, are homogeneous, comprising a molten crystal mixture that gives a bulk analysis of the sample.

The heated sample after calculating the LOI (0.8grams) and X-ray flux (8grams of 57% Lithium Tetraborate and 43% of Lithium Metaborate or 100% Lithium Tetraborate Flux, sample depending) are mixed to create fused beads. Post LOI samples are used to reduce volatilization of minerals such as carbonate which can cause analytical error. This mixture is transferred to a metal crucible and put in the XRFuse instrument with the flat tray moulds in the appropriate holders. The instrument is set to the long fusion program setting; the lid is lowered, the mixture is melted and poured into the flat tray moulds and start to cool. The flat tray mould will still be hot and need to be carefully taken out of the XRFuse and eventually labelled and taken out of the tray mould. The fused bead is now ready to be put in the XRF scanner.

To make the pressed pellets, 10 grams of dried, milled and unheated rock powder is mixed with 10-20 drops of PVA binder and poured into a labelled aluminium cup. Once the powder is pressed uniformly into the cup with a spatula, it needs to be put in the FluXana powder holder and pressed with a pressure of 20 t for one minute. The pellet is then removed and placed in a 45ºC oven overnight to evaporate the PVA binder. If the pellet has successfully been pressed, it is ready to be analysed in the XRF scanner.

The fused beads and the PPP's are put in the XRF scanner, and the sample details and LOI information are logged, the samples can now be scanned. All samples were prepared and analysed at the School of Agriculture and Environment, Massey University Palmerston North.

4.5 Petrography

Thirty-five samples were selected for petrographic microscopy (either one from homogeneous or two or three from bedded units). Thin sections were made from samples that were firstly dried in an oven at 65 degrees ºC for more than 48 hours. The samples were then vacuum impregnated with epotech epoxy (resin and hardener), vacuumed and cured at 65ºC for an hour. Once the epoxy had cured, the samples were cut and dried for another 24 hours, surface vacuum impregnated, vacuumed and cured again. Once dry, the samples were ground evenly to 1200 grit (15micron), and hot mounted to a petrographic glass slide which had been frosted with 400 grit (~23micron). The samples were then cut leaving a thin slice of sample attached to the glass slide; this remaining sample was ground and polished to 30 microns. All thin sections were described, and a selection was chosen for point counting.

4.6 Point Counting

Point counts were undertaken on 24 samples which were sandstones and mudstones that contained countable grains (nine samples had grains too small to distinguish). A minimum of 300 mineral grains was counted using a grid causing a unbiased and quantified result. Overall grain size was not measured and was not the focus of this petrography.

4.7 Micropaleontology

Forty mudstone samples (either one from homogeneous or two or three from bedded units) were processed for microfossils and microfauna using the method outlined in Harris et al. (1989). The samples are disaggregated, weighed, sieved, washed (water, soap and if needed hydrofluoric acid or bleach), filtered, dried and ready for separating individual fossils. There are different washing methods for certain rock types, and if a rock cannot be disaggregated, microfossils may not be possible to extract. Individual microfossils are secured by using a black numbered-grid picking tray under a binocular microscope with a 20-50X magnification, with a very fine paintbrush with adhesive. Microfossils were identified for age determination. The percentage of planktic and benthic species was calculated to determine the environment of deposition or redeposition. Microfossils are identified by their cast characteristics and can be environmentally specific. The aim for using this technique is to refine the depositional environments and ages of Miocene aged units, as well as confirm microfossil data from previous studies. Samples were processed and results confirmed at GNS by Hugh Morgan.

4.8 Macropaleontology

Samples of macrofossils were collected in situ at Waipatiki and transported blocks of fossiliferous mudstone were found throughout the majority of the streams as limestones. Many specimens were fragmented and unidentifiable. Coherent fossils were identified with the help of knowledgeable palaeontologists.

Chapter 5 Stratigraphy

5.1 Introduction

The Akitio sub-basin contains a Late Cretaceous to Late Miocene sedimentary succession consisting of nineteen New Zealand Stages (Fig. 5.1). In areas nearby, the underlying Glenburn Formation is exposed but is not found in the Weber mapping area. Immediately overlying the Glenburn Formation is the Whangai Group is the oldest (Late Cretaceous) (Qmap Map - Lee et al. (2002)). As the sub-basin has developed, the depositional environment and lithofacies have changed from deep marine to neritic over a relatively small distance (approximately 13 km wide). The Cretaceous to Oligocene geology has been described in previous publications (Table 1), however, the Miocene geology of this area has not and is the focus of this study. Hayward (1986) defines a framework of paleodepth and shelf position of East Coast microfossils which has been applied to this study (Fig. 5.2). A new 1:25,000 map (Fig. 5.26) has been compiled based on field investigations of the Weber Region is presented below. A stratigraphic summary is presented on the map and stratigraphic columns are in Appendix Two and Cross Sections as Appendix Three. These have been compiled through field observations and biostratigraphy primarily to differentiate the age and depositional environment. For the informally named Early to Late Miocene units, there is age overlap due to a consistently changing depositional environment, however, because of the changing environment, the units can be divided and distinguished in the field by the onset of different sedimentary features such as bedding thickness and later supported by microfossil data. The following detailed descriptions are of the geological units found in the Weber area.

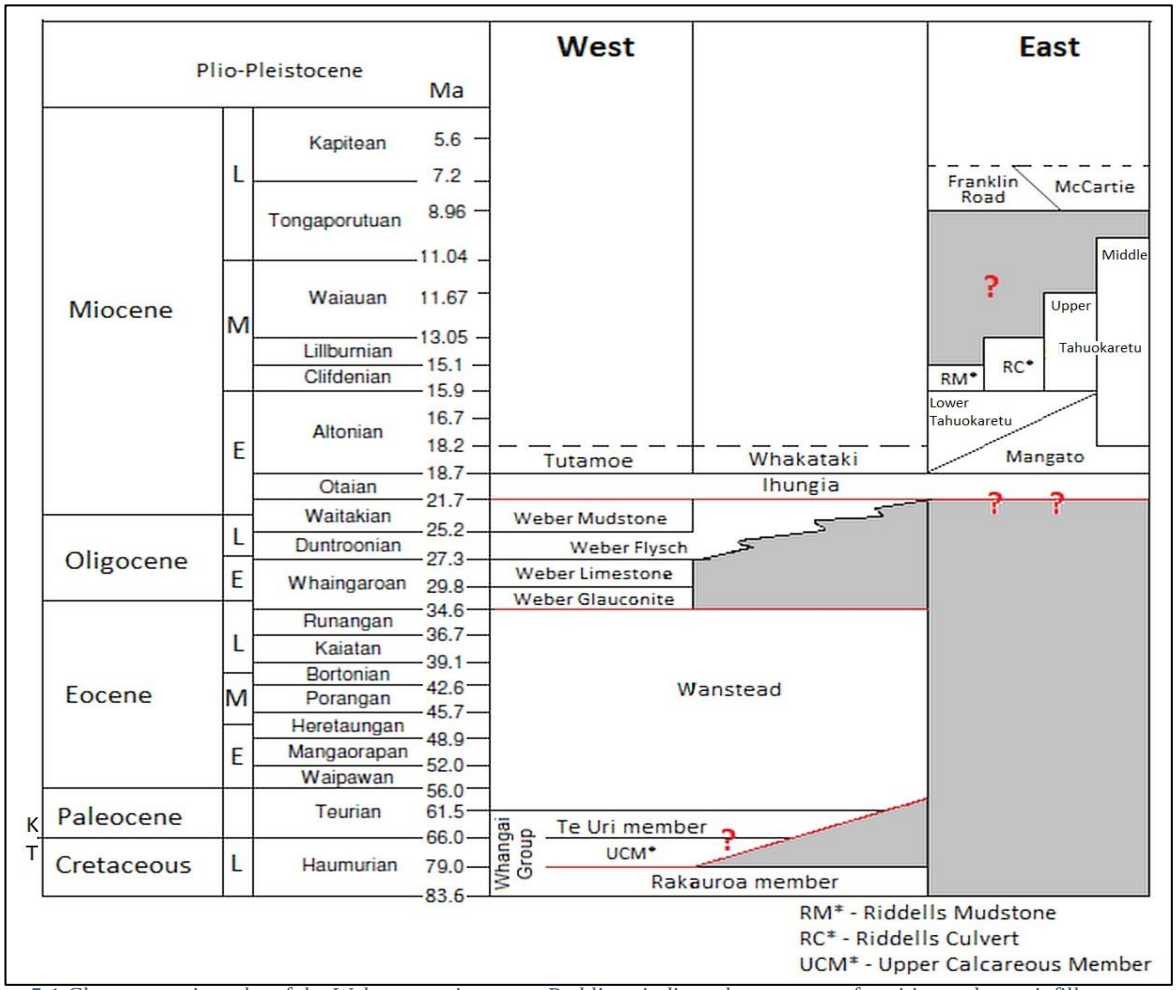

Figure 5.1 Chrono-stratigraphy of the Weber mapping area. Red lines indicate known unconformities and grey infill represents no deposition or erosion

5.2 Whangai Group

The Whangai Group in the mapping area comprises of three members, Rakauroa member, Te Uri member and Upper Calcareous member (UCM) which range in age from (80-66 Ma) Cretaceous/Tertiary boundary (K/T). Due to the age and nature of the geological outcrop, the K/T boundary is visible in the Tawanui district (Fig. 5.3). At the K/T boundary there is a change in foraminiferal content from being very abundant in the Upper Calcareous member and poor in the Te Uri (results based on microfossil data Appendix four). The Porangahau member (Whangai Zebra facies) and Kirks Breccia are not present in the Weber mapping area.

5.2.1 Whangai – Rakauroa Member

Description

The lowermost Whangai unit, Rakauroa member is medium grey mudstone which weathers red and black (Fig. 5.2). This Whangai member is firm, fractured, blocky and has an angular weathering pattern. It lacks any structures or textures, poorly bedded, bioturbated and is non-calcareous. The Rakauroa member is approximately 350- 400 m thick and is largely exposed in the Akitio river. The base of this unit was not seen in the mapping area.

Figure 5.2 Rakauroa Member of the Whangai. Note the red and black weathering

Paleoecology (Sample # F50857)

Limited fossil material was observed or recovered for this unit due to its hardness, however it includes moderately abundant fish teeth and a few broken *Bathysiphon* sp. fragments. Other macrofossils have been found in the Rakauroa member throughout the ECB, however, none were found during fieldwork for this study.

Paleoenvironment

Foraminifera indicate an upper Haumurian (80-66 Ma) to lower Teurian age (66-56 Ma). Bioturbation is ubiquitous. Although a constrained depositional environment cannot be determined with this sample, elsewhere in the basin Moore (1988b) suggests a shelfal depth (50-200 m).

5.2.2 Whangai – Upper Calcareous Member (UCM)

Description

The UCM is a light grey/blue firm mudstone, moderately calcareous, bioturbated, and displays a conchoidal weather pattern (Fig. 5.3). This poorly bedded unit is fractured, contains glauconitic sand sized grains and is micro-fossiliferous. It contains no macrofossils and is approximately 50 metres thick at Tawanui.

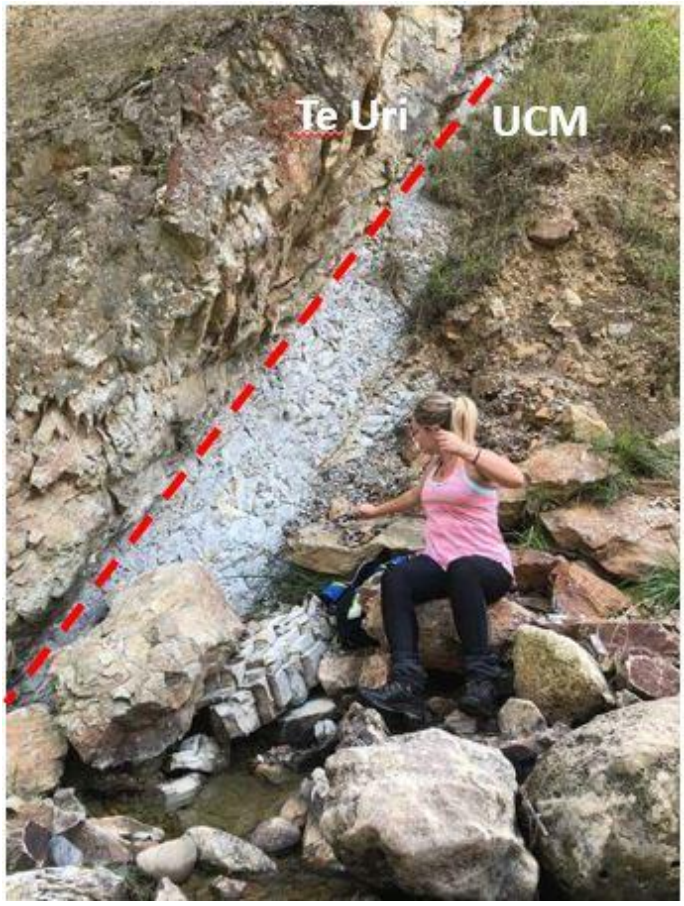

Figure 5.3 The Te Uri (left - light grey) and Upper Calcareous Member (right) of the Whangai Formation and the K/T boundary is the contact in between (red line).

Paleoecology (Sample # F50854)

The presence of the benthic foraminifera *Spiroplectammina piripaua, Stensioeina beccariiformis, Matanzia varians, Gaudryina healyi, Notoplanulina rakauroana*, and *Dorothia elongata* and the planktic foraminifera *Gublerina sp.* and *Rugoglobigerina rugosa* indicate a late Haumurian age (Late Cretaceous; 79.0-66.04 Ma).

Paleoenvironment

The presence of *Rzehakina epigona, Matanzia varians, Alabamina creta* and *Spiroplectammina* indicate a middle to lower bathyal paleodepth (600-1000 m), however, Moore (1988a) suggests a shelf environment and Hines (2018) suggests a upper to middle bathyal environment with a deepening from west to east during this time.

5.2.3 Whangai - Te Uri Member

Description

The Te Uri Member is a light grey/tan, fine grained, glauconitic sandstone (Fig. 5.3). It is indurated, is poorly bedded, slightly calcareous in places and is said to disconformably overly the UCM, however this is variable along the ECB. Although variable thickness across the region, it is approximately 30 metres thick at Tawanui and is intensely bioturbated. The upper part consists of a glauconite rich bed and has

been interpreted as the Waipawa equivalent (Hollis et al., 2014; Rogers et al., 2001). The Te Uri Member is regarded as a local member and is only found in a few locations of the ECB.

Paleoecology (Sample # F50855)

No foraminifera were obtained from the Te Uri, but moderately abundant fish teeth were recovered. Shark teeth and fish teeth have been reported by previous work (Hines, 2018). No paleodepth or environmental data was confirmed from this sample but Hines (2018) suggests an age of 66 Ma to 58.7 Ma.

Paleoenvironment

The top of the Te Uri is marked by *Zoophycos*, *Teichichnus* and contains *Chondrites* which indicate particularly difficult living conditions of bathyal environments and of near anoxic conditions (Hines, 2018; Leckie, 1992).

5.3 Wanstead Group

Description

The Wanstead Group consists of two facies, mudstone and glauconitic sand (Fig. 5.4). The Wanstead Mudstone is a light grey/blue, calcareous claystone which is moderately soft and easily eroded. It is very poorly bedded, no distinguishable sedimentary features and no macrofossils were found (expect one specimen of *Perploma* bivalve (Neef, 1995)); but contains abundant benthic foraminifera (Elgar, 1997). When a sample is wet, it is a medium-dark grey and easily moulds into a paste. The unit is approximately 50-80 m thick. The Wanstead glauconitic sandstone is a result from a depositional change of the formation and the exact thickness is not exposed but is presumed to be 1-2 m thick. Because of this, it is not mapped separately.

Paleoecology (Sample # F50867)

The presence of the benthic foraminifera *Stensioeina beccariiformis*, *Matanzia varians*, *Gaudryina whangaia*, *Allomorphina allomorphinoides* and *Cibicides* "teuria" indicates a Teurian age (Paleocene; 66.0–56.0 Ma).

Figure 5.4 Wanstead outcrop near Tawanui, Akitio River

Paleoenvironment

The presence of benthic foraminifera *Matanzia varians, Hyperammina sp., Glomospira charoides, and Stensioeina beccariiformis* sugguests a paleodepth of lower bathyal (1000 m or greater), however, there is minor indication of redeposition of shelf material (shelfal species found at bathyal depths). The planktic percentage is less than 1%, indicating a sheltered inner neritic water mass.

5.4 Weber Group

The Weber Group consists of four members; Weber Glauconitic sandstone, Weber Limestone, Weber flysch and Weber Mudstone. The difference between Weber flysch and Weber mudstone is that the flysch has a stratified fine to medium sandstone and mudstone gradation, whereas the Weber mudstone is homogeneous. The Weber Group is Late Oligocene to Miocene in age and the sequence can be found in the Waipatiki/western area of the Akitio River. The total thickness of the Weber Group in the mapped area is 650-700 m and it unconformably overlies the Wanstead Formation. This group has an approximate age of 25-23 Ma (Waitakian).

5.4.1 Weber – Glauconitic sandstone

Description

This member is a green/grey colour (Fig. 5.5) with a 10 m sandy bedded base (Fig. 5.6) that grades to a sandy mudstone that contains visible grains and is firm. The bedded base consists of 10-15 cm sandy layers with sandy mud interbeds with sharp contacts. The bedded base grades up to a near massive moderately grey mudstone with some glauconitic grains. This sample was not examined for microfossils but a shelfal depth with high iron supply and sub-oxic conditions is indicated by the glauconitic sand content. The total thickness of the unit is 90-110 m.

Figure 5.6 Weber Glauconitic sand found in Akitio River

Figure 5.5 Bedded base of Weber Glauconitic sandstone

5.4.2 Weber – Limestone

Description

The Weber limestone is a light grey colour, hard and has a conchoidal weathering fracture (Fig. 5.7). It is massive, silty, and a very calcareous mudstone. It is moderately firm but loses all strength with water. No macrofossils were seen during this study and has an approximate thickness of 150 m. Morgans (2016) noted its strong petroliferous smell.

Paleoecology (Sample # F50869)

The presence of both *Globoquadrina dehiscens* and *Globigerina euapertura* places this sample in the early Waitakian (latest Oligocene; 25.2–ca. 23.03 Ma). Fish teeth, mollusca, and radiolaria were also recovered and previous research also mentions the presence of *Zoophycus* (Bland et al., 2013) and small mollusa, rugose coral, *Flabellum* and a 2 cm wide amber (Morgans, 2016).

Paleoenvironment

The benthic foraminiferal fauna contains *Schenkiella weymouthi, Pleurostomella sp., Gyroidinoides neosoldanii, Cibicides robertsonianus,* and *Planulina wuellerstorfi* and indicates a deep middle bathyal paleodepth (700 – 1000 m).

Figure 5.7 Weber Limestone (left) and Weber Flysch (right) found in the Akitio River

5.4.3 Weber – Flysch Member

Description

Weber flysch ranges from a moderate to dark grey siltstone with definite light grey/tan medium to fine sand beds (seen at Tawanui (Fig. 5.8)) to a moderately grey siltstone with slightly less prominent sand beds (seen at Millstream Road (Fig. 5.9)). Bed thickness vary from a few centimetres to over 30 cm depending on the location. Sand beds commonly weather to an orange-rust colour. No macrofossils were found, and none have been recorded by earlier work. Weber flysch covers a large proportion of the mapping area and has an approximate total thickness of 350 m.

Paleoecology (Sample # F50858)

Weber Flysch units contains a low to medium diversity foraminiferal fauna including the planktic foraminifera *Globoquadrina dehiscens, Globigerina euapertura, Catapsydrax dissimilis* and the benthic foraminifera *Sigmoilopsis neocelata*, indicating an early Waitakian age (latest Oligocene; 25.2–ca. 23.03 Ma)

Figure 5.8 Weber Flysch at Tawanui from Bland et al. (2013)

Paleoenvironment

The benthic faunal assemblage includes *Schenkiella weymouthi, Nodosarella, Pleurostomella sp. Gyroidinoides neosoldanii* and indicates middle bathyal (>700 m) or deeper.

Figure 5.9 Weber Flysch outcrop beside the Akitio River

5.4.4 Weber – Mudstone Member

Description

The Weber Mudstone member is very hard to find and distinguish in the field. Bland et al. (2013) describes it as mudstone facies; a light creamy-grey, soft mudstone that is only seen at Weber and at Tinui. This unit is early Waitakian age and can be misidentified for Wanstead Formation.

5.5 Ihungia Formation

Description

Ihungia Formation is a dark blue grey, moderately soft, bedded mudstone. The beds are a few centimetres thick and have a straight sharp contact with the overlying and underlying mudstone. It does not contain macrofossils but contains abundant microfossils. The beds are regularly layered and uniform thickness (approximately 2-5 cm). It is well exposed on Tahuokaretu Road and is often very eroded (Fig. 5.10) and has a total thickness of 300 metres.

Paleoecology (Sample # F50859, F51132, F51133)

The presence of *Catapysdrax dissimilis, Globigerina woodi,* and *G. connecta* gives a late Waitakian to early Otaian age (Early Miocene; 23.03 – 18.7 Ma). While presence of *Paragloborotalia incognita, Globoquadrina dehiscens, Textularia miozea* and advanced specimens of *Haeuslerella hectori* indicate an age in the late Otaian, probably quite near the Po/Pl boundary.

Paleoenvironment

The samples of Ihungia contain a diverse benthic and planktic foraminiferal fauna. The benthic foraminiferas *Karreriella cushmani, Chilostomella ovoidea, Cibicides robertsonianus, Cibicides Ihungia* and *K. bradyi* indicate a middle bathyal deposition (700–800 m) or deeper, however the presence of *Karreriella cylindrica* indicates the paleodepth is at least deep upper bathyal (>400 m). Fish teeth and otoliths were also recovered. Planktic abundance of the three samples ranges from 10% to 40% indicates an inner to outer neritic water mass. This is due to the transport of the planktic foraminifera into middle bathyal deposits.

Figure 5.10 Ihungia outcrop on Mangatoitoi Station, Tahuokaretu Road. Note thin sandstone bedding.

5.6 Whakataki Formation

Description

The Whakataki Formation consists of a sequence of very well bedded brown//tan sandstone and dark grey mudstone (Fig. 5.11). The beds range from 5 cm to 50 cm thick (an occasional bed is up to 80 cm). The sandstone and mudstone are ripple laminated and the organic matter component is seen as black flowlines. The sandstone beds also pinch out in places. The Whakataki Formation is also well exposed at Mataikona/Castlepoint and at Mangatoitoi Station, central Tahuokaretu Road. The Whakataki Formation is interpreted as turbidites (Broome, 2015) and all bouma horizons are present. The basal sandstone is normally graded and is overlain by mudstone. The Whakataki Formation has a total thickness of 120metres.

Paleoecology (Sample # F50860)

A well-preserved fauna with 11 benthic and 57 planktic foraminifera species was indentfied. The presence of a single sinistral specimen of *Globorotalia miozea*, may restrict this to the Altonian to Clifdenian (Early Miocene; 16.7–15.1 Ma), but the age could be younger in the Miocene.

Paleoenvironment

From the mudstone there is not much evidence, but the benthic fauna is most likely bathyal, how deep cannot be determined, but possibly middle bathyal (> 600 m).

Figure 5.11 Whakataki outcrop, Mangatoitoi Station, Tahuokaretu Road

5.7 Tutamoe

Description

The Tutamoe facies has a sharp basal contact with the underlying Ihungia unit (Fig. 5.12). The sand base is a moderately hard light brown/grey, fine sandstone that is bioturbated. The overlying bedded sand layers vary from 40 cm to less than 10 cm and the lower sand bed contact is sharp and grades upwards to a fine mudstone and siltstone. The sand layers are nearly massive, and the layers are regarded as event deposits. The moderately grey mudstone layers increase in thickness towards the top of the unit and can contain macrofossil lenses. The top of the unit is not exposed in the mapping area. It is well bedded and has a sand base that is approximately 5 metres thick. It has an approximate age of 20-18 Ma (Otaian) and thickness of 50 metres. The base is called the Westcott sandstone by Reid (1998) and has a reworked macrofossil layer on both the upper and base contact.

Paleoecology (Sample # F50856)

The planktic percentage is less than 5%, and on the presence of the planktic *Paragloborotalia incognita* (late Po–early Pl), and the absence *Globoquadrina dehiscens* and any *Globorotalia spp*. indicates the age is likely to be late Otaian to early Altonian (Early Miocene; ca. 20.2–18.2 Ma). Although not well documented, there is evidence that *Globoquadrina dehiscens* became locally extinct in the New Zealand region in the early Altonian (*G. incognita* zone) (Scott et al., 1990; Walters, 1965). Fish-teeth, echinoid spines, shell-hash and ostracoda were also recovered. The macrofossils that are present are shown in Appendix Four.

Figure 5.12 Tutamoe overlying Ihungia, Akitio River. The red dashed line highlights the contact boundary

Paleoenvironment

The presence of *Pullenia bulloides* indicates an upper bathyal (200–400 m) paleodepth. Planktic abundance is 5 % indicating a sheltered inner neritic water mass overlay the site of deposition.

5.8 Riddells Group

This group may be differentiated Ihungia facies but they have been described and mapped separately by lithology. The group have been informally named the Riddells group as nearly all the facies are found on the Riddells property. The group is mostly made up of mudstone with sandstone beds which vary in thickness and that are very erosion prone. As shown in Figure 5.1 and Appendix Three, the Riddells Group is only found in the eastern part of the mapping area and stratigraphically overlies Ihungia and Whakataki units.

5.8.1 Mangato Mudstone

Description

The Mangato Mudstone unit is a light grey, moderately soft mudstone with thicker sandstone beds (50-70 cm) (Fig. 5.13 & Fig. 5.14). Beds are regularly spaced, have consistent thickness and the mudstone is very similar to Ihungia. No macrofossils were seen, and the sandstone beds are easily seen up high on exposed hills due to erosion. Colourful oil streams were seen after rain in the eroded unit (Fig. 5.14). Contacts between beds are sharp, the sandstone beds show mild flow banding and the unit has a total thickness of 150 metres. No sample of this unit was analysed for microfossils; however, its age is determined stratigraphically at 17-11 Ma. Its probable depositional environment is 600-800 m with the sandstone beds being transported from shallow shelf setting.

Figure 5.14 Mangato Mudstone with sandstone beds

Figure 5.13 Colourful oil streaming down eroded Mangato Mudstone after recent rain

5.8.2 Lower Tahuokaretu

Description

The Lower Tahuokaretu is a moderate to dark grey mudstone and is moderately soft and erodes easily. This unit looks very similar to Ihungia with sandstone beds that are less than 5 cm thick (Fig. 5.15), but the sand beds are more regular, show slight flow features, and are slightly thicker. It contains no macrofossils and was not analysed for microfossils. It has an approximate thickness of 210 metres. The depositional environment would be like the Ihungia mudstone with an estimated paleodepth of 700-800 m but with more shelfal sand input and its age is also likely to be near 16-11 Ma due to stratigraphy.

Figure 5.15 Lower Tahuokaretu Mudstone found in Tahuokaretu Stream near the Riddells sheep yards

5.8.3 Middle Tahuokaretu

Description

The Middle Tahuokaretu unit is a light grey colour when dry but is a moderate to dark grey when wet (Fig. 5.16). It is moderately soft and erodes easily. The Middle Tahuokaretu Mudstone very similar to Ihungia and Lower Tahuokaretu Mudstone, but it is distinguishable by its very thin bedding (less than 3 cm). This unit contains no macrofossils and structural measurements are difficult to obtain due to erosion and inaccessibility. It has an approximate thickness of 120 metres.

Paleoecology (Sample # F51128 & F51134)

The presence of *Globorotalia praescitula, G. zealandica, Globigerinoides bisphericus*, *Orbulina suturalis* and some advanced to *Orbulina universa*, *Globorotalia miotumida* (sinistral), *Paragloborotalia mayeri*, *Fohsella peripheroronda*, a couple of sinistral specimens of *Globorotalia miotumida*, forms close to *Praeorbulina* or *Universa suturalis*, *Globoquadrina dehiscens*, roughly equal numbers of sinistral and dextral coiling *Globorotalia miozea* (29s:23d), *Globigerinoides trilobus*, and *Paragloborotalia bella* indicate an age of Early to Middle Miocene (18.2-11.04 Ma). Echinoid spines, micro-gastropods and diatoms were also recovered.

Paleoenvironment

The benthic foraminifera *Karreriella cylindrica, Sigmoilopsis schlumbergeri*, *Pleurostomella*, *Chilostomella,* and *Gyroidinoides neosoldanii* indicate shallow middle bathyal paleodepths (600-800 m). However, the presence of *Tritaxilina zealandica* places the paleodepth at deep lower bathyal (>1500 m) or deeper with a middle neritic water mass (sandstone beds) input. Planktic abundance is more than 80% indicating a sub-oceanic water mass.

Figure 5.16 Middle Tahuokaretu Mudstone found in Tahuokaretu Stream. The exposed edges show the thin sandstone beds.

5.8.4 Upper Tahuokaretu

Description

The Upper Tahuokaretu sandstone beds are a light brown/grey colour and the mudstone is medium grey (Fig. 5.17). The sandstone layers show some flow banding. Both sandstone and mudstone beds are firm which makes it not as erosion prone as the other mudstones of the group. The mudstone contains very small pieces of fossil shell material but are undecipherable due to being fragmented. This unit is easier to distinguish due to the noticeable thicker (10-15 cm) sandstone beds. The sandstone beds and mudstone beds are of similar thickness. The bottom contact of the sand layers is sharp and grades into mudstone. The unit has a total thickness of 60 metres.

Figure 5.17 Upper Tahuokaretu Mudstone found in Tahuokaretu Stream

Paleoecology (Sample # F1571 & F1581)

The benthic foraminifera *Sigmoilopsis schlumbergeri, Karreriella cylindrica, Planulina wuellerstorfi,* and *Tritaxilina zealandica* indicate deep lower bathyal paleodepths (>1500 m) with some inner neritic overlay. Planktic foraminifera abundance is about 90% indicating near fully oceanic conditions. Echinoid spines, fish teeth and diatoms were also recovered.

Paleoenvironment

The presence of *Globoquadrina dehiscens,* advanced specimens of *Praeorbulina, Orbulina suturalis, Orbulina universa,* a sinistral population of *Globorotalia miotumida*, sinistral *G. miotumida*, >5% *Paragloborotalia mayeri, Globorotalia miozea, Globorotalia* cf. *zealandica, Paragloborotalia bella, and Fohsella peripheroronda* indicate a Clifdenian to middle Waiauan age (Middle Miocene; ca. 15.9–11.04 Ma).

5.8.5 Riddells Mudstone

Description

Riddells Mudstone is a dark grey, very soft, near massive, and slightly sandy mudstone (Fig. 5.18). It is distinguishable due to its lack of sedimentary features. It contains occasional chert beds, no macrofossils and is erosion prone. It has a conchoidal weather fracture and is slightly blocky and a total approximate thickness of 200 metres.

Paleoecology (Sample # F50861)

The paucity of *Globorotalia* specimens in this sample is a problem. The bulk of the planktic fauna *Globoquadrina dehiscens, Globigerinoides trilobus, Globigerinoides bisphericus, Globigerina woodi, Globigerina connecta* and *Sphaeroidinella grimsdalei* indicates Early Miocene or younger. A single sinistral specimen of *Globorotalia* identified as *G. miozea* may restrict the age to late Altonian to Clifdenian, and no *Orbulina* taxa (Sl-Rec) were recovered, but the identification cannot be certain (Early to middle Miocene; 15.9–15.1 Ma). Fish teeth were also recovered.

Paleoenvironment

The presence of *Tritaxilina zealandica* indicates paleodepths at deep lower bathyal (>1500 m).

Figure 5.18 Riddells Mudstone and chert beds found in Tahuokaretu Stream

5.8.6 Riddells Culvert Member

Description

This unit was first seen (as the name suggests) in the culvert next to the track up to the Riddells stock yards (Fig. 5.19)and was later found in the stream on the Ernslaw forestry area. The sandstone is a light brown to grey colour and the mudstone is a dark grey to nearly black colour but weathers light grey colour. It is a very well bedded sandstone and mudstone and the mudstone contains very small shell fragments. The beds vary in thickness and the bottom contact of the sandstone beds is sharp and grades into a slightly wavy and laminated mix of sand and mud to lastly a mudstone. The Riddells Culvert member has a total thickness of 110 metres.

Figure 5.19 Riddells Culvert

Paleoecology (Sample # F50862)

The presence of small specimens of *Praeorbulina circularis* and a couple of *Globorotalia*, one possibly *miotumida* and the other possibly *miozea* gives a Clifdenian or younger, possibly no younger than Lillburnian age. (Middle Miocene; 15.9–13.05 Ma). Otoliths were also recovered.

Paleoenvironment

The presence of the benthic foraminifera *Tritaxilina zealandica* places the paleodepth at deep lower bathyal (>1500 m).

5.9 Franklin Road

Description

The Franklin Road unit is a light grey mudstone and dark grey/brown fine sandstone (Fig. 5.20). This unit contains 30-50 cm thick sand beds and 40-70 cm thick mudstone interbeds. The upper and lower sandstone contacts are sharp, and both the sandstone and mudstone are typically moderately hard unless weathered. The mudstone contains broken fossil shell fragments and microfossils. The sandstone beds were regularly deposited and are of consistent thickness. The alternating layers look very similar to Tutamoe but are more consistently deposited and have a regular bed thickness and it has a total approximate thickness of 315 metres. The Franklin road member may be included in the Riddell Group but is individually differentiated because of its lithology, bedding and microfossil indicated age. It is found on Franklin Road and Geologist Road (Ernslaw Forestry Road).

Paleoecology (Sample # F50864)

The presence of sinistral *Globorotalia miotumida* (10 sinistral and no dextral), generally with 4-4.5 chambers in the final whorl, the presence of *Bolivinita pliobliqua* (Tt–Wn) and the absence of *Globoquadrina dehiscens* (Lw–early Tt) indicates a late Tongaporutuan age (Late Miocene; 8.96–7.12 Ma). Ostracoda were also recovered.

Paleoenvironment

There is evidence for shelf, even shallow shelf sediments, with *Notorotalia hurupiensis* and *Zeaflorilus parri*, yet *Karreriella cylindrica* (>400 m) and *Stilostomella sp.* and *Cibicides ihungia* indicate possible middle bathyal 600–1000 m paleodepths. It seems that some shelf material was being transported into middle bathyal depths. Planktic abundance of 7% indicates an inner neritic water mass.

Figure 5.20 Franklin Road which is located on Franklin Road and Geologist Road.

5.10 McCartie Group

5.10.1 McCartie Mudstone

Figure 5.21 McCartie Mudstone found at Mt McCartie cliff seen from Franklin Road. Note person in centre for scale.

Description

The McCartie mudstone is homogeneous mudstone with two thick (3-5 m) sandstone beds and is named a mudstone in order to distinguish from the overlying McCartie Sandstone. The mudstone layers are a light to moderate grey colour, hard and is occasionally macro-fossiliferous with millimetre sized shell fragments (Fig. 5.21). The sandstone beds are also hard and is a brown/grey colour. It has a sharp contact with the overlying McCartie sandstone. The sandstone beds have some wavy banding near the upper contact with the mudstone, but it is only a few centimetres thick, otherwise the rest of the layer is nearly massive, and it has a total approximate thickness of 30 metres.

The McCartie mudstone is located under the McCartie sandstone at 390 m elevation in the forestry near the cliff to the right of Franklins road (Mt McCartie). It is not well exposed, and most outcrops are hard or difficult to reach.

Paleoecology (Sample # F51119, F51118 & F51122)

The presence of *Bolivinita pliobliqua, Globorotalia miotumida* (all sinistral), *Bolivinita pliozea, Neogloboquadrina pachyderma,* and the absence of *Globoquadrina dehiscens*, gives a late Tongaporutuan age. 8.96-7.2 Ma

Paleoenvironment

The presence of *Karreriella cylindrica* indicates a deep upper bathyal paleodepth (400-600 m). Planktic abundance of 30-40% indicates an outer neritic water mass.

5.10.2 McCartie Sandstone

Description

The McCartie sandstone is a soft, medium to fine grained sandstone which is orange/tan in colour and is very micaceous (Fig. 5.22). It can weather to a darker orange or slightly black colour. It is one of the youngest deposits in the mapping area, with an approximated age of 5 Ma (Kapitean to Opotian) based on stratigraphy. It is nearly massive and has no bedding or textural features. It has poor stability but is stable with vegetation cover. Its approximate thickness is 15 metres. This unit was not analysed for microfossils; however, its depositional environment is likely to be rather shallow water in order to incorporate lots of fragile and light-weight biotite fragments.

Figure 5.22 McCartie Sandstone found on Franklin Road

5.11 Limestone units

There are three limestone facies found in the area and they have been given the informal names of Te Awaputahi Limestone, Scallop Limestone, and Hillcap Limestone. Their age is presumed to be Plio-Pleistocene. They all have been transported due to being found in displaced blocks or as a conglomerated deposit. Their original outcrop site is not found in the mapping area and the true thicknesses are unknown. The limestone units are Plio-Pleistocene age based on visible macrofossils. Furthermore, this indicates that the limestone units were deposited after they were formed from surrounding structural highs. The only visible unit contact for any of the limestone units is the Scallop Limestone which has sheared off small hill tops (Fig. 5.25). Due to the sharp, unconformable contact and the orientated mixture of varying clasts (or rocks) of the unit, the likelihood of event or sudden deposition is likely.

Figure 5.24 Te Awaputahi Limestone block found up

Figure 5.23 Scallop Limestone block found in Tahuokaretu Stream and Akitio River

5.11.1 Te Awaputahi Limestone

The Te Awaputahi Limestone has estimated equal parts of a medium grey, muddy sandstone matrix with orientated fossil shell fragments (Fig. 5.23). It is very hard and can spark when hit with a hammer. The Te Awaputahi Limestone is found in big blocks (5 m+ diameter) and is located up Titoki road which leads up to Mt Te Awaputahi. The blocks of limestone are flaggy and rather weathered.

Figure 5.25 Hillcap Limestone which is found on Riddells property and Tahuokaretu Road as a loosely packed conglomerate

5.11.2 Scallop Limestone

Scallop Limestone contains many intact scallops and other tan/light brown shell material with calcium carbonate matrix (Fig. 5.24). It also contains small pebbles and the shell material is orientated. It is

moderate to hard firmness. It is found often small boulders (1 m diameter), but occasionally in relatively big blocks (2 m+).

5.11.3 Hillcap Limestone Conglomerate

Hillcap Limestone contains rounded amalgamated cream/tan coloured shell-hash rocks (less than 20 cm diameter) as well as concretions and other foreign material (Fig. 5.25). It is found in two known places, one across the road from the small fault on Tahuokaretu Road and on the other side of Riddells Valley. The outcrop has sheared off the top of the hills (sharp bottom contact with mudstone) and could potentially be from a pre-existing fluvial channel.

5.12 Stratigraphy Summary

- During the Eocene to Oligocene there is high bio-productivity and low to moderate siliciclastic deposition.
- The Miocene onset of the modern-day subduction interface increased tectonic uplift of terranes and therefore influx of siliciclastic material that dominates the succession at this time.
- Lastly in the Pliocene, the return of increased biotic activity due to shoaling and shallowing resulted in high ocean productivity and essentially Te Aute Limestone suite of the East Coast.

Geology of Weber, Akitio Sub-Basin, East Coast, North Island, New Zealand

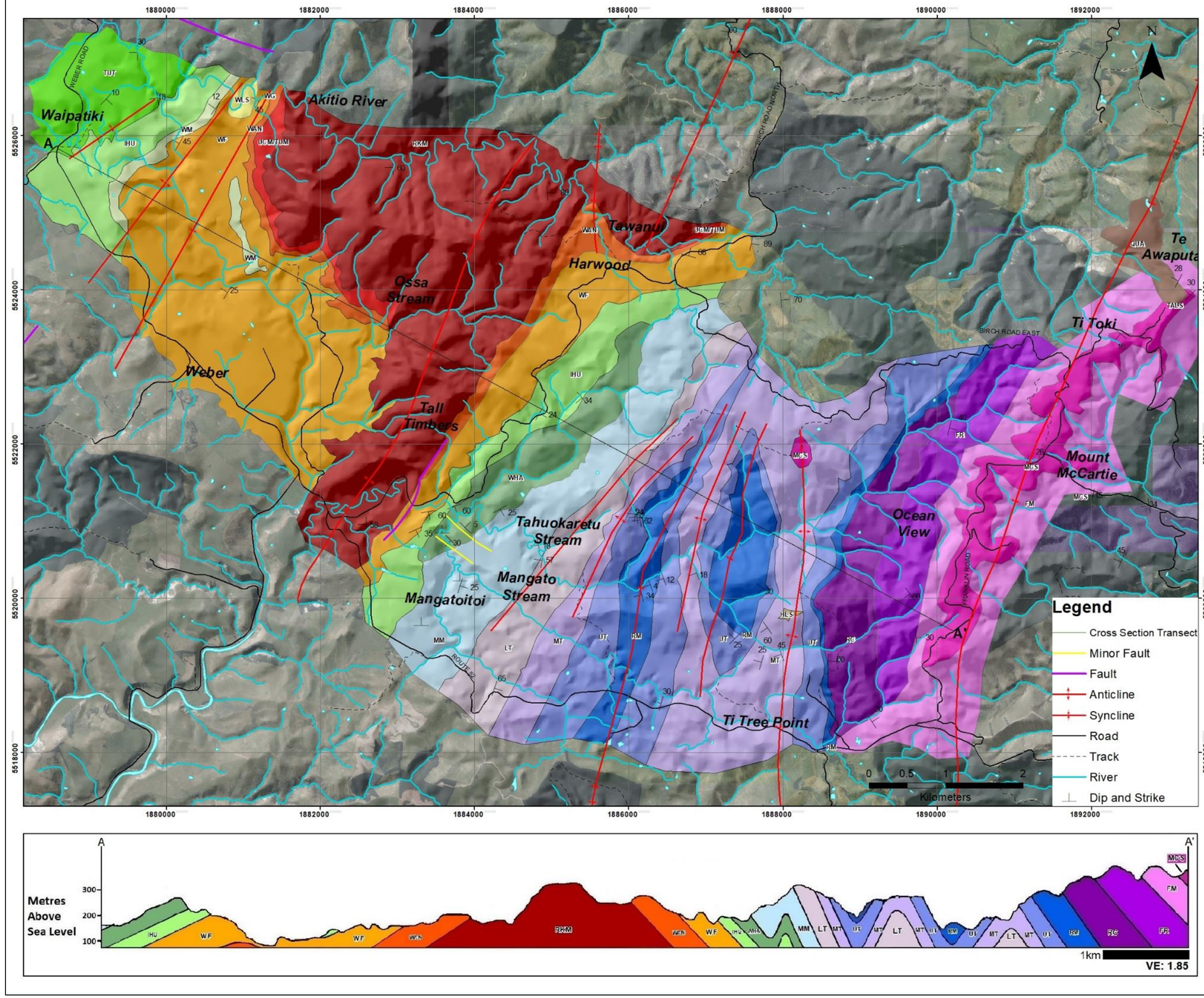

Figure 5.26 The Geology of the Weber area (1:25,000)

Chapter 6 Petrography and Geochemistry

Petrography is the study of the composition of rock to gain more information about its composition such as its depositional environment, deformation/alteration and provenance. Many analytical procedures that can be used to study rock composition, either by bulk analysis or single grains. For example, thin sections and point counting, Quartz-Feldspar-Lithics (QFL), Quartz undulosity and crystallinity, Loss on Ignition (LOI) and X-ray fluorescence (XRF). McLennan et al. (1993) shows many principles that show either processes of petrographical or provenance environmental interactions. For this project, the processes of weathering, diagenesis, sorting, sedimentary sorting, and terrane type will be investigated. By using these concepts and comparing data of this project to previous New Zealand studies, petrographic and geochemical interpretations will be made. Radiogenic isotopes are not used in this study.

6.1 Thin Sections

6.1.1 Introduction

From the 35 thin sections made, 24 slides have minerals of distinguishable size and which were point counted (Appendix Six). There are four main lithologies, limestones, sandstone, mudstone and glauconitic sands. The limestones were not counted or described due to being transported and of Plio-Pleistocene age; Late Cretaceous to Miocene geology are of petrographic focus. Photos were taken at x10 magnification, and each complete field of view is 2mm (width).

6.1.2 Rakauroa Member

The Rakauroa Member is composed mostly of quartz, calcite, glauconite and mud matrix (Fig. 6.1). Minerals are sub-rounded, poorly sorted, slightly orientated, and is as a silt to fine silt to silt. Using Folk (1980) classification this is a lithic greywacke.

6.1.3 Upper Calcareous Member

The Upper Calcareous Member is composed of calcite, quartz, iron oxides, glauconite and mud matrix (Fig. 6.2). The minerals are sub-rounded, poorly sorted and is a silt to fine silt. It is classified as a lithic greywacke.

6.1.4 Te Uri Member

The Te Uri Member is composed of quartz, glauconite, plagioclase feldspar and minor mud matrix (Fig. 6.3). The minerals are sub-rounded, poorly sorted and is a sandy mudstone. Using Folk (1980) classification this is a litharenite.

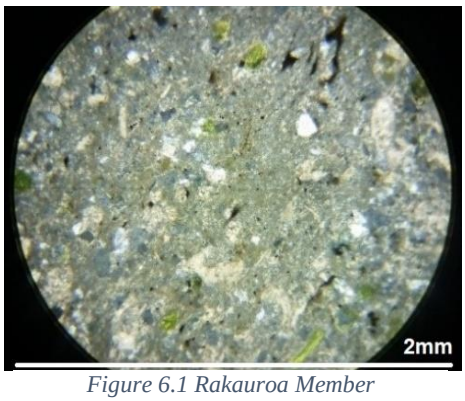

Figure 6.1 Rakauroa Member

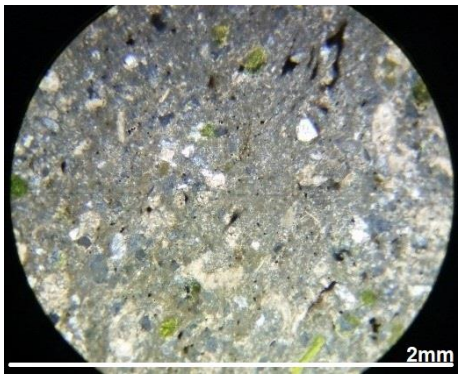

Figure 6.2 Upper Calcareous Member

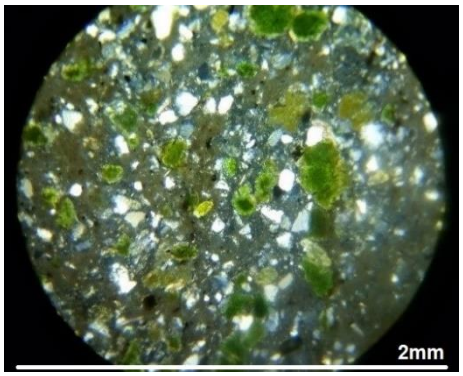

Figure 6.3 Te Uri Member

Figure 6.4Wanstead Glauconite

6.1.5 Wanstead and Wanstead Glauconitic Sand

The Wanstead Formation is composed of quartz, glauconite and calcite matrix whereas the Wanstead Glauconitic sand is largely made up of glauconite and quartz with some iron oxides (Fig. 6.4 & Fig. 6.5). Minerals are sub-rounded, and sorting is poor and is classed as a lithic greywacke.

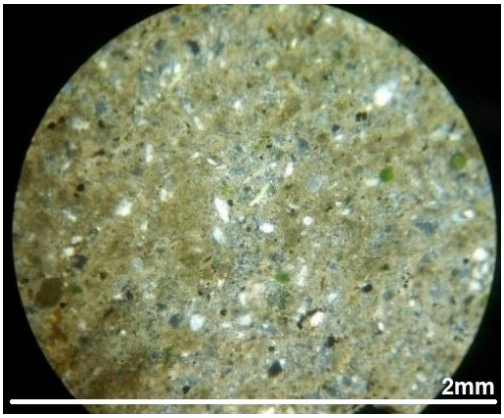

Figure 6.5 Wanstead

6.1.6 Weber Glauconitic Sand

Weber Glauconitic sand is composed of quartz, glauconite, and iron oxides (Fig. 6.6). Minerals are sub-angular, poorly sorted and is clast supported. It is a moderate to fine sand grain size and is classed as a litharenite.

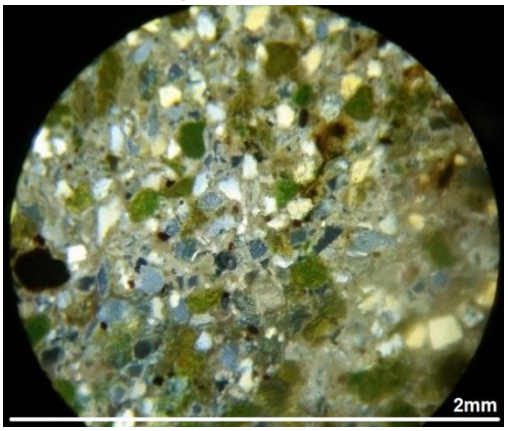

Figure 6.6 Weber Glauconitic Sand

6.1.7 Weber Limestone

Weber Limestone is composed of calcite matrix, quartz, plagioclase feldspar, iron oxides and glauconite (Fig. 6.7). Minerals are sub-rounded, moderately sorted and has a fine silt/clay grain size.

Figure 6.7 Weber Limestone

6.1.8 Weber Flysch

Weber Flysch has a sandstone and mudstone bedding (Fig. 6.8). The sandstone is composed of mostly quartz, plagioclase feldspar, glauconite, calcite matrix and iron oxides. The mudstone is made up of quartz, glauconite, plagioclase feldspar, biotite, and fossil shell fragments. Minerals are sub-angular and sub-rounded, moderately sorted and are fine sand or fine silt. Weber Flysch sand is classified as a sub-arkose and Weber Flysch Mud is classified as a sub-litharenite.

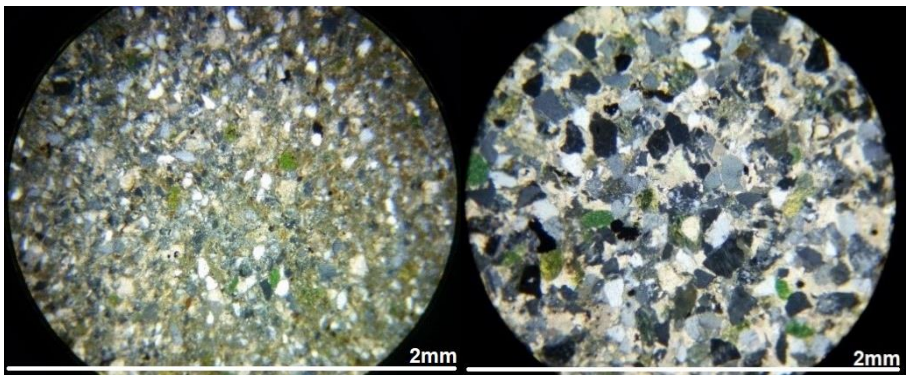

Figure 6.8 Weber Flysch Sand (right) and Weber Flysch Mud (Left)

6.1.9 Ihungia

The Ihungia Formation is composed of quartz, calcite, glauconite, pyrite and mud matrix (Fig. 6.9). Minerals are sub-rounded, moderately poorly sorted and are fine silt. It classed as a lithic greywacke and its fabric is near homogenous.

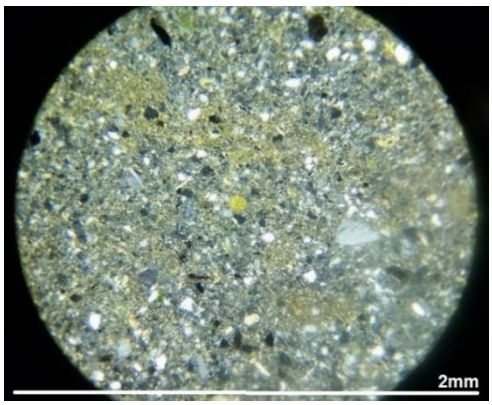

Figure 6.9 Ihungia

6.1.10 Whakataki

The Whakataki Formation consists of bedded sandstone, organic-rich mudstone and mudstone (Fig. 6.10 – Fig. 6.12). The sandstone is made up of quartz, glauconite, iron oxides, organic matter and clay matrix. The minerals are sub-rounded, poorly sorted and clast supported. There is no obvious granular orientation and is a fine sand grainsize. The organic rich mudstone is made up of the same minerals as the sandstone but has a higher organic matter, clay matrix content and lower glauconite; quartz grains are also significantly smaller. The organic matter is strongly orientated and is visible to the naked eye. The mudstone component also is made up of the same minerals but contains more quartz and clay matrix and less organic matter. Minerals are more rounded and more sorted than the sandstone and organic rich mudstone. Whakataki is classified as a sub-litharenite.

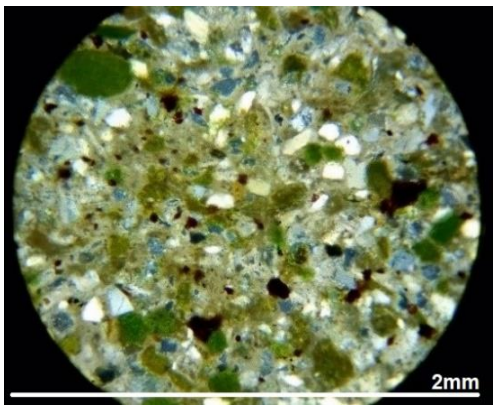

Figure 6.11 Whakataki Sandstone

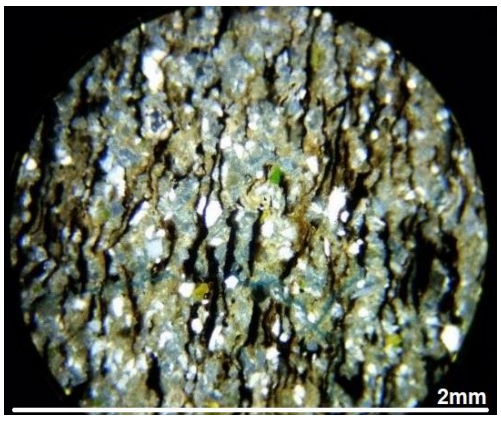

Figure 6.10 Whakataki Organic rich mudstone

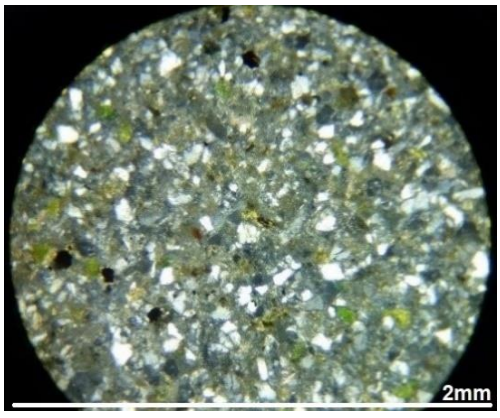

Figure 6.12 Whakataki mudstone

6.1.11 Tutamoe

The Tutamoe Formation consists of bedded fine sandstone and fine siltstone (Fig. 6.13). Both lithologies contain quartz, glauconite, calcite, organic matter and iron oxides. The mudstone contains more opaque material, glauconite and matrix than the sandstone. Minerals are sub-rounded, have no orientation and is classed as a lithic greywacke. Sorting is moderately and the rock has a homogenous fabric.

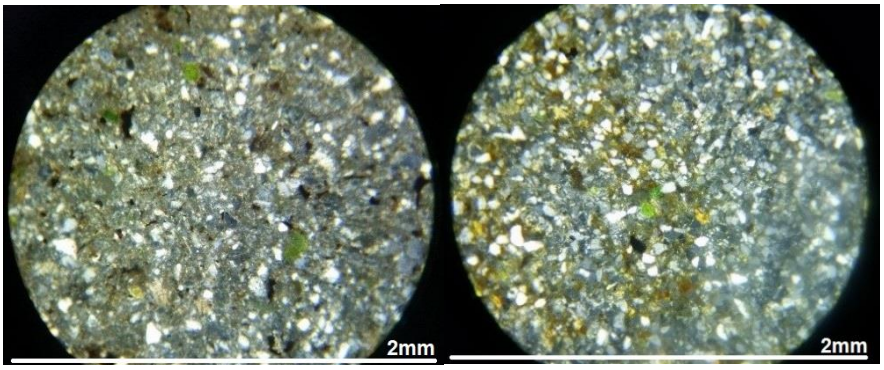

Figure 6.13 Tutamoe Mudstone (left) and Tutamoe fine sandstone (right)

6.1 12 Riddells Mudstone

Riddells Mudstone is made up of quartz, calcite, glauconite, organic matter and mud matrix (Fig. 6.14). Minerals are sub-round and are poorly sorted. The fabric is homogenous, medium silt grain size and classed as a litharenite. The minerals are matrix supported and

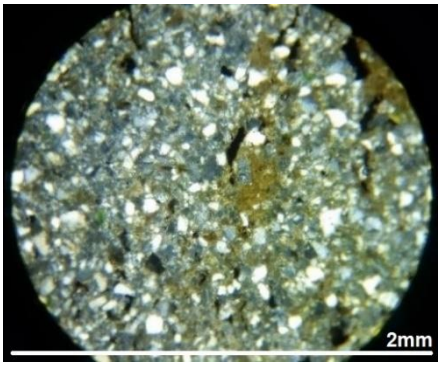

Figure 6.14 Riddells mudstone

6.1.13 Riddells Culvert

Riddells Culvert is a bedded fine sandstone and fine siltstone (Fig. 6.15 & Fig. 16). The sandstone consists of mostly quartz as well as calcite, glauconite, plagioclase feldspar and the siltstone are made up of quartz, calcite, glauconite and silt matrix. Minerals are sub-rounded, moderately to poorly sorted and have no orientation. The sandstone is clast supported whereas the siltstone is matrix supported.

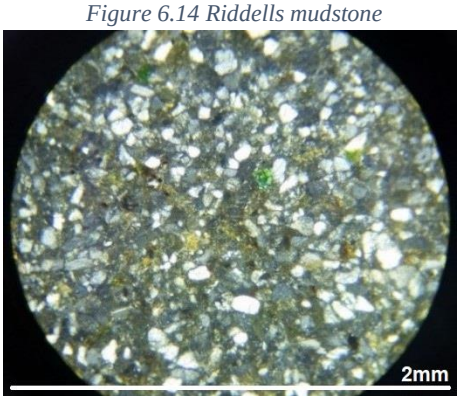

Figure 6.16 Riddells Culvert sandstone

Figure 6.15 Riddells Culvert mudstone

6.1.14 Franklin Road

Franklin Road is made up of bedded sandstone and fine siltstone (Fig. 6.17). The sandstone is composed of quartz, glauconite, and calcite/fossil material and is poorly sorted whereas the siltstone also contains organic matter and is moderately sorted. The sandstone is patchy and has two lithologies where grain/mineral size dramatically changes from a clast supported moderate sandstone to matrix supported fine sandstone. The fine siltstone also contained visible fossil material, such as foraminifera. Neither of the Franklin Road lithologies show orientation. The sandstone is classified as a lithic greywacke and siltstone as a greywacke.

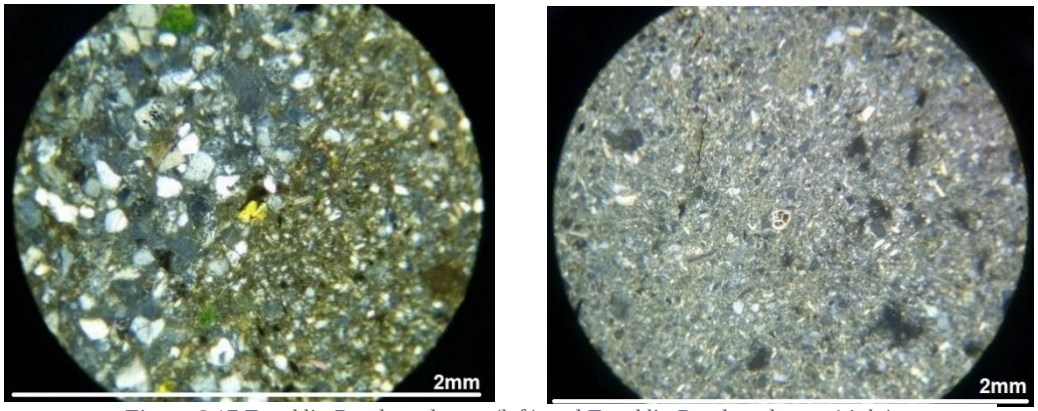

Figure 6.17 Franklin Road sandstone (left) and Franklin Road mudstone (right)

6.1.15 McCartie Sandstone

The McCartie Sandstone is composed of mostly quartz, plagioclase and potassium feldspar, biotite, calcite and glauconite (Fig. 6.18). Mineral grains are sub-angular to sub-rounded, clast supported and has no orientation. Sorting is poor and is classified as a sub-arkose.

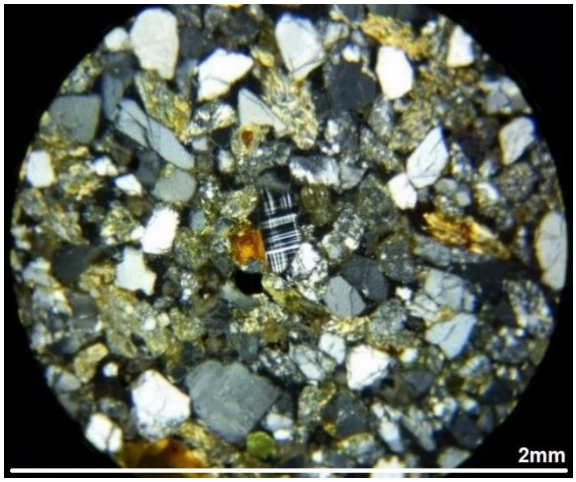

Figure 6.18 McCartie Sandstone with a central potassium feldspar

6.2 Point Counting

Point counting minerals from thin section is a powerful tool for quantifying mineralogy and possible sediment provenance usually determining and indicating maturity. Maturity indicates whether minerals have been altered physically or chemically. The crystallinity (mono or poly) and undulosity of quartz were noted as well as other minerals found in the thin sections (Appendix Five). Quartz and feldspar are the most common components of most samples other than glauconite dominant in some samples. The proportion of potassium feldspar is low compared to plagioclase feldspar. Biotite mica and calcium carbonate (matrix and fossils) are found in the sandier lithologies whereas glauconite and opaque minerals (pyrite, magnetite) are found in most samples. Most samples contain tiny mineral fragments that could not be identified under the microscope. Because quartz is a robust mineral resistant to weathering, it is the dominant mineral found in most samples, and less weathered samples contain more feldspar. Most mudstones share similar mineral types and are homogenous whereas sandstones display more varied mineralogy.

6.2.1 Quartz, feldspar and lithics (QFL)

Point counting was performed on 24 thin sections; 300 points were counted from each thin section in order to quantify mineralogy (Fig. 6.19). Quartz undulosity was recorded as either greater or equal to and less than five degrees as well as its degree of crystallinity (monocrystalline, polycrystalline 2-3 units per grain or more than three units per grain). Other minerals that were present were also recorded. From these data QFL, and Basu Quartz diagrams were plotted.

The higher proportion of quartz and lithics and a lesser proportion of feldspar show a cluster of points in the mid to upper pole of the QFL diagram. Miocene aged samples display a wider compositional range whereas Late Cretaceous samples are clustered together. When comparing the QFL diagram of this research to Dickinson et al. (1983), the results indicate a mostly recycled orogen provenance and continental block provenance. A continental block provenance is defined as a platform or shield or a faulted basement block whereas a recycled orogen provenance is defined as a source which is deformed and uplifted due to subduction zones, collision orogens and foreland of fold-thrust belts which is seen structurally for the ECB.

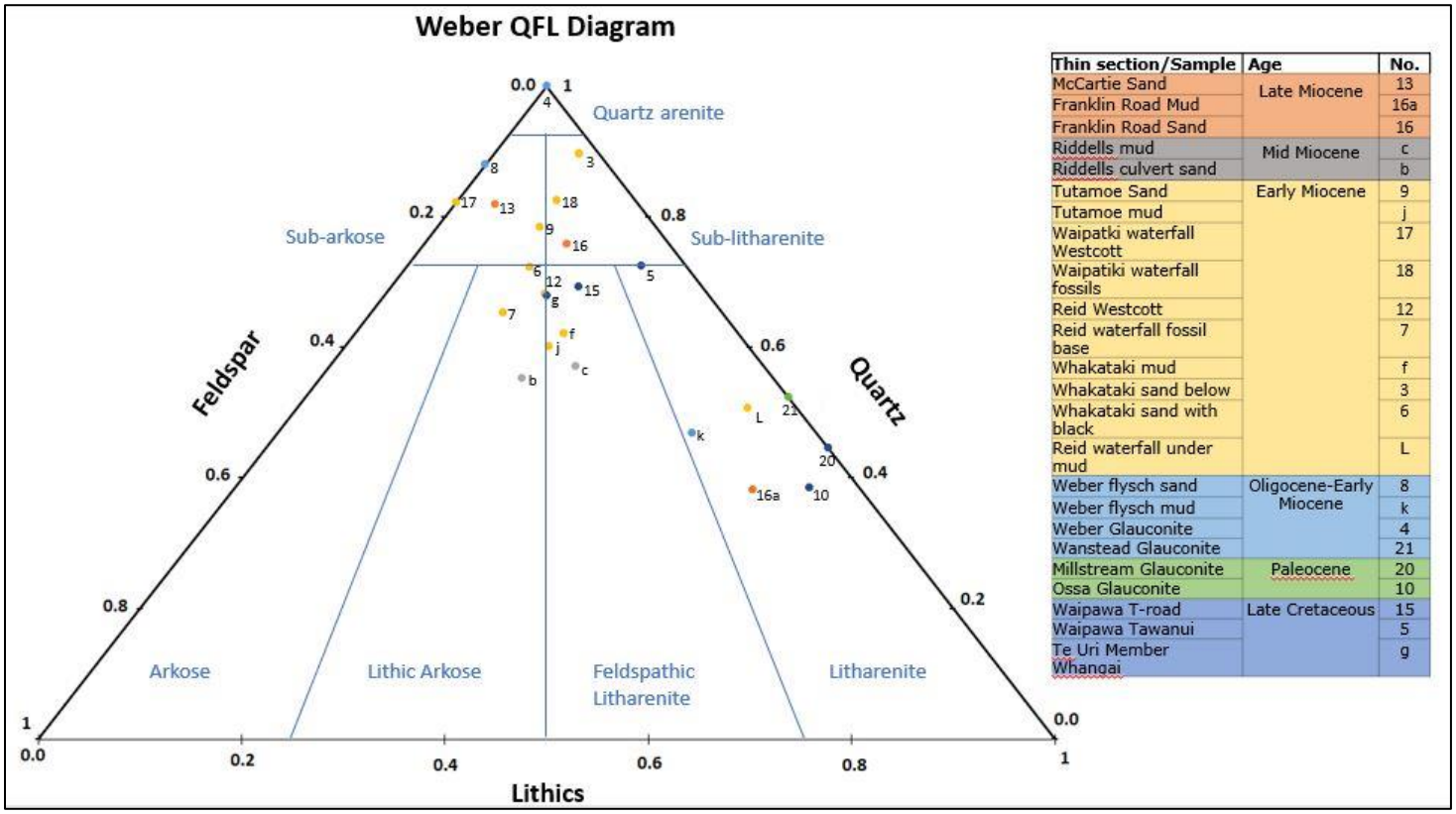

Thin section/Sample	Age	No.
McCartie Sand	Late Miocene	13
Franklin Road Mud		16a
Franklin Road Sand		16
Riddells mud	Mid Miocene	c
Riddells culvert sand		b
Tutamoe Sand	Early Miocene	9
Tutamoe mud		j
Waipatki waterfall Westcott		17
Waipatiki waterfall fossils		18
Reid Westcott		12
Reid waterfall fossil base		7
Whakataki mud		f
Whakataki sand below		3
Whakataki sand with black		6
Reid waterfall under mud		L
Weber flysch sand	Oligocene-Early Miocene	8
Weber flysch mud		k
Weber Glauconite		4
Wanstead Glauconite		21
Millstream Glauconite	Paleocene	20
Ossa Glauconite		10
Waipawa T-road	Late Cretaceous	15
Waipawa Tawanui		5
Te Uri Member Whangai		g

Figure 6.19 Weber QFL diagram regards to Folk classification (Folk, 1980).

6.2.2 Basu Quartz Diagram

The ratio of mono- to polycrystalline undulatory to non-undulatory quartz were recorded. Samples showed mostly polycrystalline undulatory quartz that contains more than three units per grain or quartz that are monocrystalline; there was no polycrystalline quartz with 2-3 units per grain. The Basu Quartz diagram (Fig. 6.20) results of this study show that in all samples the quartz to be derived from a low-rank metamorphic source, therefore that the rock units have not faced significant metamorphic strain due to not being tectonized enough or deep enough in the crust for the quartz to be altered. This further supports that the rock unit provenance is from pre-existing rock sediment of the Gondwana margin.

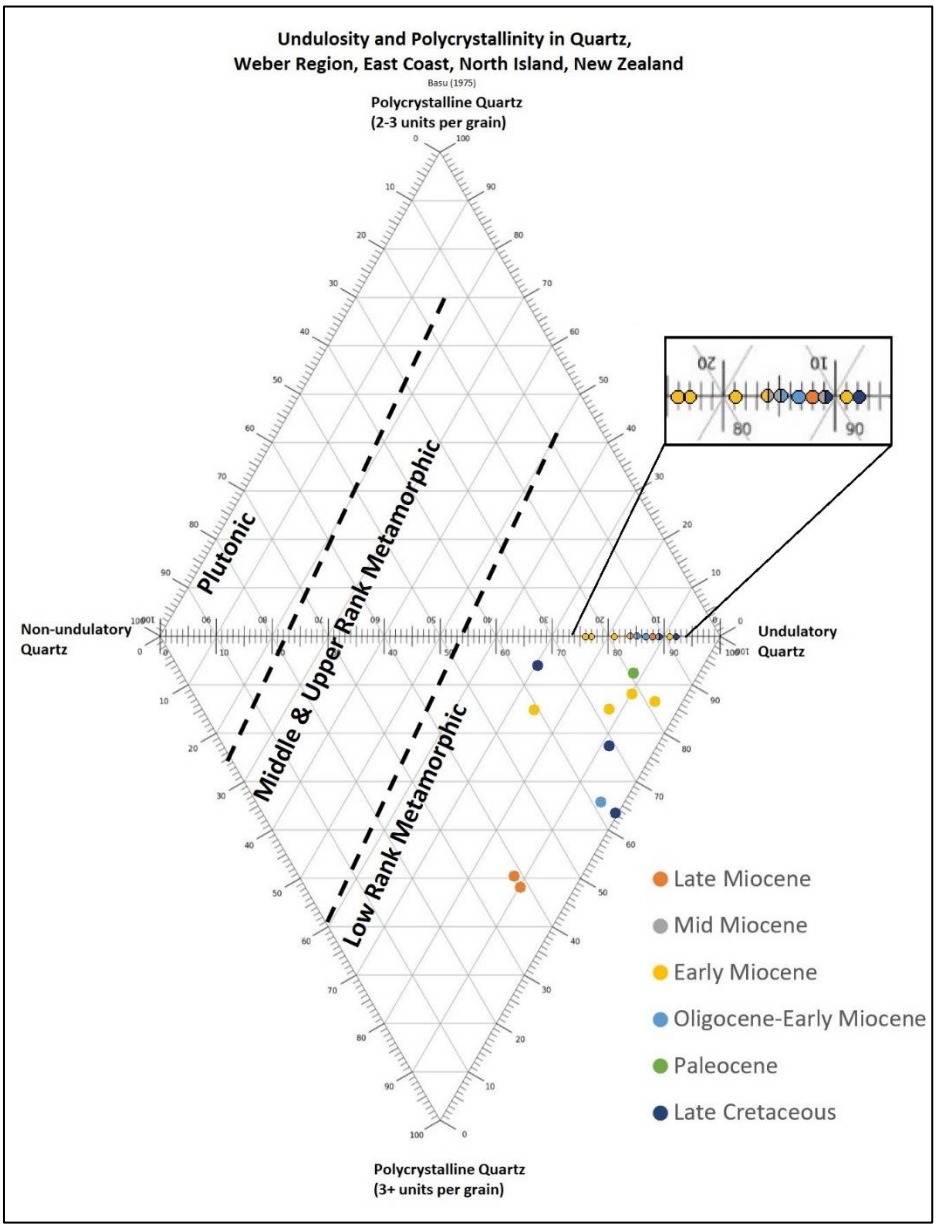

Figure 6.20 Diagram showing this studies Quartz data applied to Basu et al. (1975)

6.3 X-ray Fluorescence (XRF) and Provenance

XRF data can be used to show indications of provenance and sedimentary processes. By comparing terrane data with the element mobility and composition, a greater understanding of how the rock unit formed and processes that were operating is achieved. All 35 samples were scanned after preforming LOI measurements (burning off organic matter and calcium carbonate – see earlier), and the results were calcium carbonate corrected, and the data also was normalised to Upper Continental Crust (UCC) (Gaschnig et al., 2014) (where most of the sediments were derived from) by Matt Sagar (GNS). When describing the XRF results, samples that are significantly glauconitic or are recognised as shell-fragment-based limestones, are often referred to as outliers due to input from glauconitic sand (iron and other elements) or calcite (CaO). Terrane data was compared and referenced from Palmer et al. (1995) and Price et al. (2015).

6.3.1 Major Elements

Major element data presented in Appendix Six have moderate to high SiO_2 content (46.47%-84.7%) with the exception of the Plio-Pleistocene limestones (28.8%-2.81%). Nearly all samples are Fe_2O_{3T} depleted, but range in value from 1.86% to 12.71% (higher percentages are due to glauconite rich samples) as well as MgO depleted (0.6% to 2.08%) when compared to the UCC average. All samples are also moderately depleted of TiO_2 (0.13%-0.445%) and Al_2O_3 (values vary from 2.25%-9.42%, with the average of 3.64% excluding outliers (Waipawa Glauconite (12.16%) equivalent and Wanstead Glauconite (12.71%)).
As shown in figure 6.21, major element levels change with time, the most obvious being the decrease in most element concentrations in the Te Uri Whangai member likely due to the K/T impact. The also is an increase of concentration of calcium carbonate during the time of the Weber deposition, a decrease with the Tutamoe and increase during the Plio-Pleistocene when the limestones were deposited. SiO_2 slightly decreases with time whereas most other elements fluctuate and overall increase in concentration during the majority of the Miocene, (except during the time of McCartie units where elements slightly increase) compared to the Cretaceous and older periods. There also is a slight increase during the deposition of Riddells mud followed by a decrease during the deposition of Riddells Culvert.

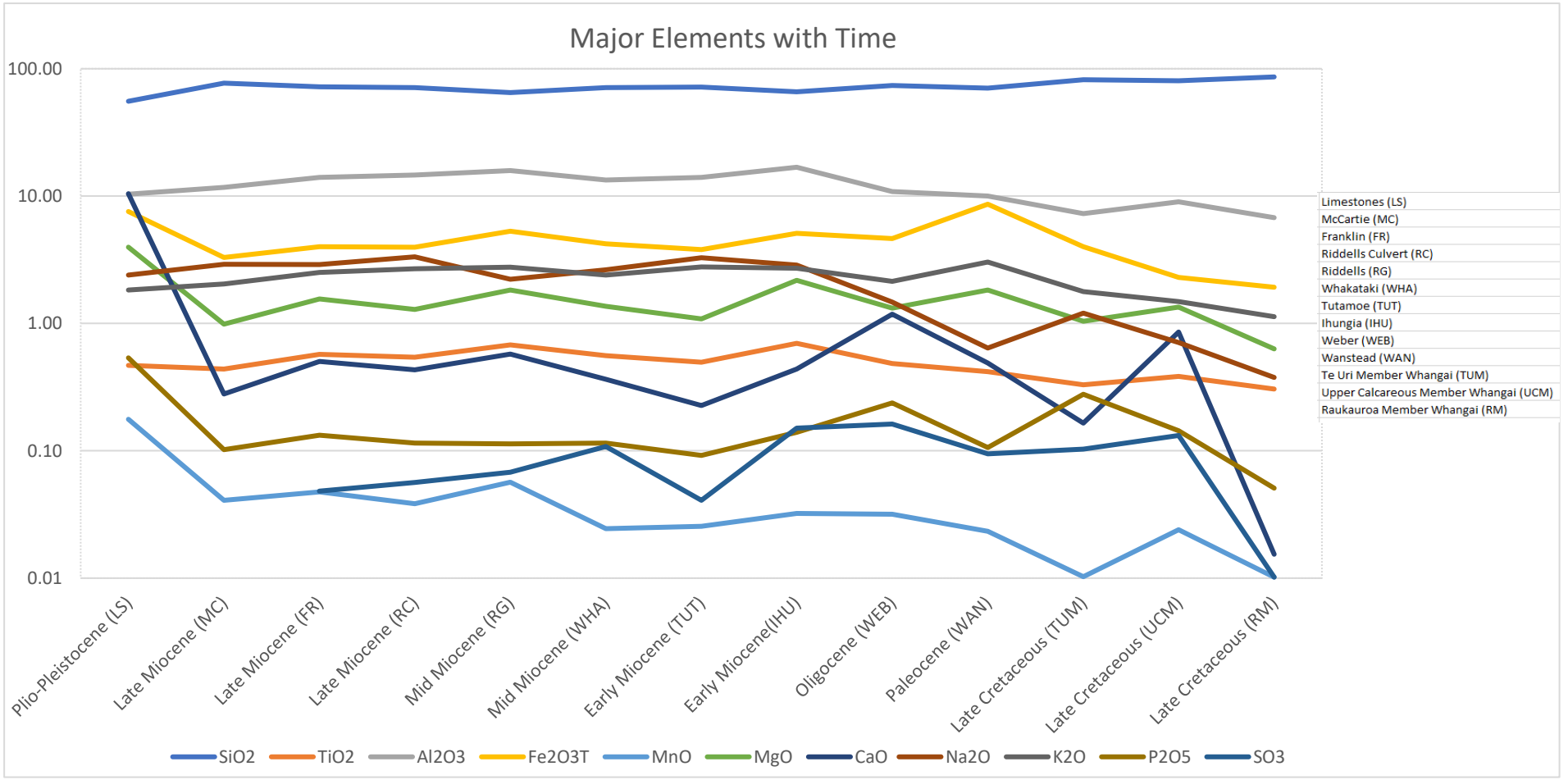

Figure 6.21The major elements with time found in the Weber mapping area

6.3.1.1 Chemical Indication of Alteration (CIA) and $Al_2O_3 + CaO^* + Na_2O + K_2O$ (ACNK)

CIA/ACNK uses molecular proportions (wt%/molecular weight) of Al_2O_3 , $CaO+Na_2O$ and K_2O plot to show the degree of weathering of siliciclastic material(Fig. 6.22) (Nesbitt et al., 1982). CIA is calculated by the following formula:

$CIA= (Al_2O_3 /(Al_2O_3 +CaO^*+Na_2O+K_2O)) *100$

CaO^* = Carbonated corrected (a strong carbonate signature can skew CIA)

CIA values range from 17.41 (limestone) to 78.91 and have an average of 63.27 excluding glauconite and limestone outliers or 59.47 including all samples. Higher the CIA value the more weathering has occurred and values less than 50 are classified as unweathered. This indicates that rock units of the Weber area are composed of slightly to moderately weathered sediment. Furthermore, the older the unit is, the more typically weathered it is, which is shown by the age gradient of point clusters along the weathering trend line.

Weathering is the alteration of sensitive minerals (i.e. feldspar and mica) to clays, and this is shown on the ACNK plot (Fig. 6.22). When comparing the results from this study to McLennan et al. (1993) it indicates a strong weathering trend and Upper Continental Crust (UCC) relationship. The XRF data was later normalised to UCC parameters due to the close correlation. There also is a noticeable glauconite and calcite effect which skews plotted points away from the overall correlation such as Plio-Pleistocene and Waipawa equivalent units. Because glauconite naturally contains higher levels of potassium (K), the CIA value is higher than expected.

The UCC and weathering trend is in between the andesite and rhyolite composition which indicates a dacitic composition. When comparing to McLennan et al. (1993), there is a clear indication that the samples are of a weathering shale composition which is transitioning to illite/clay with time.

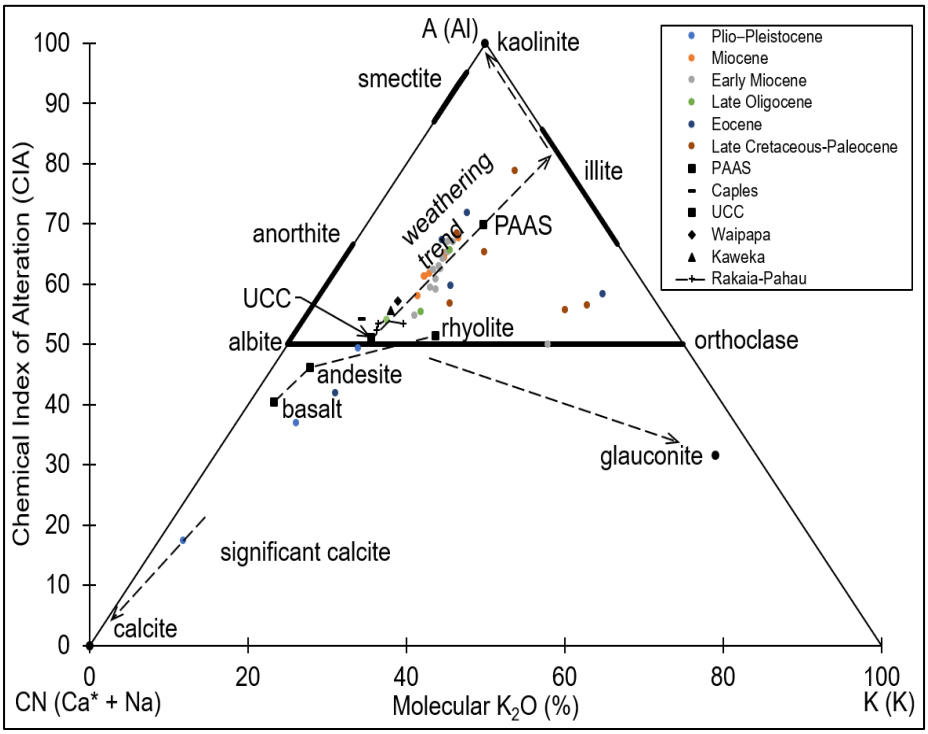

Figure 6.22 ACNK/CIA weathering plot

6.3.1.2 Function One-Function Two (F1-F2)

A F1-F2 plot identifies terrane type by grouping samples based from standard data (previous New Zealand terrane data to differentiate provenance. Roser et al. (1988) applies unstandardized discriminant function coefficients to major element data to calculate F1 and F2 to classify data. This plot (Fig. 6.23), like the CIA/ACNK plot shows a glauconite and calcite effect due to being diagenetic and a dacite derivation; the samples are derived from a Rakaia and Pahau (Torlesse Composite) Terrane. The likely glauconite effect gives the impression that the samples are derived from the Greenland Group (Buller Terrane).

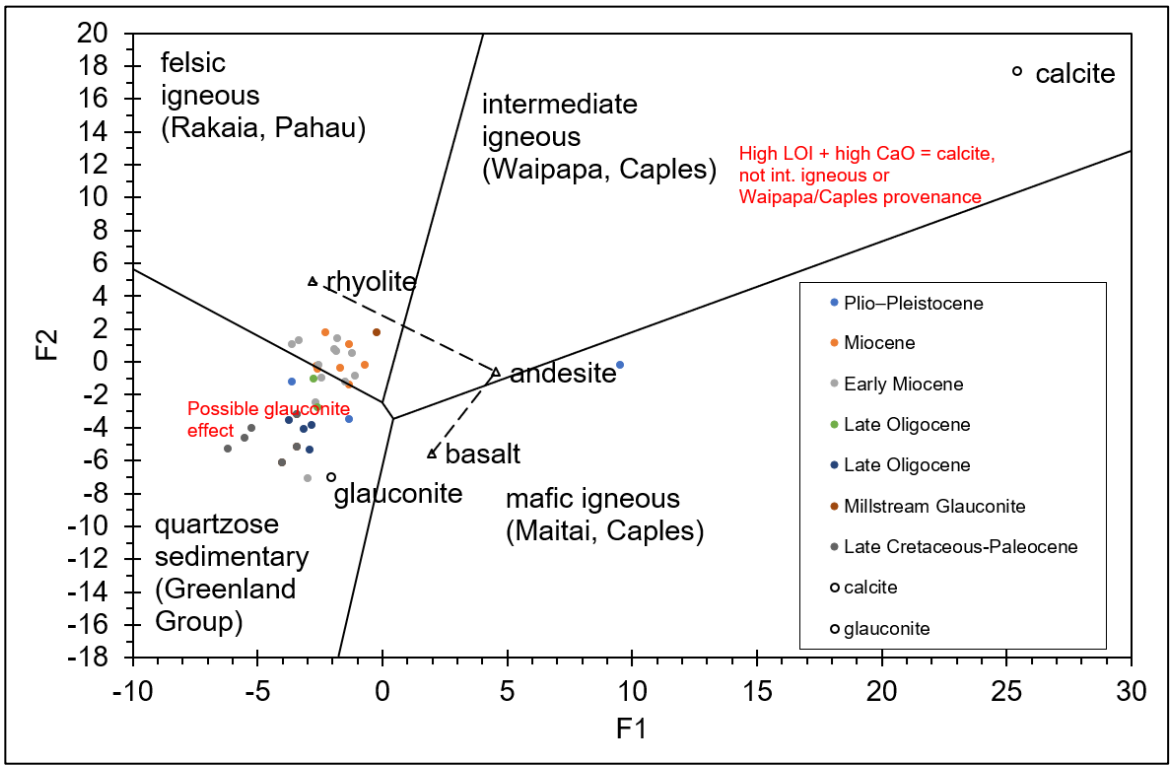

Figure 6.23 Weber F1 and F2 plot results

6.3.2 Trace Elements

Trace elements, rare earth elements (REE) and high field strength elements (HFSE) are typically immobile below surface conditions and reflect the tectonic setting and provenance. Mobile or easily weathered elements such as K, Na, Mg, Sr, Rb, U, Ba, and Ca show significant variation whereas elements such as Ti, Zr, Nb, Y, Th, Sc and REE's are more durable and are more consistent (immobile). Mobile elements can be present for several environmental reasons and not reflect provenance. Most samples when compared to the UCC average are slightly depleted of Th with the range of 3-70pmm (limestones have high ppm) but have an overall average of 6ppm excluding outliers. Samples are also depleted in Sr, P, Sc, Cr and Nb. The samples show a Zr range of 0ppm to 491pmm and has a similar average compared to UCC of 192pmm excluding outliers. There also is an enrichment of Ti, Nb, and Ce. When observing immobile elements with time (Fig. 6.24), like the major elements with time, there is a notable decrease at the end of the Late Cretaceous and Paleocene, presumably due to the K/T event. During Early Miocene there in an increase of immobile elements and a slight decrease towards the end of the Miocene. There also is a decrease of immobile elements during the Oligocene. The following ratio graphs present data from this study that are applied to Bhatia et al. (1986) ratio concepts of element mobility. The resulting graphs are also compared to New Zealand terrane from Palmer et al. (1995) and Price et al. (2015) in order to provide a provenance overview. Each terrane has an immobile element ratio signature, so by comparing ratios of this study to previous terrane data, preliminary provenance comparisons and interpretations can be made.

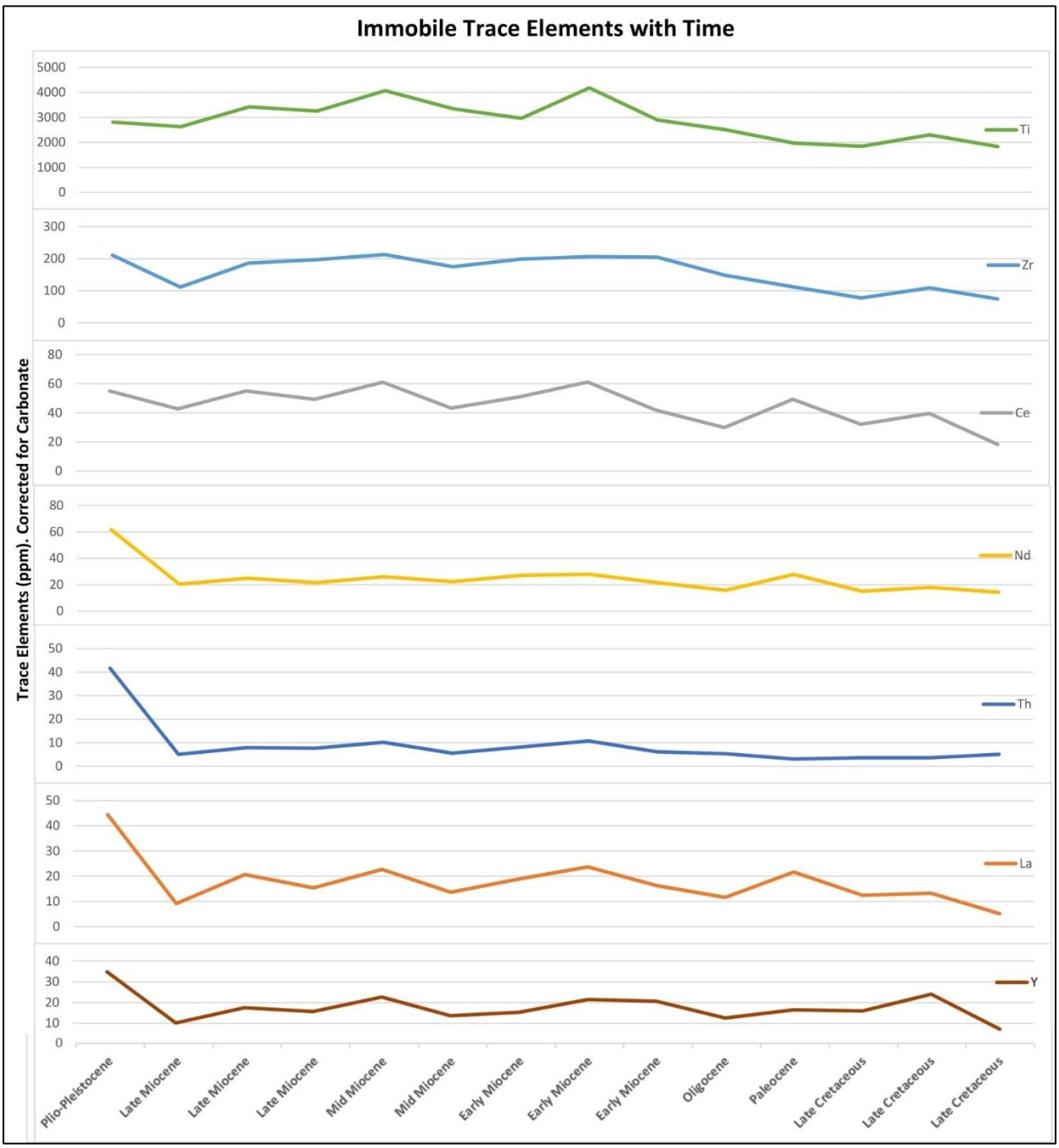

Figure 6.24 Immobile trace elements with time. The impact of the K/T event is seen by a reduction of most element concentrations (towards the end of the Late Cretaceous) with a later decrease during the Oligocene (reduction of deposition) to a wavering increase until the Late Miocene where Immobile concentrations increase with increased deposition with the activation of the

6.3.2.1 Spider Diagrams

The UCC normalised data is used to plot provenance, weathering and sedimentary processes and shows either a depletion or excess of an element compared to the UCC standard (Fig. 6.25 – Fig. 30). This also shows the mobility (or lack of) for trace elements and are compared to terrane data to show sedimentary process correlation. Samples are grouped together to show variation with time and enrichment and depletion are shown in relation to the value of one. The availability for substitution of trace elements to a major element within a mineral is shown on the x-axis (shown from compatible to incompatible). Incompatible elements are depleted in the mantle but enriched in the continental crust and vice versa.

When comparing units that were deposited during a common geological stage, commonalities and variation is observed, for example, during the Late Cretaceous and Paleocene Th values were very similar but P and Cr (Fig. 6.26) were variable. Variation or lack of trend shows changes of depositional input during that time which is shown with incompatible elements during the Early Miocene but shows a common trend for compatible elements. For the Eocene, since there were very different lithofacies deposited this is reflected in the spider diagram. This trace element data is also reflected to known terrane data to determine provenance.

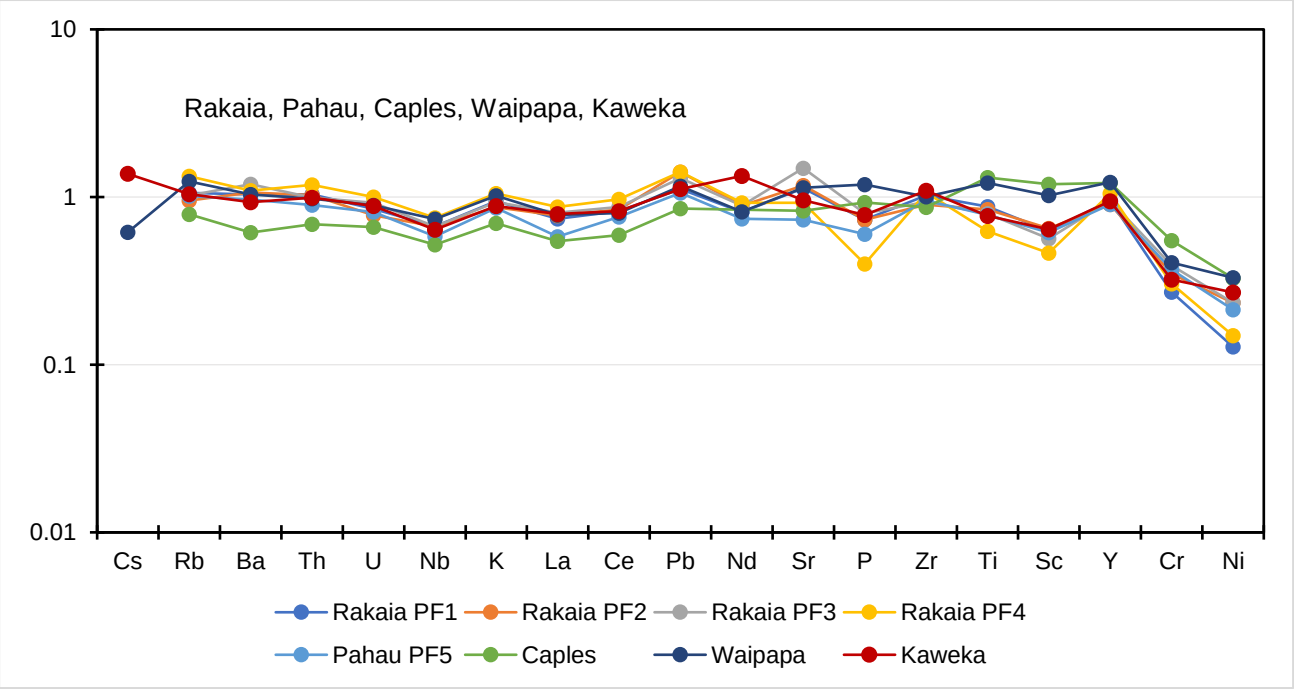

Figure 6.25 New Zealand terrane spidergram plot

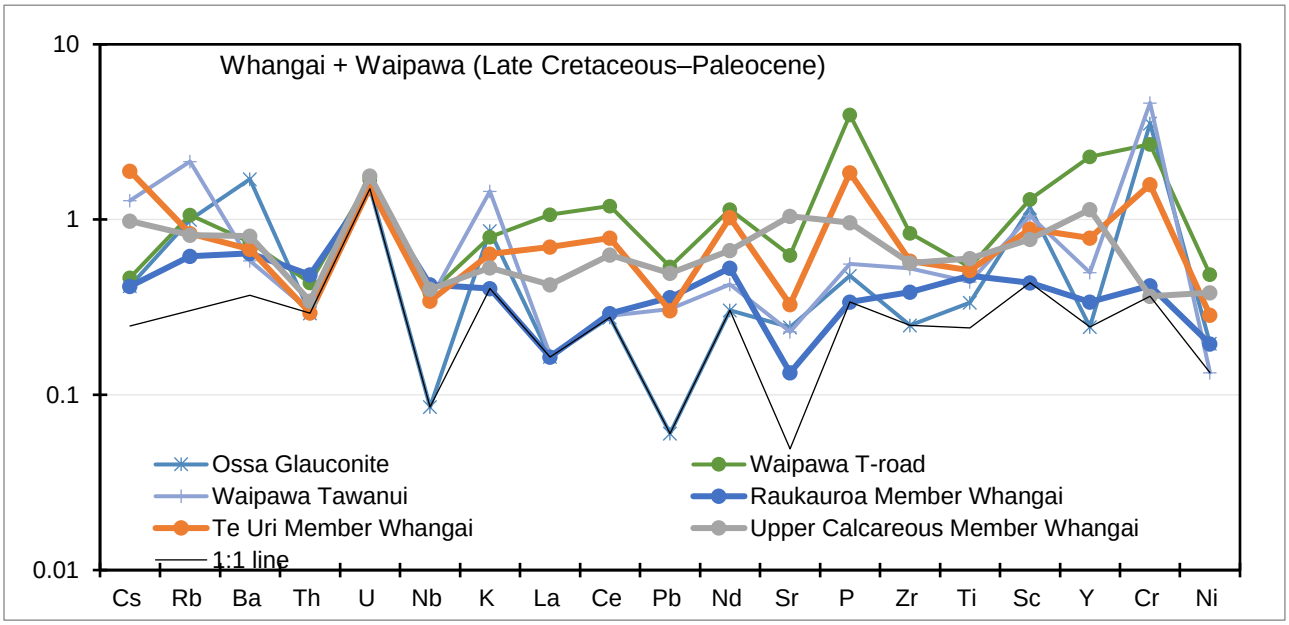

Figure 6.26 Weber area Whangai and Waipawa spidergram

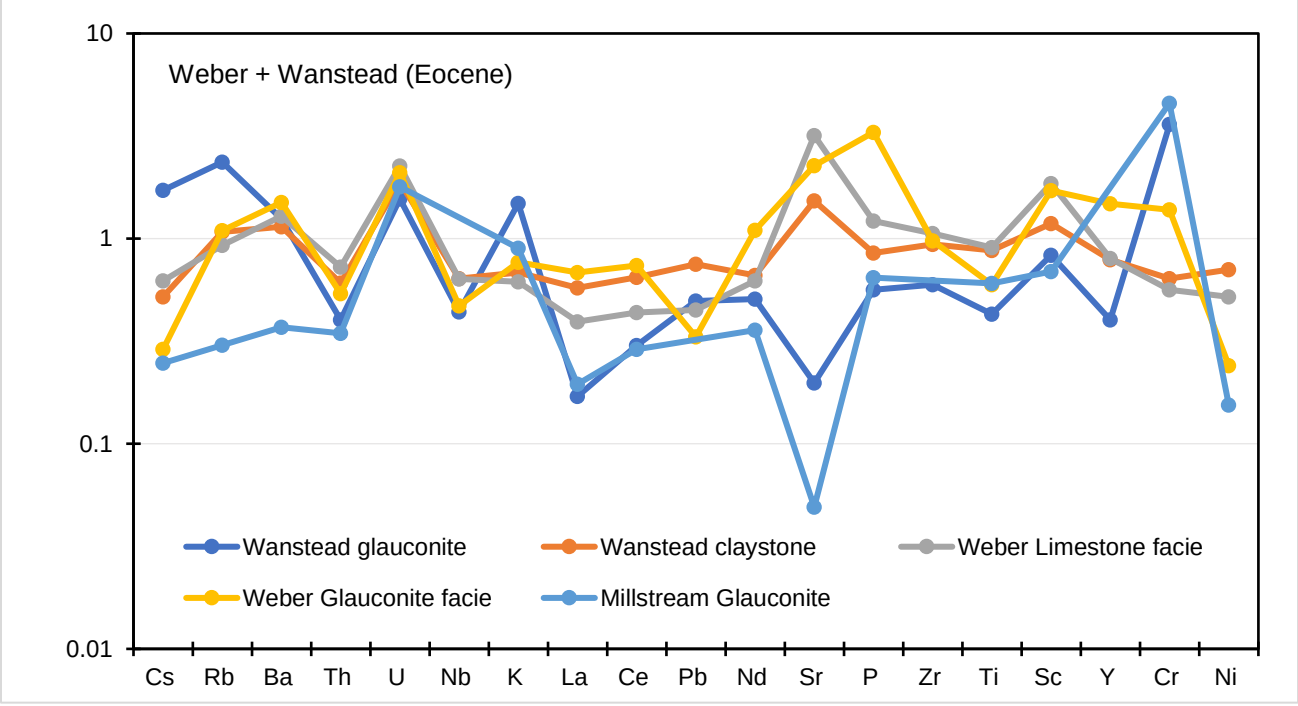

Figure 6.27 Weber and Wanstead spidergram

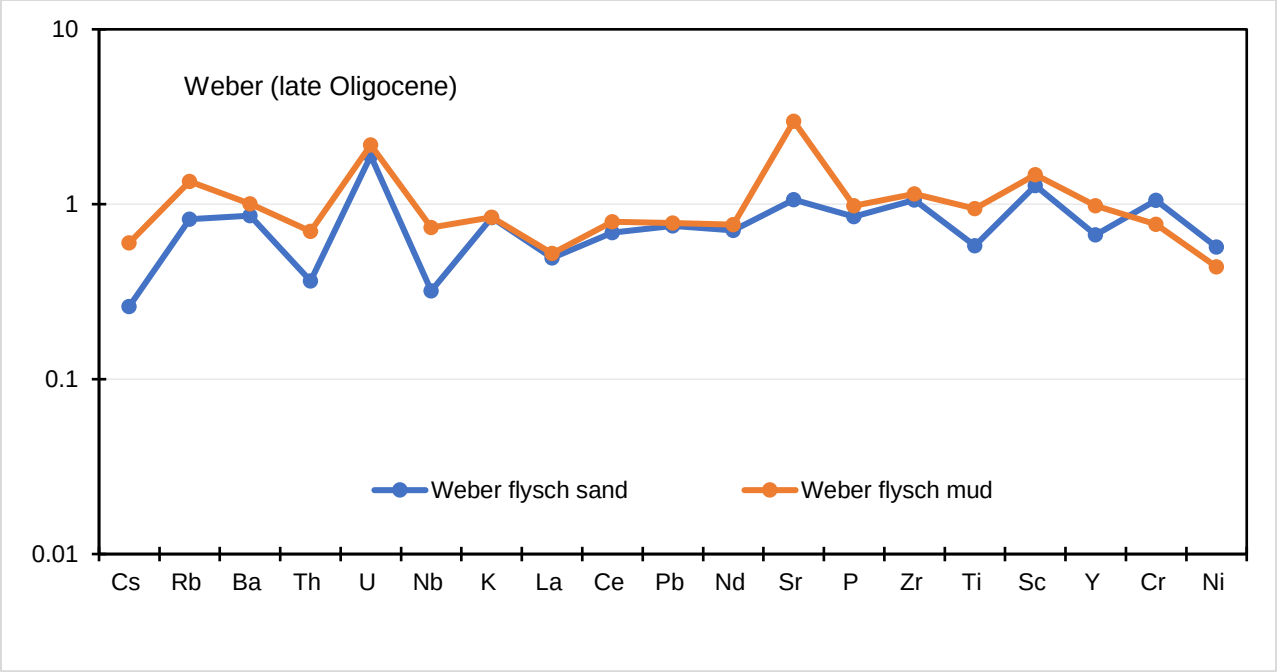

Figure 6.28 Weber flysch spidergram

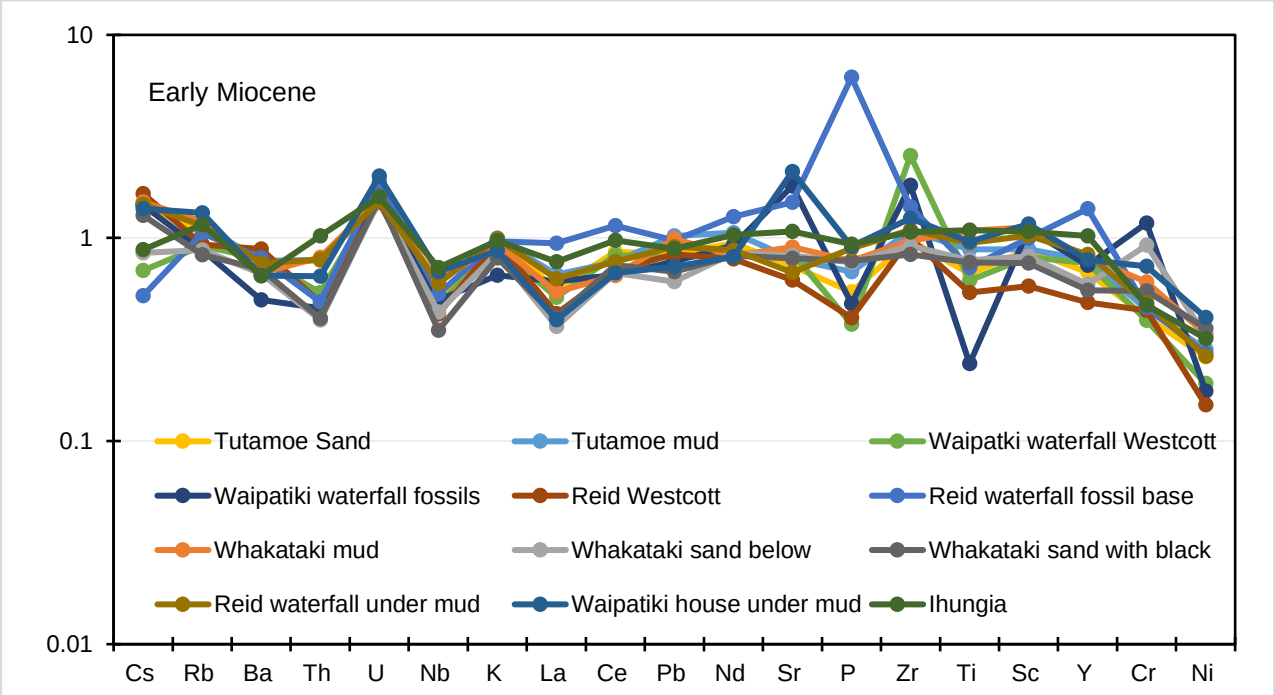

Figure 6.29 Early Miocene spidergram

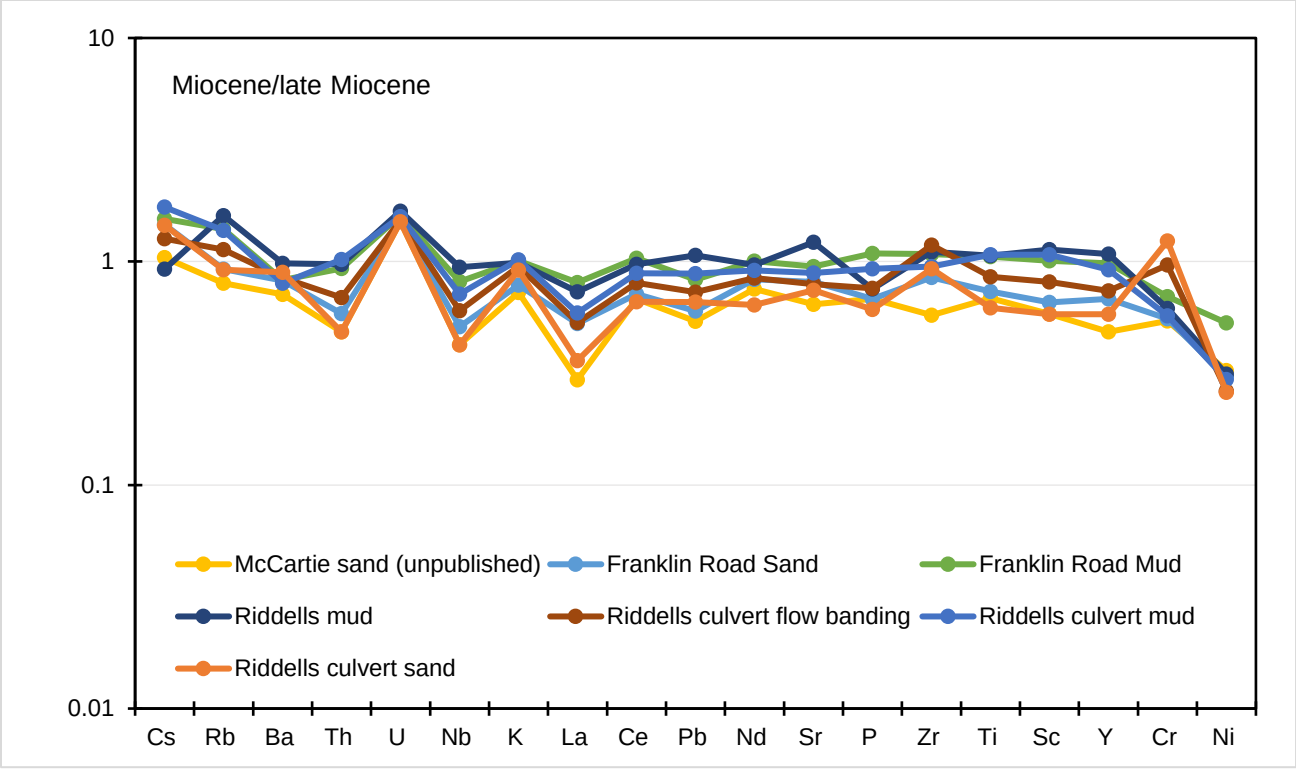

Figure 6.30 Middle to Late Miocene spidergram

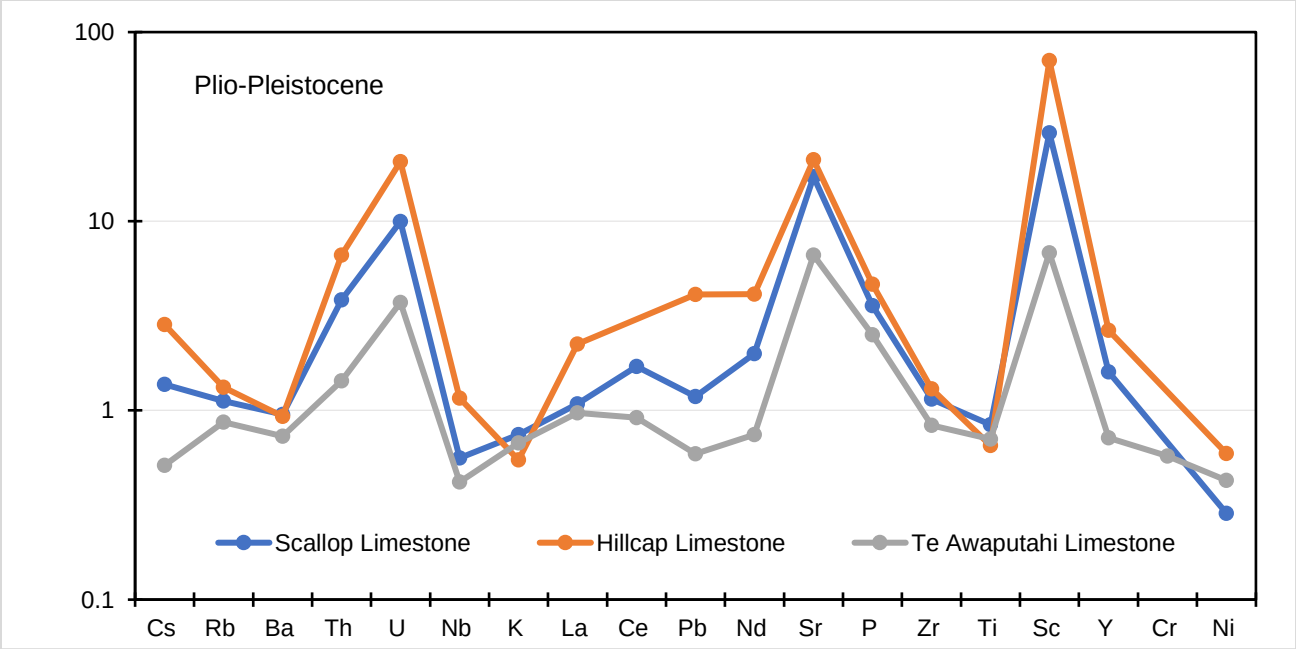

Figure 6.31 Plio-Pleistocene spidergram

6.3.2.2 La-Th

For this study La ranges from 5.09 to 69.62ppm with an average of 18.31 as well as Th ranges from 3.07 to 69.62 with an average of 9.14ppm (Fig. 6.32).The La/Th ratio average is 2.648ppm and this typical for continental island arc greywackes (2.4±0.3) as shown in Bhatia et al. (1986). When compared to terrane data, Rakaia-Pahau (Th 10.78ppm, La 23.4ppm) has the closest correlation with overall ratio averages.

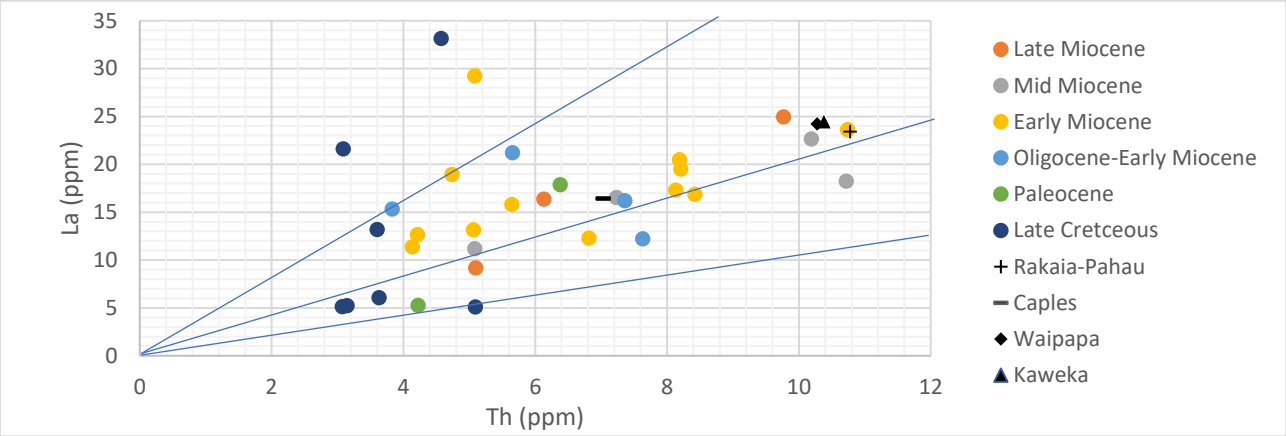

Figure 6.32Weber La/Th provenance plot

6.3.2.3 Th-Zr

Greywackes typically have a positive Th and Zr correlation (Bhatia et al., 1986). Th values range from 3.07 to 69.63ppm with an average of 9.14ppm whereas Zr values range from 0ppm (glauconite outlier) to 491.15ppm and have an average of 186.53 including outliers (Fig. 6.33). According to Bhatia, continental island arc Zr/Th ratios are between 10 and 35ppm and the Zr/Th ratio average for this study is 29.79ppm. When compared to terrane data, Rakaia-Pahau (Th 10.5ppm, Zr 193) has the closest correlation of the overall ratio averages.

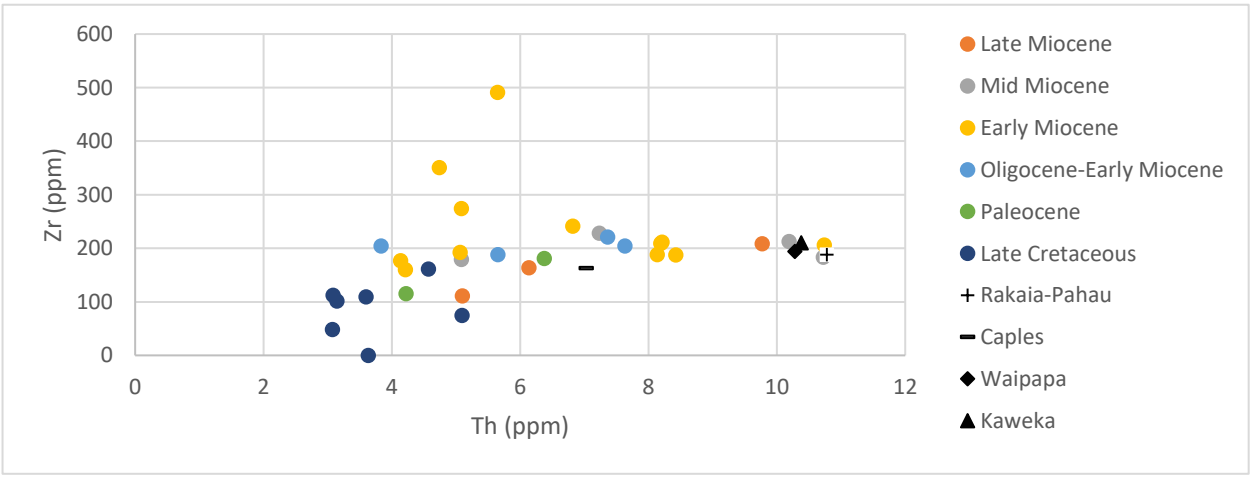

Figure 6.33 Weber Zr/Th provenance plot

6.3.2.4 Ti/Zr-La/Sc

Continental island arcs typically have a Ti/Zr ratios between 10 and 35 and a La/Sc ratio between 1 and 3 (Bhatia et al., 1986). This study has Ti/Zr ratios between 2.63 and 26.77 and an average of 16.1, as well as La/Sc ratios between 0.07 and 2.09 and an average of 1.09 (Fig. 6.34). When comparing terrane data ratios, Waipapa (La/Sc 1.69, Ti/Zr 23.91) has the closest match to the overall ratios.

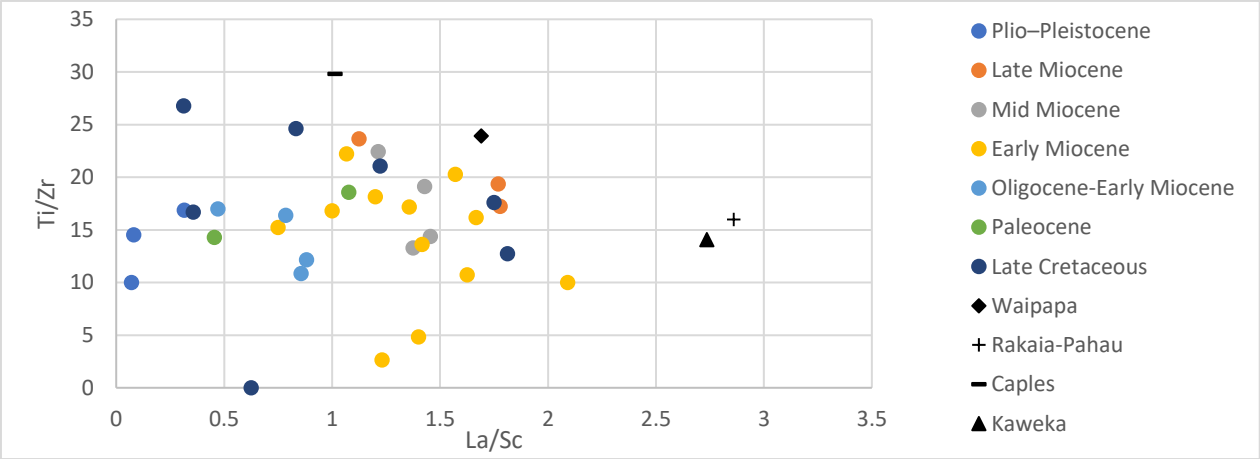

Figure 6.34 Weber Ti/Zr-La/Sc plot

6.3.2.5 La/Y-Sc/Cr

Continental island arc's typically have La/Y ratios between 0.5 and 1.0 and Sc/Cr ratios between 0.2 and 0.4 (Bhatia et al., 1986). This study has La/Y ratio from 0.5 to 2 and an average ratio of 1, as well as Sc/Cr ratios between 0.02 and 1.8 with an average of 0.25 (Fig. 6.35). When comparing terrane data, Waipapa (La/Y 0.94, Sc/Cr 0.38) has the closest match to the overall ratio averages.

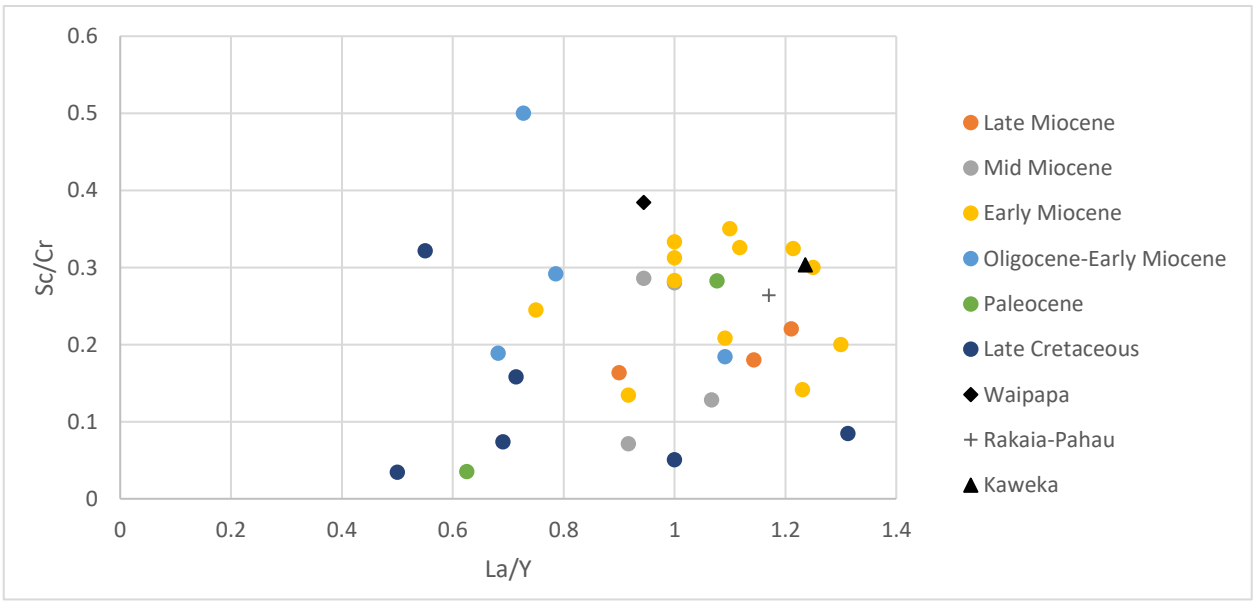

Figure 6.35 Weber Sc/Cr-La/Y plot

6.4 Petrology and Provenance Summary

- The QFL plot indicates a mixture of Lithic Arkose, Feldspathic Litharenite and both sub – Arkose and sub-litharenite rock with a cluster of Litharenitic samples. These results show that there is a significant proportion of quartz with some lithic material and minor feldspar. This indicates that the source material is quartz rich and the samples have a feldspar and lithic sub-componentry.
- As shown by the adapted Basu et al. (1975) Quartz diagram, the quartz reflects a recycled orogen and low metamorphic rank, therefore mild tectonic influence and supports a crustal surface correlation.
- As shown by the CIA/ACNK plot the geology is moderately weathered.
- All plots show a glauconite and calcium carbonate influence on element plots due to a geological alteration or specific depositional environment.
- There is a decrease of immobile and mobile elements during the end of the Late Cretaceous and Paleocene which is likely due to the K/T event.
- During the Miocene, due to tectonic activation, the input of immobile elements increased and fluctuated whereas during the Paleocene and towards the end of the Cretaceous immobile elements decreased and slowed and deposition slowed.
- The rock units are mostly Rakaia-Pahau derived with a Waipapa provenance influence.

Chapter 7 Evolution of the Akitio Sub-basin

Introduction

The Akitio Sub-basin contains rock of Late Cretaceous (~80 Ma) to the end of the Miocene (~5 Ma) with eroded and transported Plio-Pleistocene and Quaternary deposits. The Akitio Sub-basin formed in an accretionary setting associated with the subduction of the Pacific plate under the Australian. The geology of the Akitio Sub-basin and Weber region reflect the tectonic phases and changing depositional environments from the separation from Gondwana, to the drift and the present-day collision that forms present-day Zealandia.

Late Cretaceous-Paleocene- Early Oligocene

During the Haumurian, the initial members of the Whangai Group were accumulating on the edge of Zealandia which was separating from Gondwana due to rifting. Paleodepth increased from the Rakauroa Member to the Upper Calcareous Member and continued to deepen into the Paleocene and Eocene. Fine silica-rich siltstone and claystone grains were being deposited and derived from Torlesse terranes. At approximately 65 Myrs the Cretaceous-Paleogene extinction event (K/T event) occurred, which caused global extermination of most flora and fauna (both marine and terrestrial). After the Te Uri Member, the Waipawa Formation, which is a well-researched source rock found along the East Coast, was deposited. As previously mentioned, the typical black shale, Waipawa, is not found in the Weber region; however, a biomarker correlative glauconitic unit is identified as a Waipawa equivalent (Hollis, 2003; Rogers et al., 2001). The deposition of the Wanstead Formation succeeded the Waipawa into the Paleocene. During the Eocene and Early Oligocene deposition significantly slowed which was disturbed by the tectonic activation of the subduction zone found in northern Zealandia 25 Mya. This Late Oligocene/Miocene change of tectonic setting caused a rapid influx of sedimentation as well as the East Coast Basin as a catchment and Hikurangi Trench as a conduit. The Torlesse terrane was being accreted, uplifted, deformed and eroded into the forearc basin and sub-basins.

Waitakian (Late Oligocene)

By this time the Akitio Sub-basin was forming due to the subduction activation which created thrust-faults, and the Weber members were being deposited followed by Ihungia Formation. The Weber members that were accumulating at 25.2-23.03 Ma have very different lithologies, which show different depositional settings and conditions. The Weber Glauconitic sandstone was deposited at a shelfal depth 50-200 m in sub-oxic conditions; the Weber Limestone (very calcareous mudstone) was deposited at a paleodepth of 700-1000 m in a low energy environment; the Weber Flysch was deposited at a depth of 700 m+ with episodic input of sand, and lastly, the Weber Mudstone is presumed to be deposited at a similar depth but during periods of quiescence. The limited distribution of the Weber Limestone suggests it was a confined unit that accumulated where living conditions were very favourable for micro-organisms due to their abundance. This environment does not indicate a transported calcareous input due to the unit being massive and showing no directional sedimentary structures, as well as macrofossils being incredibly rare (only one has ever been found (Lillie, 1953)). The Weber Glauconite and Weber Mudstone also have limited distribution suggesting a specific depositional environment. The Weber flysch was not as environmentally selective and is found over a large proportion of the Weber mapping area. The Weber Flysch formation consists of mid-bathyal mudstone with intermittently supplied sandstone beds.

The deposition of the Ihungia Formation followed during the Late Oligocene and continue through to the Early Miocene, more specifically at 23.03 Ma. After this time, the Whakataki Formation began to be deposited and continued through to the Early Miocene. The Whakataki Formation contains complete Bouma sequence layers suggesting turbidite deposition. The Akitio sub-basin is a juvenile basin, and the Whakataki turbidites in the Weber mapping area were deposited from a local-scale sub-marine fan that was likely confined to the central area of the mapping area. The channel that fed the submarine fan has eroded and is no longer present. Following the deposition of the Whakataki Formation, the Weber area became siliciclastic dominated until 15.1 Ma when the supply of sand became readily onset through to 5 Ma. This change of inconsistent supply of sand to consistent suggests a significant change of the larger surrounding depositional environment, likely due to the uplift of the Cape Turnagain structural high (Fig. 3.2). The deformation and deposition of the East Coast show an ongoing and repeating series of the uplifting of structural highs (thrust

faults) which causes an influx of sandstone lithologies which later become inconsistent and the strata become mudstone dominant. As the following structural high forms, the tectonic pressure intensely folds the mudstone until the next structural high becomes exposed and causes an influx of sandstone lithologies once again. Therefore, the East Coast is made up of near parallel structural highs and sub-basins. Furthermore, the Central East Coast, because of its position in regard to the tectonic margin, has faced significant uplift, exposing the Akitio Sub-basin, and intense folding of basin in-fill strata.

Miocene

At the start of the Miocene, the deposition of the Weber Formations, the Ihungia and Whakataki was concluding, and the deposition of the Riddell members and Tutamoe commenced.

During this time, the compression of the subducting Pacific Plate under the Australian Plate caused further thrust faulting and folding throughout the East Coast, especially in the central regions due to the present-day position of the tectonic boundary (New Zealand Petroleum & Minerals, 2014). The accretionary motion created areas of uplift and sub-basins which were progressively eroded and rapidly filled. The uplifted areas caused shoals which supplied the sub-basins with both sand and fine-grained sediment which is reflected throughout the Miocene and continues offshore today. As uplift progressed, so did erosion, therefore, transportation and deposition down to basins and the marine landscape.

During the Late Miocene, at approximately 15.09 Ma, deposition of mudstone dominated rock units transitioned to prominent sandstone deposition. This signals a time of shallowing of local and regional depositional environments which continued into the Plio-Pleistocene which caused the notable limestone deposition of the East Coast. This shallowing is seen on both borders of the Weber mapping area with the deposition of the Tutamoe Formation in the west and Riddells Culvert, Franklin Road Formation and McCartie Formations. The Tutamoe sharply and unconformably overlies the Ihungia Formation which indicates a time of erosion or no deposition whereas in the east the shallowing progression appears continuous.

The base of the Tutamoe, identified as the Westcott Sandstone by Reid (1998) contains an upper and lower contact layer of macrofossils such as *Flabellum circulare* and *Glycymerita rangatira* (Appendix Five of Early and Mid-Miocene age with some showing reworking of older fossils which are likely to be transported

from further inland Oligocene fossiliferous units. Fossil lenses are also found in the mudstone beds of the Tutamoe. Fossils that were able to be identified were found in the reworked upper Westcott base of the Tutamoe and the upper mudstone beds (as fossil lenses) of the Tutamoe. Because the Tutamoe unit was deposited by event deposition, older fossils were incorporated making the age-span of the fossils larger.

In the western part of the mapping area, the progression to the McCartie Sandstone from Riddells Mudstone is shown by increasing thickness of sandstone beds. The Riddell Members show a progression of deep-water deposition which was influenced by a time of folding which created a marine landscape of small platforms and dips which accumulated eroding sediment. There is a likely but not confirmed unconformity between the Riddells Mudstone and Riddells Culvert units. The McCartie Sandstone (and Franklin Road) is notably recognised by its friable micaceous nature of the sand, and for the biotite to be present, it was likely to be derived from a nearby metamorphic source, likely the North or Eastern South Island. Throughout the derivation of the older Torlesse and Whangai Formations, easily weathered minerals were washed out of Oligocene and Miocene units, and stable minerals such as quartz and feldspar became prominent in the rock composition.

With the activation of the subduction margin, deep bathyal environments that were catchments for mudstone began to be uplifted and shallow which encouraged the input of coarser grained beds. This transgression is shown by the Tahuokaretu, Riddell and Franklin Road Formations as the proportion and regularity of sandstone beds increases with time. However, the transgression is not seen as a unit by unit consistently, but as in some cases, mudstone is abruptly underlying alternating sandstone and mudstone (Riddells Mudstone and Franklin Road) which is dependent on sand supply during the Miocene. As the Pacific Plate has subducted and pressure build-up has continued, thrust faults have formed and caused zones of folding in between. The Weber mapping area does not contain any large thrust faults, but they are either side of the mapping area, therefore, is an area of major and minor folding. The major folds of the Weber area are what has been named the McCartie Syncline (this publication, also named the Akitio Syncline in other publications), Ossa Anticline and the Waipatiki Syncline by Ongley (1935) (Appendix 1.1 – 1.3).

Post Miocene

After the Miocene, as marine regression and accretion continue, Zealandia proceeded to be uplifted out of the ocean. Because of this, the Akitio Sub-basin is now exposed, and a large amount of erosion has occurred throughout the East Coast which has transported sediment out to offshore basins. As the Hikurangi Margin continues to compress and be uplifted offshore basins are being exposed, and new ones continue to form offshore. Throughout the mapping area, there are McCartie Sandstone and Plio-Pliocene Limestone shoals that have been deposited after a time of significant erosion which is seen by the sharp unconformity of overlying strata that is >2 Myrs older. This further shows that during the Clifdenian-Liliburnian tectonic motion caused additional deformation in the centre of the Eastern part of the mapping area, which was followed by the intermittent influx of sediments. As the Plio-Pleistocene and Quaternary proceeded, the once deep marine landscape became exposed. During the Quaternary, most of Zealandia was submerged under the ocean and continued to be uplifted and exposed. This exposure is marked by an erosional surface which is witnessed by flat top hills which either remain eroded or are capped. The Plio- Pleistocene/Quaternary erosion surface has caused limestones from either side of the mapping area to be eroded and dropped onto the uplifted plains.

Chapter 8 Discussion

Ongley (1935) mapped and identified multiple synclines and anticlines in the Weber area. Because of the scale of the map, some geological units have been grouped, but the boundaries of the geological units do show the overall distribution. Ongley (1935) does not include the Mapiri series in the Weber mapping area but does include the Waihoki Series. The Waihoki Series is not currently found on top of the McCartie Syncline, but with more analysis, Riddells Culvert could potentially be identified as Waihoki Series as the unit's appearance found in the field looks similar to that found in Neef (1992b). Lillie (1953) also identifies the Mapiri Formation of being present in the Weber mapping area. The boundaries from Lillie's map can be interpreted downwards towards the Akitio River, and it shows that the Whangai Formation is found centrally with younger Miocene units either side, however Lillie shows that the Mapiri Formation is found overlying the Tutamoe Formation in the East which is not the case for this research as the McCartie Sandstone is found overlying the Franklin Road Members. Lillie (1953) also shows two faults in the Akitio River which are concluded to be folds in this study as no distinct displacement is seen. Overall, Lillie's (1953) map is a relatively accurate depiction of the geology north of the mapping area, and unit boundaries are easily linked to this study.

Although Reid (1998) covers a small portion of the Weber mapping area and the geological units have been further differentiated, the distribution and differentiation are precise. The Tunakore mudstone and the base of the Westcott Sandstone are the Tutamoe Formation and the unit named the Mangapuku Mudstone is the Ihungia Formation. The structure of Reid's (1998) map matches what is seen in the field, and the lithology has provided much-needed detail in order to describe Miocene-aged units.

Lastly, Lee et al. (2002) which covers the entire Weber mapping area, shows a valid distribution of the geological groups based on age. It does show major structural features such as anticlines and synclines but misses the minor folding in between. Although the Miocene geological boundaries have been inferred for the Eastern part of the mapping area, the boundaries between Early, Mid and Late Miocene show the overall transition of becoming younger towards the East of which is seen in the field the Lee et al. (2002) map, which

is compiled from previous maps, was a vital foundation for this project and now the undifferentiated Miocene geological units have been distinguished due to this study.

When considering the structure of the Weber mapping area, the Whangai Members break through younger geological units, as Kingma (1958) suggests, however, for this case it is due to folding and erosion not faulting. There also is substantial evidence for the activation of the subduction margin at 25 Myrs, but deposition rapidly increased at 23.03 Myrs with the onset of the Weber Formation and other Late Oligocene-Early Miocene aged lithologies. This may mean that geological units found in closer proximity to the tectonic margin activated earlier compared to those on either side of the margin (Raukumara and Pegasus Basin) but more research is needed for this to be concluded. The stratigraphy of the Weber area indicates a deep-water environment with moderate deposition during the Late Cretaceous to Paleocene, in which the paleodepth deepens but deposition slows, only to be accelerated at 23.03Myrs (Late Oligocene) followed by constant shallowing with high deposition and high erosion to the present day. This change of depositional environment of Cretaceous accretion, Paleogene subduction and Miocene uplift throughout time coincides with most East Coast studies.

The Tawanui type section has been examined in detail before this study (Hollis, 2003; Rogers et al., 2001); however, it is still an essential site for mapping and contains important age markers. Other type sections have also been studied (Bland et al., 2013; Bland et al., 2014; Clowes et al., 2016) and have been a significant contributor to this study by providing insights into stratigraphic relationships and the depositional environment. Because the Miocene rock units are being deposited rapidly, distinct unit boundaries are rarely seen as well as due to erosion. However, due to rapid lithology changes between nearby outcrops, distinguishing the unit boundaries of the strata was achieved.

As the lithologies and depositional environment changed, so did the microorganisms. Microfossil analysis was used to gain better age control and to achieve a better understanding of the depositional environment throughout time. Morgans (2016) examines the Whangai, Wanstead and Weber Formation biostratigraphy which gave a foundation to the Late Cretaceous to the start of the Early Miocene. Little information was known about other Miocene biostratigraphy before this study. Results from this study align with Morgans (2016) findings and differentiate the Miocene strata found in the mapping area. The Miocene microfossil

analysis, lithology and stratigraphy from this study (Appendix Two – Appendix Four) shows the shallowing and increasing proportion of sand sediments into the Akitio sub-basin with time as well as turbidite deposition, event deposition, reworking and unconformity forming.

The geochemistry and petrology data shows results are similar to Moore (1988a) and indicates that younger geological units with similar geochemistry to the Whangai Formations (such as the Wanstead and Weber) are likely to be eroded and formed from the Whangai or a similar source (Torlesse Terrane). There also is no evidence for a volcanic content, but the ACNK/CIA plot does suggest a possible dacite signature before weathering. This dacite signature could be from the Waipapa Terrane material or transported material from the Taupo region yet no volcanic deposits are found in the Weber mapping area. Moore (1988a) also mentions that the Whangai is influxed with terrigenous sediment which is also reflected in the younger rock units. Moore (1988a) also suggests that due to dilution the Whangai shows a decline in terrigenous sediment input and an increase in biological activity before the K/T impact. It is also stated that the Wanstead has a close relationship and is likely to be sourced from the Whangai group. Moore (1998a) also shows the overall change of Whangai geochemistry and rock distribution from North to South which shows the variation of depositional environment and provenance. This is also reflected in the results of this study.

The quartz data also shows a low-grade metamorphic rank, as well as a Torlesse-derived provenance like Lillie (1953) and Smale (1993) suggested. When compared to the Makara Basin, which has a plutonic or upper metamorphic rank and feldspathic litharenite or lithic feldsarenite sandstones, it shows how nearby basins can be very different considering the Akitio Sub-basin has low metamorphic rank, and the sandstones are litharenite/sub-litharenite as well as sub-arkose. This may mean that the Makara Basin has had more significant influence from the Taupo Volcanic Zone than the Akitio Sub-basin and that weathering and tectonics have played a different role despite their proximity. The geochemistry, when compared to previous terrane studies, shows that the provenance of the Weber area is of Rakaia-Pahau (composite Torlesse) and Waipapa Terrane derivation. Hines (2018) showed that Western Terrane Provenances can be found for East Coast Basin strata but are expected from rock units older than 83Myrs. Because the Whangai is of Late Cretaceous age (83Myrs+), this explains why there is an indication of Waipapa Terrane influence. When comparing to the Makara basin, paleocurrent data from this study during the Mid-Miocene (Waiauan stage)

currents were coming from the south whereas in the Late Miocene currents came from the north and west. Overall, the Makara basin Miocene flysch came from the Akitio basin and was eventually separated by uplifting anticlines. This makes the Makara Basin and Akitio basin very similar until the Miocene separation and shows that due to folding and uplift, the provenance can change.

The thin sections and lithology reflect the evolution of the Akitio Sub-basin by showing the deposition of mudstone with glauconitic sand until the Weber Formation was deposited at 25Mys when there was an influx of coarser sand grains due to the initiation of the subduction zone. Periods of interbedded sandstone such as the Weber Flysch and Whakataki show the ongoing change of surrounding depositional environment due to increasing sand input while deeper water mudstone setting was being rapidly infilled. By 18-15 Ma, the Western part of the Akitio Sub-basin sand input was decreasing but continued and became consistent in the Eastern part of the Sub-Basin as the subduction zone accreted more material and tectonic pressure built up structural highs. As this structural high uplifted, the deposition of more fossiliferous units became more prominent, which is seen in Tutamoe mudstone and Franklin Mudstone thin sections and stratigraphy and later the Plio-Pleistocene Limestones.

When regarding the petroleum potential of the Akitio Sub-basin, Miocene aged units are yet to be thoroughly analysed for their potential. With observations of oil or gas streaming out of eroded Mangato Mudstone and other Riddells Group Mudstones combined with this study has highlighted that the Riddells Group should be of further research interest. Younger sandy units such as the Tutamoe or McCartie Group had no visible signs of petroleum potential, but further research can only determine this.

The purpose of this study was to map and provide higher detailed analysis of the geology-reflected evolution of the central ECB by studying the stratigraphy and geology of the Akitio Sub-basin. Thin sections, biostratigraphy and geochemistry, show the changes through time and story of sediment input to the basin, provenance and depositional environments.

Chapter 9 Conclusions

This study produced a 1:25,000 map of the Weber area and the Akitio sub-basin, that identifies nine units through more detailed stratigraphic and sedimentological analysis and further defines the Miocene aged units. The petrography and whole-rock geochemistry (XRF) of each unit was analysed and aided in developing an increased temporal understanding of the provenance of the units within the sub-basin that showed that the Whangai and Wanstead Formations were sourced from distal terranes such as the Waipapa and proximal terranes such as Rakaia-Pahau and as the Akitio Sub-basin established, Weber and other Miocene sources were more proximal and localised. The biostratigraphic analysis found by that using macro and microfossils better stratigraphic control could be achieved through better constraining the mapped lithologies (and sedimentological changes) to specific periods of basin change. The detailed biostratigraphy allowed for a better understanding of the timing of different phases of sediment input and changing depositional environments reflecting basin formation, infill and uplift.

An interpretation of the Late Cretaceous (80 Ma) to Late Miocene (5 Ma) stratigraphy has been presented showing that the basin formed in response to accretionary action due to the subduction margin and thrust faulting of the ECB. The basin formed primarily due to the tectonic evolution of the area and lithologies is representative of the depth of the near shelf environment in which they were deposited.

9.1 Key findings

The key finding can be summarised as follows:

- Biostratigraphy shows varying basin depositional environments during the Miocene, such as shelfal with high iron supply and sub-oxic conditions (Weber Glauconitic Sand), deep middle bathyal (Weber Limestone and Weber Flysch Formations), middle bathyal with shelfal input (Ihungia Formations), upper bathyal (Tutamoe), deep lower bathyal (Riddells Group) and neritic (sandstones of Tutamoe Formation, Franklin Road and McCartie Sandstone).
- The geochemistry shows rather siliceous rock with an overall increasing concentration of immobile elements. The immobile elements increased during the Late Cretaceous until the Paleocene or K/T impact where immobile elements dropped due to a decrease of deposition due to Zealandia being

relatively tectonically quiet and drifting. Immobile elements very slowly increased until the start of the Miocene where the influx dramatically increased rapidly due to the formation of the subduction zone/collision. And due to the uplift during the Plio-Pleistocene sandstone and limestone deposition increased due to a shallower depositional environment.

- The Weber area has experienced extensive folding and erosion from the Mid to Late Miocene onwards with regional and local structural highs having formed due to accretionary induced thrust faulting and intermittent zones of folding.
- Authigenic glauconite is found in every thin section sample which indicates areas of restricted deposition and reworking.
- The Akitio Sub-basin geology reflects the phases of deposition and Zealandia separating from Gondwana (Whangai Group), to the drifting of Zealandia (Wanstead Formation), to the onset of the subduction zone at 25 Ma (Weber Group), and lastly the Akitio Sub-basin infill (Ihungia Formation and Riddells Group) and uplift (Tutamoe, Franklins Road and McCartie Groups).
- The Akitio Sub-basin has shortened by 27.1% or 4.36km due to the accretionary action.
- Due to the onset of the subduction margin at 25 Mya, a range of depositional environments occurred in a localised (80 km^2) area that changed rapidly; this is reflected by the Weber Formations.
- Due to rapid infill and shallowing, macrofossils were disintegrated or transported and deposited as lenses in the Tutamoe and Franklin Road Formations.

9.3 Suggestions for further study

To extend the research of this study, mapping the adjacent area and correlating Miocene strata recognised in the Weber area would be valuable to further support the analysis of the ECB structures and gain a wider context of the succession of depositional environments of the Central East Coast Basin.

Zircon and radiogenic isotope analysis of the Weber and surrounding area is also recommended to further age control on the newly identified units, especially of the differentiated Miocene aged units. Better age control will contribute to better understanding the evolution of this sub-basin but also allow correlations to possibly

be made to other basins to determine the of succession basins throughout the East Coast. Lastly, Clay mineralogy, Total Organic Carbon (TOC) and porosity analysis of the Miocene units within this basin and regionally should be undertaken to examine the petroleum potential of the studied lithologies.

References

Bailleul, J., Chanier, F., Ferriere, J., Robin, C., Nicol, A., Mahieux, G., . . . Caron, V. (2013). Neogene evolution of lower trench-slope basins and wedge development in the central Hikurangi subduction margin, New Zealand. *Tectonophysics, 591*, 152-174. doi:10.1016/j.tecto.2013.01.003

Barnes, P. M., Lamarche, G., Bialas, J., Henrys, S., Pecher, I., Netzeband, G. L., . . . Crutchley, G. (2010). Tectonic and geological framework for gas hydrates and cold seeps on the Hikurangi subduction margin, New Zealand. *Marine Geology, 272*(1-4), 26-48. doi:10.1016/j.margeo.2009.03.012

Basu, A., Young, S. W., Suttner, L. J., James, W. C., & Mack, G. H. (1975). Re-evaluation of the use of undulatory extinction and polycrystallinity in detrital quartz for provenance interpretation. *Journal of Sedimentary Research, 45*(4), 873-882.

Bhatia, M. R., & Crook, K. A. W. (1986). Trace-Element Characteristics of Graywackes and Tectonic Setting Discrimination of Sedimentary Basins. *Contributions to Mineralogy and Petrology, 92*(2), 181-193. doi:10.1007/Bf00375292

Bland, K. J., Morgans, H. E. G., & Strogen, D. P. (2013). *Record of geological observations and sample collection from Late Cretaceous–Early Miocene strata in the southern Hawke's Bay-Wairarapa areas, 10–15 February 2013, for micropaleontological, petrographic, and source rock analyses.* GNS Science Internal Report 2014/04. GNS Science. Lower Hutt.

Bland, K. J., Strogen, D. P., Morgans, H. E. G., & Ventura, G. (2014). *Record of section descriptions and sample collection from the Tahuokaretu and Taylor-White sections, southern Hawke's Bay, 1–3 May 2014, for micropaleontological and source rock analyses.* . GNS Science Internal Report 2014/03. GNS Science. Lower Hutt.

Broome, S. J. (2015). *Depositional model for the early Miocene turbidite sequence, the Whakataki Formation, NZ.* (Masters by Research). Retrieved from https://eprints.qut.edu.au/90732/

Burgreen-Chan, B., Meisling, K. E., & Graham, S. (2016). Basin and petroleum system modelling of the East Coast Basin, New Zealand: a test of overpressure scenarios in a convergent margin. *Basin Research, 28*(4), 536-567. doi:10.1111/bre.12121

Campos, N., Roser, B., & Sampei, Y. (2002). Organic carbon and carbonate contents of black shales from the lower Cretaceous Paja Formation (Colombia) by loss on ignition and CHNS analysis: comparison of methods. *Geoscience Reports of Shimane University, 21*, 9-26.

Chanier, F., & Ferriere, J. (1991). From a Passive to an Active Margin - Tectonic and Sedimentary Processes Linked to the Birth of an Accretionary Prism (Hikurangi Margin, New-Zealand). *Bulletin De La Societe Geologique De France, 162*(4), 649-660.

Chanier, F., Ferriere, J., & Angelier, J. (1999). Extensional deformation across an active margin, relations with subsidence, uplift, and rotations: The Hikurangi subduction, New Zealand. *Tectonics, 18*(5), 862-876. doi:10.1029/1999tc900028

Clare, A., & Wunderlich, A. (2017). Sedimentary supply and distribution in a slope basin province - East Coast Basin, New Zealand. In. Wellington.

Clowes, C. D., Bland, K. J., Morgans, H. E. G., & Hines, B. R. (2016). *Record of geological observations and sample collection from Late Cretaceous-ealy Miocene strat in southern Hawkes's Bay, 04-08 April 2016*. Lower Hutt: GNS Science Internal Report 2016/14.

Crouch, E. M., & Brinkhuis, H. (2005). Environmental change across the Paleocene–Eocene transition from eastern New Zealand: a marine palynological approach. *Marine Micropaleontology, 56*(3-4), 138-160.

Davy, B., & Wood, R. (1994). Gravity and Magnetic Modeling of the Hikurangi Plateau. *Marine Geology, 118*(1-2), 139-151. doi:10.1016/0025-3227(94)90117-1

Dickinson, W. R., Beard, L. S., Brakenridge, G. R., Erjavec, J. L., Ferguson, R. C., Inman, K. F., . . . Ryberg, P. T. (1983). Provenance of North-American Phanerozoic Sandstones in Relation to Tectonic Setting. *Geological Society of America Bulletin, 94*(2), 222-235. doi:10.1130/0016-7606(1983)94<222:Ponaps>2.0.Co;2

Elgar, N. E. (1997). *Petroleum geology and geochemistry of oils and possible source rocks of the southern East Coast Basin, New Zealand.* Victoria University, Wellington.

Field, B. D., & Uruski, C. I. (1997). *Cretaceous-Cenozoic geology and petroleum systems of the East Coast region, New Zealand* (Vol. 1): Institute of Geological & Nuclear Sciences.

Folk, R. L. (1980). *Petrology of sedimentary rocks*: Hemphill Publishing Company.

Francis, D. A. (1990a). Tour Guide: Akito Syncline, Fingerpost Syncline, Turnagain Syncline. In: Geological Society of New Zealand miscellaneous publication 50B: 241-247.

Francis, D. A. (1990b). *Report on the geology of coastal Wairarapa, between Riversdale and Porangahau, adjacent to offshore prospecting leases 38318 and 38323. New Zealand open-file petroleum report 2138 for Amoco New Zealand Exploration Company. New Zealand*. Wellington: New Zealand Ministry of Economic Development.

Francis, D. A., Bennett, D., & Courteney, S. (2004, 7-10 March). *Advances in understanding of onshore East Coast Basin structure, stratigraphic thickness and hydrocarbon generation.* Paper presented at the New Zealand Petroleum Conference Proceedings Report.

Gaschnig, R. M., Rudnick, R. L., McDonough, W. F., Kaufman, A. J., Hu, Z., & Gao, S. (2014). Onset of oxidative weathering of continents recorded in the geochemistry of ancient glacial diamictites. *Earth and Planetary Science Letters, 408*, 87-99.

Graham, I. (2008). *A Continent on the Move : New Zealand Geoscience into the 21st Century*. Wellington: Geological Society of New Zealand in association with GNS Science.

Harris, A. G., & Sweet, W. C. (1989). Mechanical and chemical techniques for separating microfossils from rock, sediment and residue matrix. *The Paleontological Society Special Publications, 4*, 70-86.

Hines, B. (2018). Cretaceous to Paleogene palinspastic reconstruction of the East Coast Basin, New Zealand.

Hollis, C. J. (2003). The Cretaceous/Tertiary boundary event in New Zealand: profiling mass extinction. *New Zealand Journal of Geology and Geophysics, 46*(2), 307-321.

Hollis, C. J., Tayler, M. J. S., Andrew, B., Taylor, K. W., Lurcock, P., Bijl, P. K., . . . Phillips, A. (2014). Organic-rich sedimentation in the South Pacific Ocean associated with Late Paleocene climatic cooling. *Earth-Science Reviews, 134*, 81-97. doi:10.1016/j.earscirev.2014.03.006

Kaiho, K., Arinobu, T., Ishiwatari, R., Morgans, H. E. G., Okada, H., Takeda, N., . . . Wada, H. (1996). Latest paleocene benthic foraminiferal extinction and environmental changes at Tawanui, New Zealand. *Paleoceanography, 11*(4), 447-465. doi:10.1029/96pa01021

Kingma, J. T. (1958). Possible of Piercement structures, local unconformities, and secondary basins in the Eastern Geosyncline, New Zealand. *New Zealand Journal of Geology and Geophysics, 1*(2), 269-274.

Kingma, J. T. (1959). The tectonic history of New Zealand. *New Zealand Journal of Geology and Geophysics, 2*(1), 1-55.

Kingma, J. T. (1960). Outline of the Cretaceo-tertiary sedimentation in the eastern basin of New Zealand. *New Zealand Journal of Geology and Geophysics, 3*(2), 222-234.

Leckie, D. A. (1992). *Stratigraphic framework and source-rock potential of maastrichtian to paleocene marine shale: East coast, North Island, New Zealand: hydrocarbon prospects* (Vol. 92): Institute of Geological and Nuclear Sciences.

Lee, J. M., & Begg, J. G. (2002). *Geology of the Wairarapa Area*. Wellington: Geological and Nuclear Sciences Ltd.

Lewis, K. B., Collot, J.-Y., & Lallemand, S. E. (1998). The dammed Hikurangi Trough: a channel-fed trench blocked by subducting seamounts and their wake avalanches (New Zealand–France GeodyNZ Project). *Basin Research, 10*(4), 441-468.

Lewis, K. B., & Pantin, H. M. (2002). Channel-axis, overbank and drift sediment waves in the southern Hikurangi Trough, New Zealand. *Marine Geology, 192*(1-3), 123-151. doi:10.1016/S0025-3227(02)00552-2

Lewis, K. B., & Pettinga, J. R. (1993). The emerging, imbricate frontal wedge of the Hikurangi margin. *Sedimentary basins of the world, 2*, 225-250.

Lillie, A. (1953). *The Geology of the Dannevirke Subdivision*. Wellington: New Zealand Geological Survey Bulletin.

McArthur, A. D., & McCaffrey, W. D. (2019). Sedimentary architecture of detached deep-marine canyons: Examples from the East Coast Basin of New Zealand. *Sedimentology, 66*(3), 1067-1101.

McLennan, S. M., Hemming, S., McDaniel, D. K., & Hanson, G. N. (1993). Geochemical approaches to sedimentation, provenance, and tectonics. *Special Papers - Geological Society of America*, 21-21.

Moore, P. R. (1988a). *Stratigraphy, composition and environment of deposition of the Whangai Formation and associated Late Cretaceous-Paleocene rocks, eastern North Island, New Zealand* (Vol. 100): New Zealand Geological Survey.

Moore, P. R. (1988b). *Structural divisions of eastern North Island* (Vol. 30): New Zealand Geological Survey, Dept. of Scientific and Industrial Research.

Morgans, H. E. G. (1977). *The Stratigraphy and Micropaleontology of the Weber Formation in its type locality at Weber, Southern Hawkes Bay*. Wellington: Victoria University.

Morgans, H. E. G. (2016). *The Weber Formation at its location in Southern Hawke's Bay, and its distribution though the East Coast, North Island, New Zealand*. Lower Hutt: GNS Science.

Morgans, H. E. G., Crundwell, M., Scott, G., & Edwards, A. (1995). Biostratigraphy of Titihaoa-1 offshore petroleum exploration well, Wairarapa coast, New Zealand. *Inst. Geol. Nucl. Sci. Client Rep. 53492A, 10*.

Mountjoy, J. J., Barnes, P. M., & Pettinga, J. R. (2009). Morphostructure and evolution of submarine canyons across an active margin: Cook Strait sector of the Hikurangi Margin, New Zealand. *Marine Geology, 260*(1-4), 45-68. doi:10.1016/j.margeo.2009.01.006

Neef, G. (1992a). Turbidite deposition in five Miocene, bathyal formations along an active plate margin, North Island, New Zealand" with notes on styles of deposition at the margins of east coast bathyal basins. *Sedimentary geology*, 111-136.

Neef, G. (1992a). Turbidite deposition in five Miocene, bathyal formations along an active plate margin, North Island, New Zealand: with notes on styles of deposition at the margins of east coast bathyal basins. *Sedimentary geology, 78*(1-2), 111-136.

Neef, G. (1992b). Geology of the Akitio area (1:50 000 metric sheet U25BD, east), northeastern Wairarapa, New Zealand. *New Zealand Journal of Geology and Geophysics, 35*(4), 533-548. doi:10.1080/00288306.1992.9514546

Neef, G. (1992b). Geology of the Akitio area (1:50 000 metric sheet U25BD, east), northeastern Wairarapa, New Zealand. *New Zealand Journal of Geology and Geophysics*, 533-548.

Neef, G. (1995). Cretaceous and Cenozoic Geology East of the Tinui Fault Complex in Northeastern Wairarapa, New-Zealand. *New Zealand Journal of Geology and Geophysics, 38*(3), 375-394. doi:10.1080/00288306.1995.9514664

Neef, G. (1997). Stratigraphy, structural evolution, and tectonics of the northern part of the Tawhero basin and adjacent areas, northern Wairarapa, North Island, New Zealand. *New Zealand Journal of Geology and Geophysics, 40*(3), 335-358. doi:10.1080/00288306.1997.9514766

Neef, G., & Bottrill, R. S. (1992c). The Cenozoic geology of the Gisborne area (1: 50 000 metric sheet Y18AB), North Island, New Zealand. *New Zealand Journal of Geology and Geophysics, 35*(4), 515-531.

Nesbitt, H. W., & Young, G. M. (1982). Early Proterozoic Climates and Plate Motions Inferred from Major Element Chemistry of Lutites. *Nature, 299*(5885), 715-717. doi:10.1038/299715a0

New Zealand Petroleum & Minerals. (2014). *New Zealand Petroleum Basins*. Wellington: Ministry of Business Innovation and Employment.

Nicol, A., Mazengarb, C., Chanier, F., Rait, G., Uruski, C., & Wallace, L. (2007). Tectonic evolution of the active Hikurangi subduction margin, New Zealand, since the Oligocene. *Tectonics, 26*(4). doi:10.1029/2006tc002090

Noda, A., & Miyakawa, A. (2017). Deposition and deformation of modern accretionary-type forearc basins: Linking basin formation and accretionary wedge growth. In *Evolutionary Models of Convergent Margins-Origin of Their Diversity*: IntechOpen.

Ongley, M. (1935). *Geological Map of the Eketahuna Subdivision (1: 253,440)*. Lower Hutt, Wellington, New Zealand: GNS.

Palmer, K., Mortimer, N., Nathan, S., Isaac, M. J., Field, B. D., Sircombe, K. N., . . . Orr, N. W. (1995). Chemical and petrographic analyses of some New Zealand Paleozoic–Mesozoic metasedimentary and igneous rocks. *Institute of Geological & Nuclear Sciences Science Report 95, 16*.

Price, R. C., Mortimer, N., Smith, I. E. M., & Maas, R. (2015). Whole-rock geochemical reference data for Torlesse and Waipapa terranes, North Island, New Zealand. *New Zealand Journal of Geology and Geophysics, 58*(3), 213-228.

Rait, G., Chanier, F., & Waters, D. W. (1991). Landward-and seaward-directed thrusting accompanying the onset of subduction beneath New Zealand. *Geology, 19*(3), 230-233.

Reid, C. M. (1998). Stratigraphy, paleontology, and tectonics of lower Miocene rocks in the Waipatiki/Mangatuna area, southern Hawke's Bay, New Zealand. *New Zealand Journal of Geology and Geophysics, 41*(2), 115-131. doi:10.1080/00288306.1998.9514796

Reyners, M. (2013). The central role of the Hikurangi Plateau in the Cenozoic tectonics of New Zealand and the Southwest Pacific. *Earth and Planetary Science Letters, 361*, 460-468. doi:10.1016/j.epsl.2012.11.010

Rogers, K. M., Collen, J. D., Johnston, J. H., & Elgar, N. E. (1999). A geochemical appraisal of oil seeps from the East Coast Basin, New Zealand. *Organic Geochemistry, 30*(7), 593-605. doi:10.1016/S0146-6380(99)00036-4

Rogers, K. M., Morgans, H. E. G., & Wilson, G. S. (2001). Identification of a Waipawa Formation equivalent in the upper Te Uri Member of the Whangai Formation - implications for depositional history and age. *New Zealand Journal of Geology and Geophysics, 44*(2), 347-354. doi:10.1080/00288306.2001.9514943

Roser, B. P., & Korsch, R. J. (1986). Determination of Tectonic Setting of Sandstone-Mudstone Suites Using Sio2 Content and K2o Na2o Ratio. *Journal of Geology, 94*(5), 635-650. doi:10.1086/629071

Roser, B. P., & Korsch, R. J. (1988). Provenance Signatures of Sandstone Mudstone Suites Determined Using Discriminant Function-Analysis of Major-Element Data. *Chemical Geology, 67*(1-2), 119-139. doi:10.1016/0009-2541(88)90010-1

Scott, G. H., Bishop, S., & Burt, B. J. (1990). *Guide to some Neogene Globorotalids (Foraminiferida) from New Zealand*: (p. 135). New Zealand Geological Survey.

Smale, D. (1993). *Heavy Minerals in Cretaceous sediments of East Coast North Island and Marlborough.* Institute of Geological and Nuclear Sciences.

Uruski, C. I. (2010). New Zealand's deepwater frontier. *Marine and Petroleum Geology, 27*(9), 2005-2026.

Van der Lingen, G., J., & Pettinga, R. (1980). The Makara Basin: a Miocene slope-basin along the New Zealand sector of the Australian-Pacific obliquely convergent plate boundary. *Sedimentation in oblique-slip mobile zones, 34*, 191.

Wallace, L. M., Beavan, J., McCaffrey, R., & Darby, D. (2004). Subduction zone coupling and tectonic block rotations in the North Island, New Zealand. *Journal of Geophysical Research-Solid Earth, 109*(B12). doi:10.1029/2004jb003241

Walters, R. (1965). The Globorotalia zealandica and G. miozea lineages. *New Zealand Journal of Geology and Geophysics, 8*(1), 109-127.

Wood, R., & Davy, B. (1994). The Hikurangi Plateau. *Marine Geology, 118*(1-2), 153-173.

Appendices

Appendix One - Previous Maps

Appendix 1.1 – Geological Map of the Eketahuna Subdivision (Ongley, 1935)

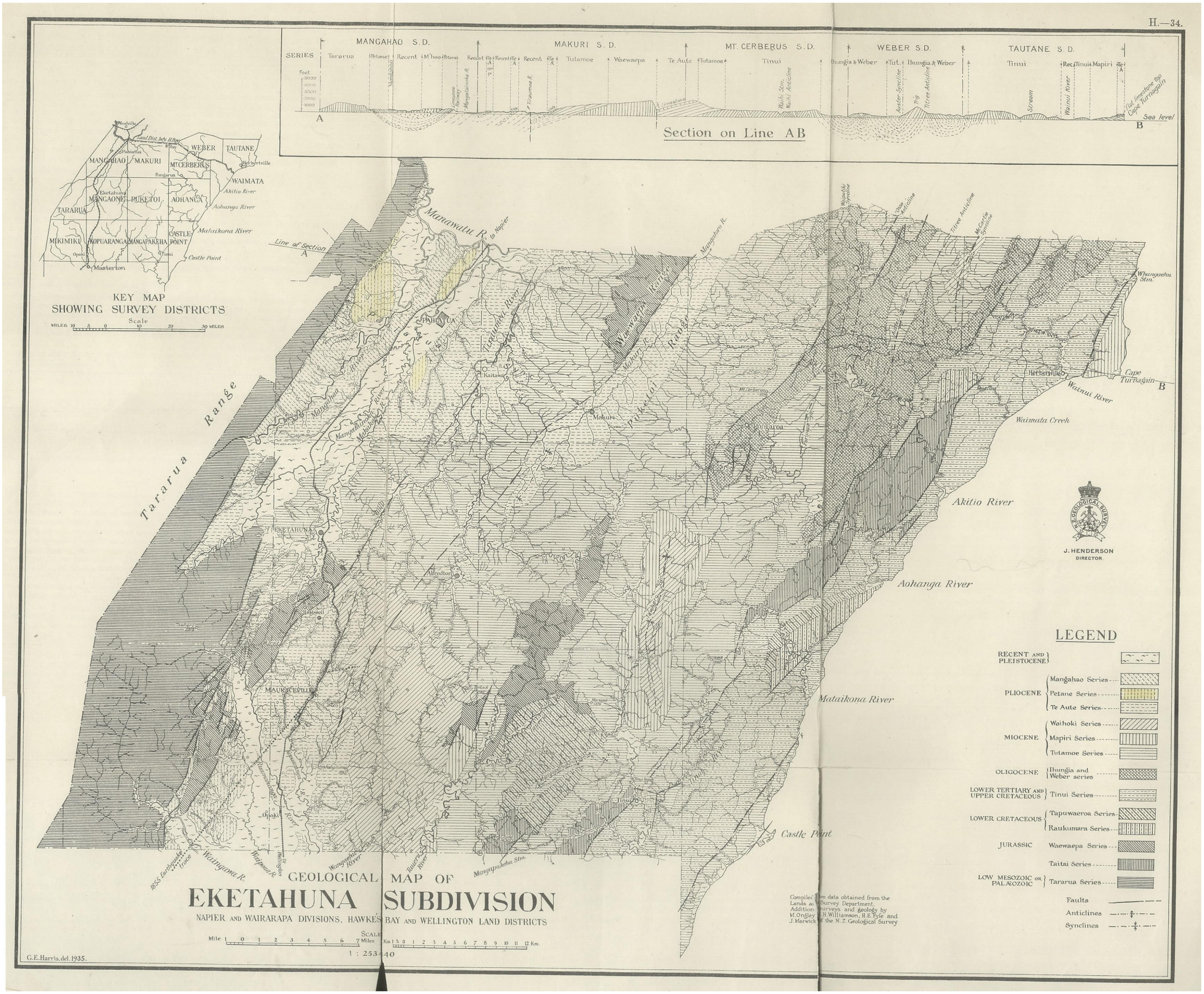

Appendix 1.2 – Close up of the Weber Geology and Cross Section (Ongley, 1935)

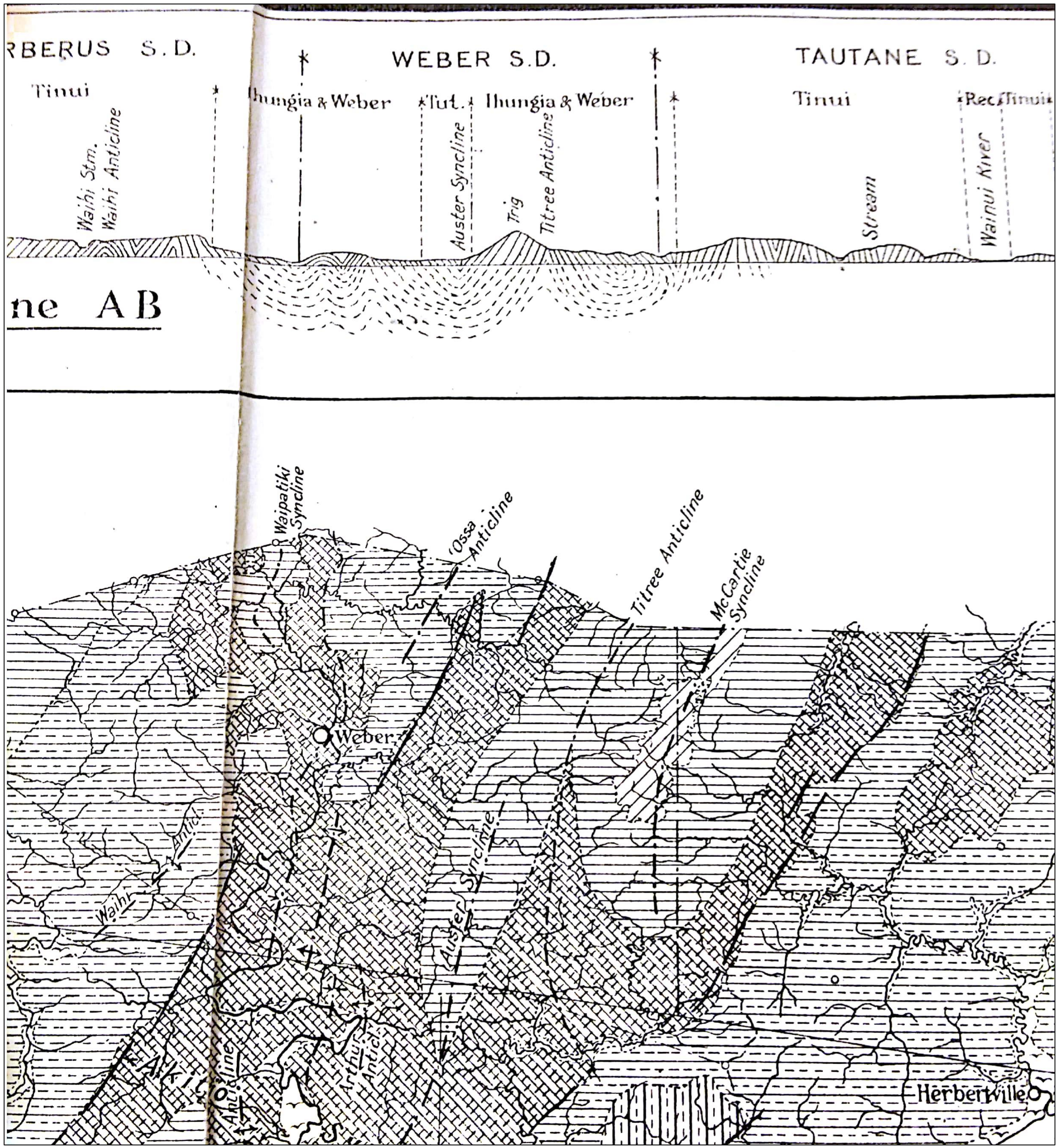

Appendix 1.3 – Geological Legend of the Geology of the Eketahuna Subdivision (Ongley, 1935)

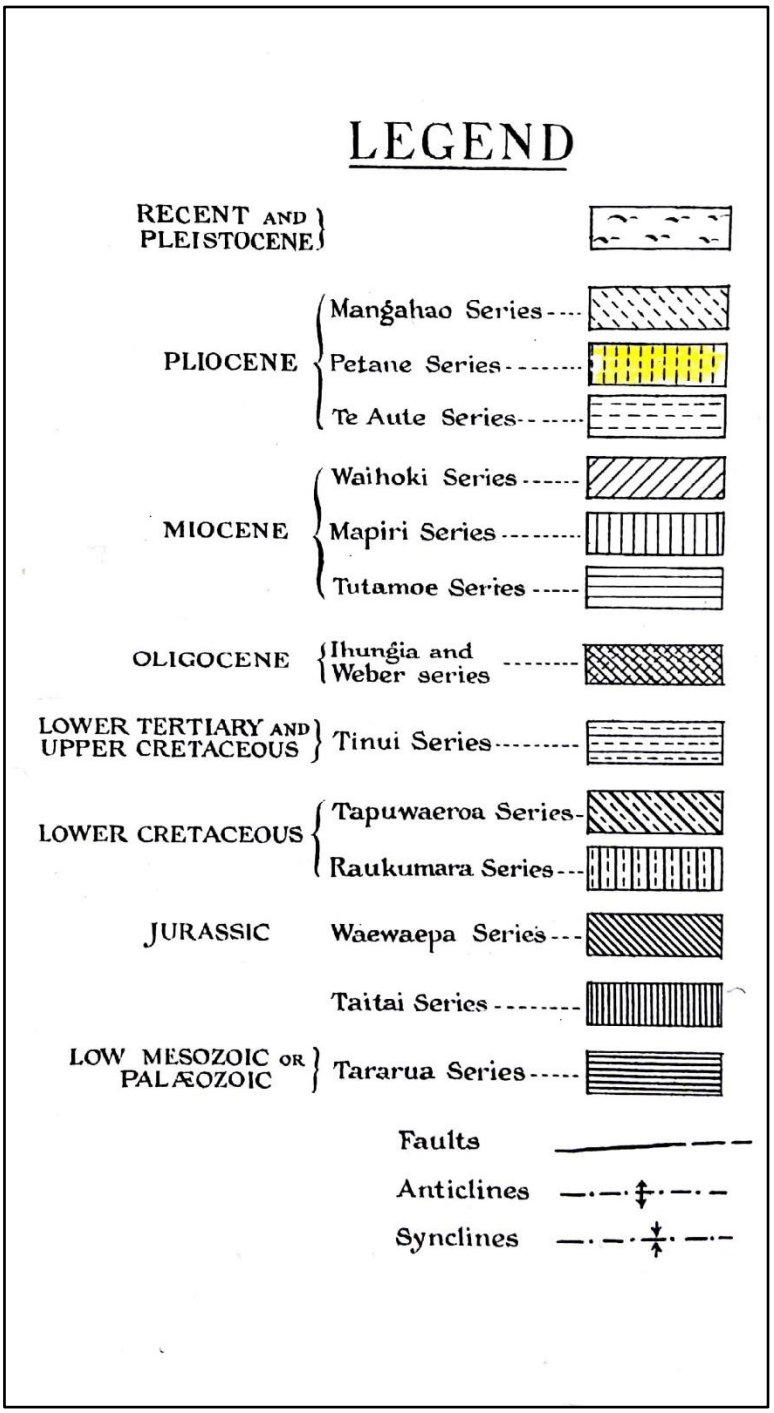

Appendix 1.4 – Geological Map of the Mangatoro and Porangahau survey district (Lillie, 1953)

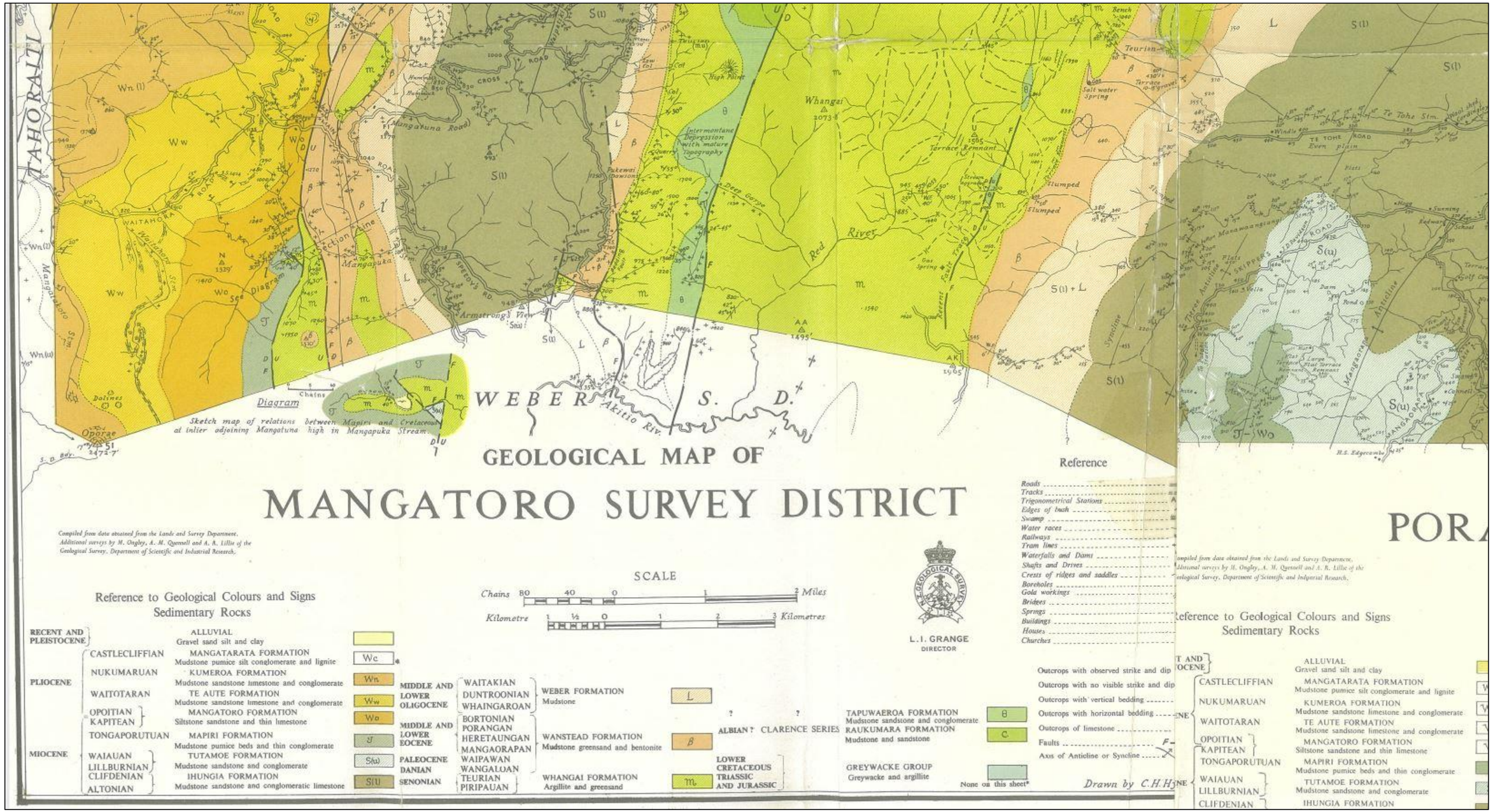

Appendix 1.5 – Geology of the Waipatiki Syncline (Reid, 1998)

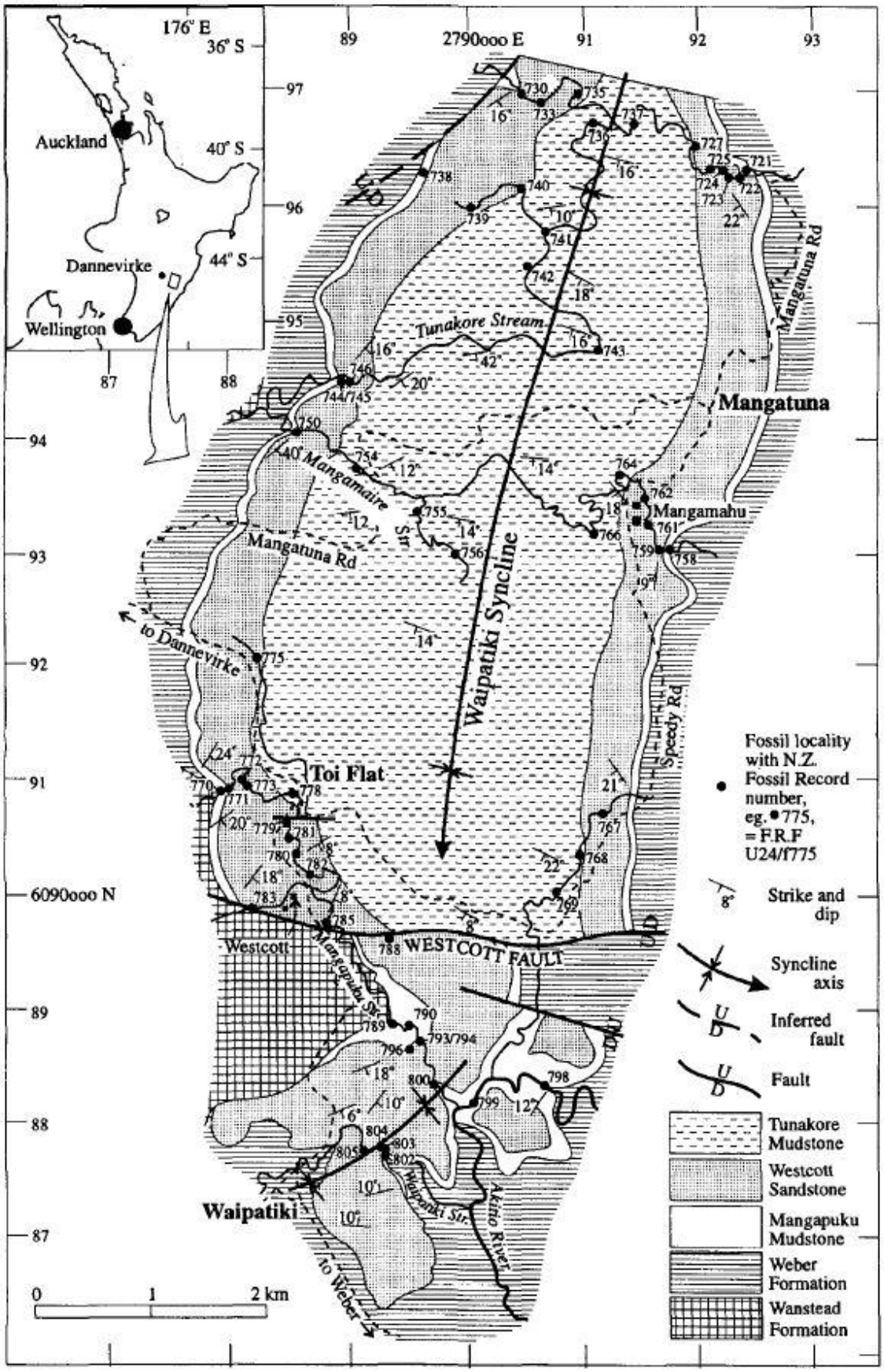

Appendix 1.6 – Partial Geology of the Wairarapa with the added Weber Region Boundary (Lee et al., 2002)

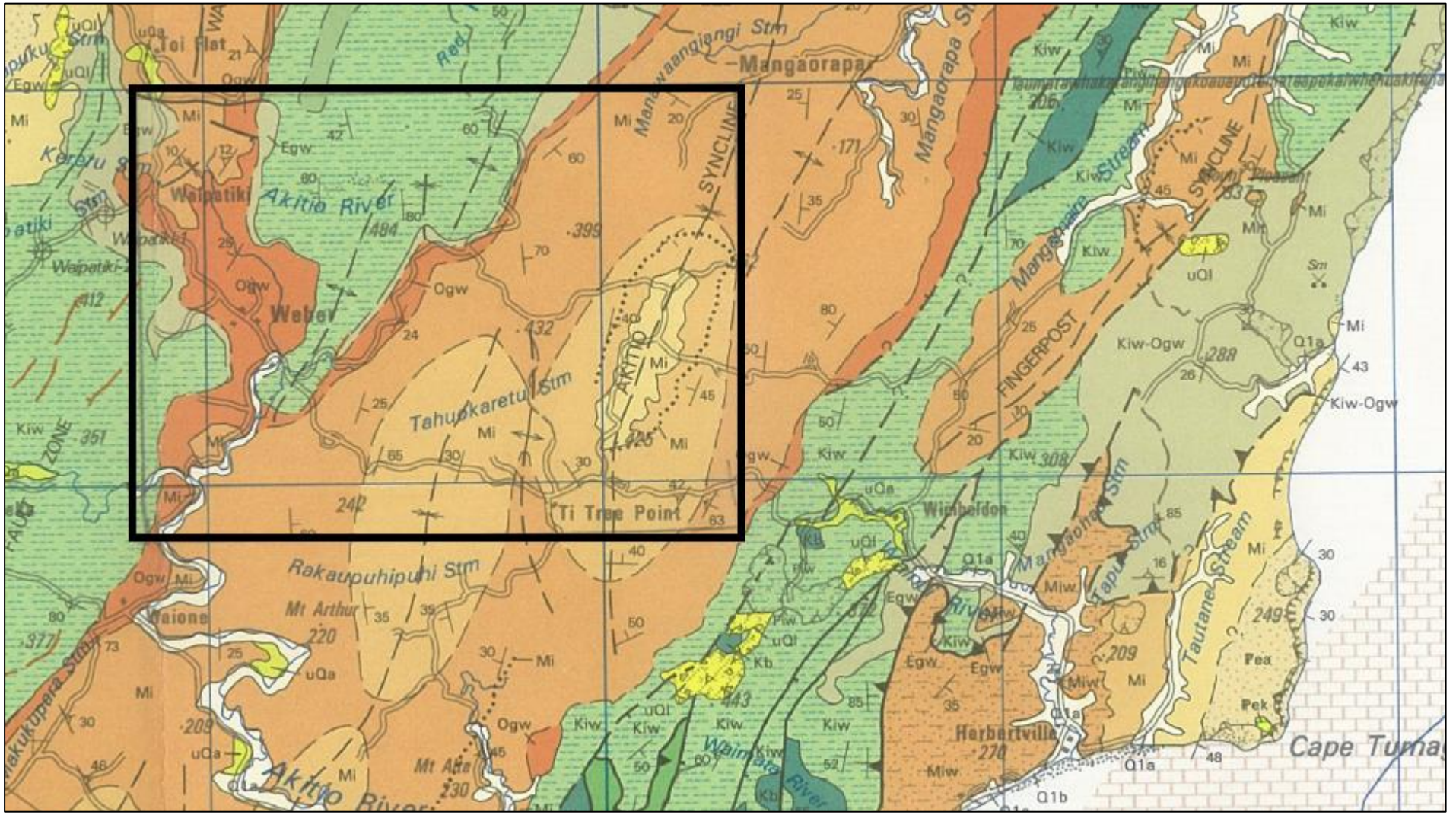

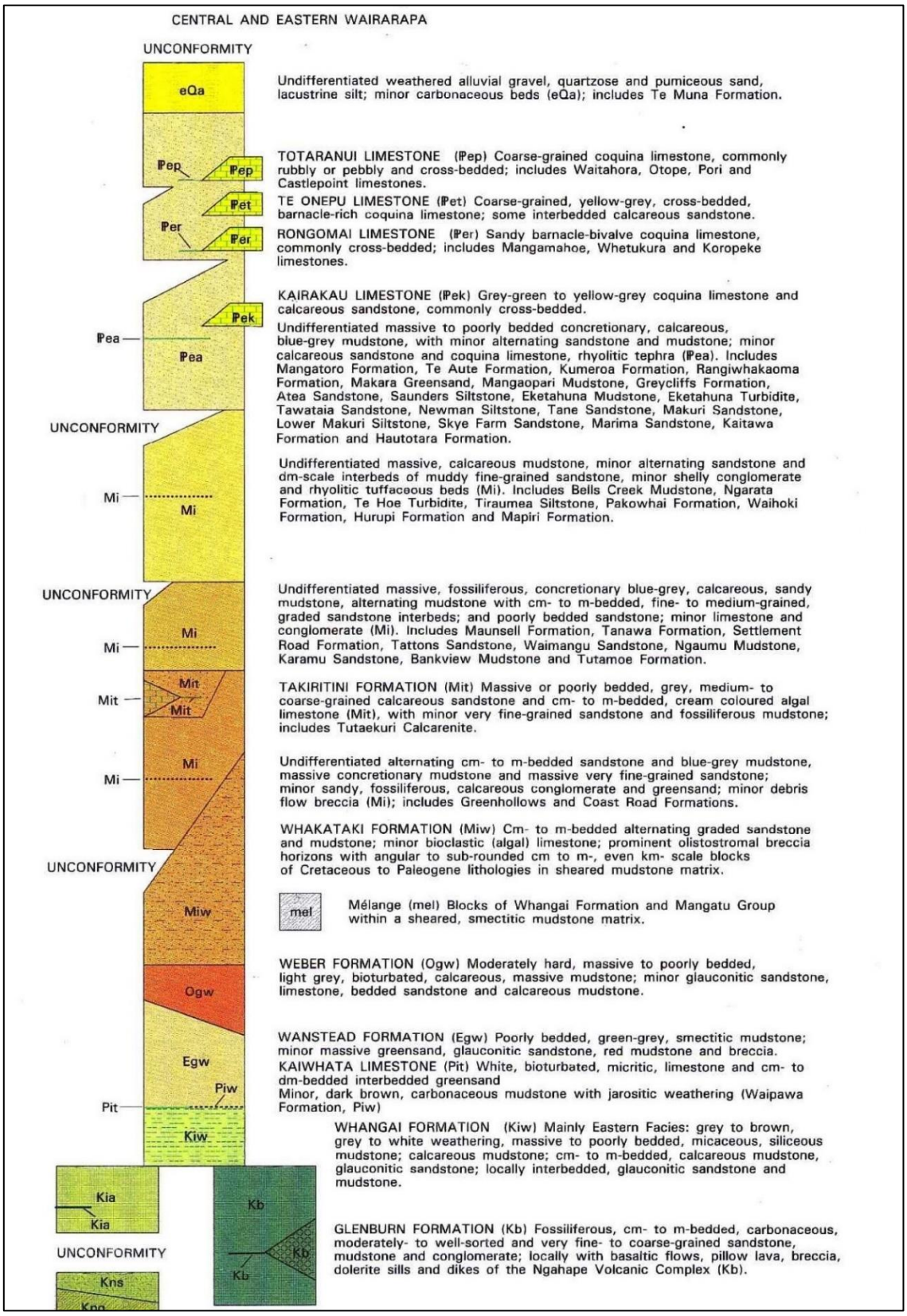
CENTRAL AND EASTERN WAIRARAPA
UNCONFORMITY
eQa
Undifferentiated weathered alluvial gravel, quartzose and pumiceous sand, lacustrine silt; minor carbonaceous beds (eQa); includes Te Muna Formation.
Pep
Pep
TOTARANUI LIMESTONE (Pep) Coarse-grained coquina limestone, commonly rubbly or pebbly and cross-bedded; includes Waitahora, Otope, Pori and Castlepoint limestones.
Pet
TE ONEPU LIMESTONE (Pet) Coarse-grained, yellow-grey, cross-bedded, barnacle-rich coquina limestone; some interbedded calcareous sandstone.
Per
Per
RONGOMAI LIMESTONE (Per) Sandy barnacle-bivalve coquina limestone, commonly cross-bedded; includes Mangamahoe, Whetukura and Koropeke limestones.
Pek
KAIRAKAU LIMESTONE (Pek) Grey-green to yellow-grey coquina limestone and calcareous sandstone, commonly cross-bedded.
Pea
Pea
Undifferentiated massive to poorly bedded concretionary, calcareous, blue-grey mudstone, with minor alternating sandstone and mudstone; minor calcareous sandstone and coquina limestone, rhyolitic tephra (Pea). Includes Mangatoro Formation, Te Aute Formation, Kumeroa Formation, Rangiwhakaoma Formation, Makara Greensand, Mangaopari Mudstone, Greycliffs Formation, Atea Sandstone, Saunders Siltstone, Eketahuna Mudstone, Eketahuna Turbidite, Tawataia Sandstone, Newman Siltstone, Tane Sandstone, Makuri Sandstone, Lower Makuri Siltstone, Skye Farm Sandstone, Marima Sandstone, Kaitawa Formation and Hautotara Formation.
UNCONFORMITY
Mi
Mi
Undifferentiated massive, calcareous mudstone, minor alternating sandstone and dm-scale interbeds of muddy fine-grained sandstone, minor shelly conglomerate and rhyolitic tuffaceous beds (Mi). Includes Bells Creek Mudstone, Ngarata Formation, Te Hoe Turbidite, Tiraumea Siltstone, Pakowhai Formation, Waihoki Formation, Hurupi Formation and Mapiri Formation.
UNCONFORMITY
Mi
Mi
Undifferentiated massive, fossiliferous, concretionary blue-grey, calcareous, sandy mudstone, alternating mudstone with cm- to m-bedded, fine- to medium-grained, graded sandstone interbeds; and poorly bedded sandstone; minor limestone and conglomerate (Mi). Includes Maunsell Formation, Tanawa Formation, Settlement Road Formation, Tattons Sandstone, Waimangu Sandstone, Ngaumu Mudstone, Karamu Sandstone, Bankview Mudstone and Tutamoe Formation.
Mit
Mit
Mit
TAKIRITINI FORMATION (Mit) Massive or poorly bedded, grey, medium- to coarse-grained calcareous sandstone and cm- to m-bedded, cream coloured algal limestone (Mit), with minor very fine-grained sandstone and fossiliferous mudstone; includes Tutaekuri Calcarenite.
Mi
Mi
Undifferentiated alternating cm- to m-bedded sandstone and blue-grey mudstone, massive concretionary mudstone and massive very fine-grained sandstone; minor sandy, fossiliferous, calcareous conglomerate and greensand; minor debris flow breccia (Mi); includes Greenhollows and Coast Road Formations.
WHAKATAKI FORMATION (Miw) Cm- to m-bedded alternating graded sandstone and mudstone; minor bioclastic (algal) limestone; prominent olistostromal breccia horizons with angular to sub-rounded cm to m-, even km- scale blocks of Cretaceous to Paleogene lithologies in sheared mudstone matrix.
UNCONFORMITY
Miw
mel
Mélange (mel) Blocks of Whangai Formation and Mangatu Group within a sheared, smectitic mudstone matrix.
Ogw
WEBER FORMATION (Ogw) Moderately hard, massive to poorly bedded, light grey, bioturbated, calcareous, massive mudstone; minor glauconitic sandstone, limestone, bedded sandstone and calcareous mudstone.
Egw
Piw
Pit
Kiw
WANSTEAD FORMATION (Egw) Poorly bedded, green-grey, smectitic mudstone; minor massive greensand, glauconitic sandstone, red mudstone and breccia.
KAIWHATA LIMESTONE (Pit) White, bioturbated, micritic, limestone and cm- to dm-bedded interbedded greensand
Minor, dark brown, carbonaceous mudstone with jarositic weathering (Waipawa Formation, Piw)
WHANGAI FORMATION (Kiw) Mainly Eastern Facies: grey to brown, grey to white weathering, massive to poorly bedded, micaceous, siliceous mudstone; calcareous mudstone; cm- to m-bedded, calcareous mudstone, glauconitic sandstone; locally interbedded, glauconitic sandstone and mudstone.
Kia
Kia
Kb
Kb
Kb
GLENBURN FORMATION (Kb) Fossiliferous, cm- to m-bedded, carbonaceous, moderately- to well-sorted and very fine- to coarse-grained sandstone, mudstone and conglomerate; locally with basaltic flows, pillow lava, breccia, dolerite sills and dikes of the Ngahape Volcanic Complex (Kb).
UNCONFORMITY
Kns
Kng

Appendix Two – Stratigraphic Columns

Legend for the following stratigraphic columns

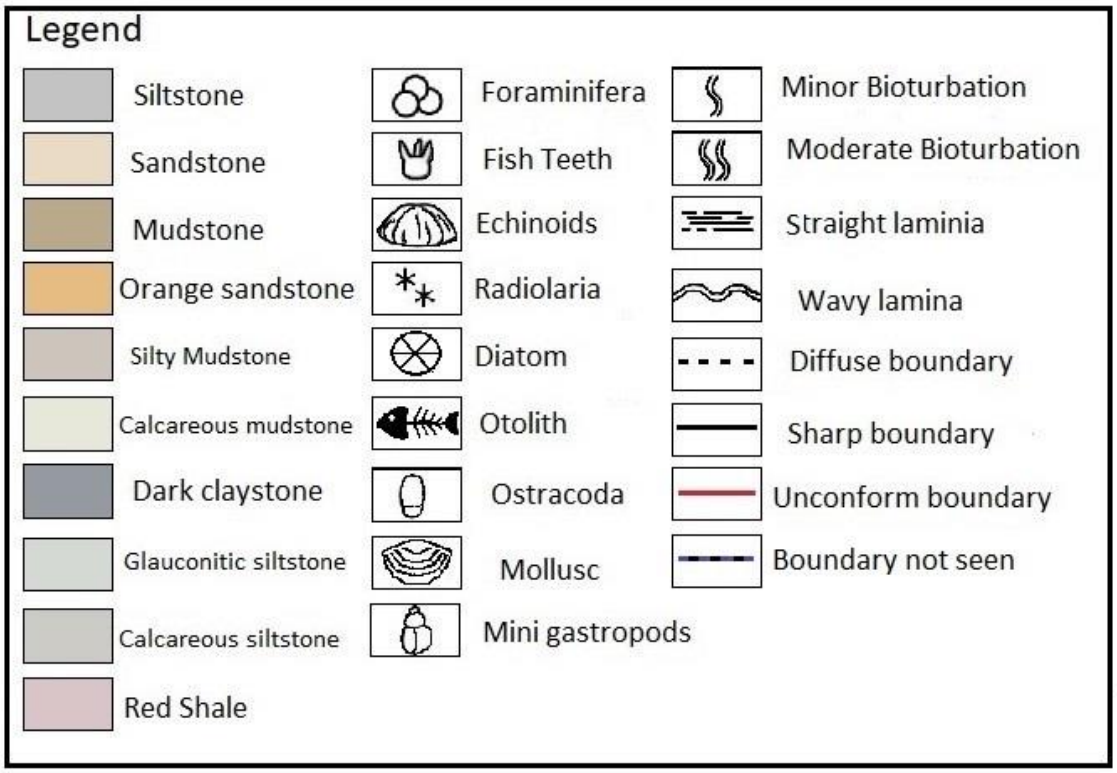

West (Waipatiki to Central Akitio River towards Tawanui)

Age	Stage	Name	Scale (x100m)	Lithology	MUD clay silt	SAND vf f m c vc	Paleodepth Neritic I M O	Oceanic U M L	Fossils	Fossil Number	Notes
Early Miocene	Otaian	Tutamoe	15							F50856	20.2-18.2Ma Thick sandstone base named Westcott in Reid (1998). Fossiliferous upper and bottom contact of Westcott and macrofossils found as lenses in mudstone
	Waitakian-Otaian	Ihungia	14							F50859 F51132 F51133	23.03-18.7Ma Soft mudstone with very thin and sharp sanstone beds (3-5cm)
		Weber Mudstone	13								Mudstone that is often misidentified as Wanstead
	Waitakian	Weber Limestone	12							F50869	25.02-23.03Ma Massive calcareous mudstone
Latest Oligocene- Early Miocene		Weber Flysch	11							F50858	25.2-23.03Ma Intermittedly sandstone bedded mudstone with sharp contacts. Sandstone beds show minor lamina and bioturbation
			10								
			9								
			8								
			7								
Paleocene	Eocene*	Weber Glauconite	6								Glauconitic mudstone with bedded glauconitic sand base
	Teurian	Wanstead	5							F50867	66.0-56.0Ma Massive and easily eroded dark grey claystone
		Te Uri								F50855	Glauconitic mudstone
	Upper Haumurian	Upper Calcerous Member								F50854	79.0-66.04Ma Very calcareous indurated mudstone
Late Cretaceous	Haumurian	Rakauroa Member	4							F50857	Red and black weather shale. No bedding evident and moderately deformed
			3								
			2								
			1								

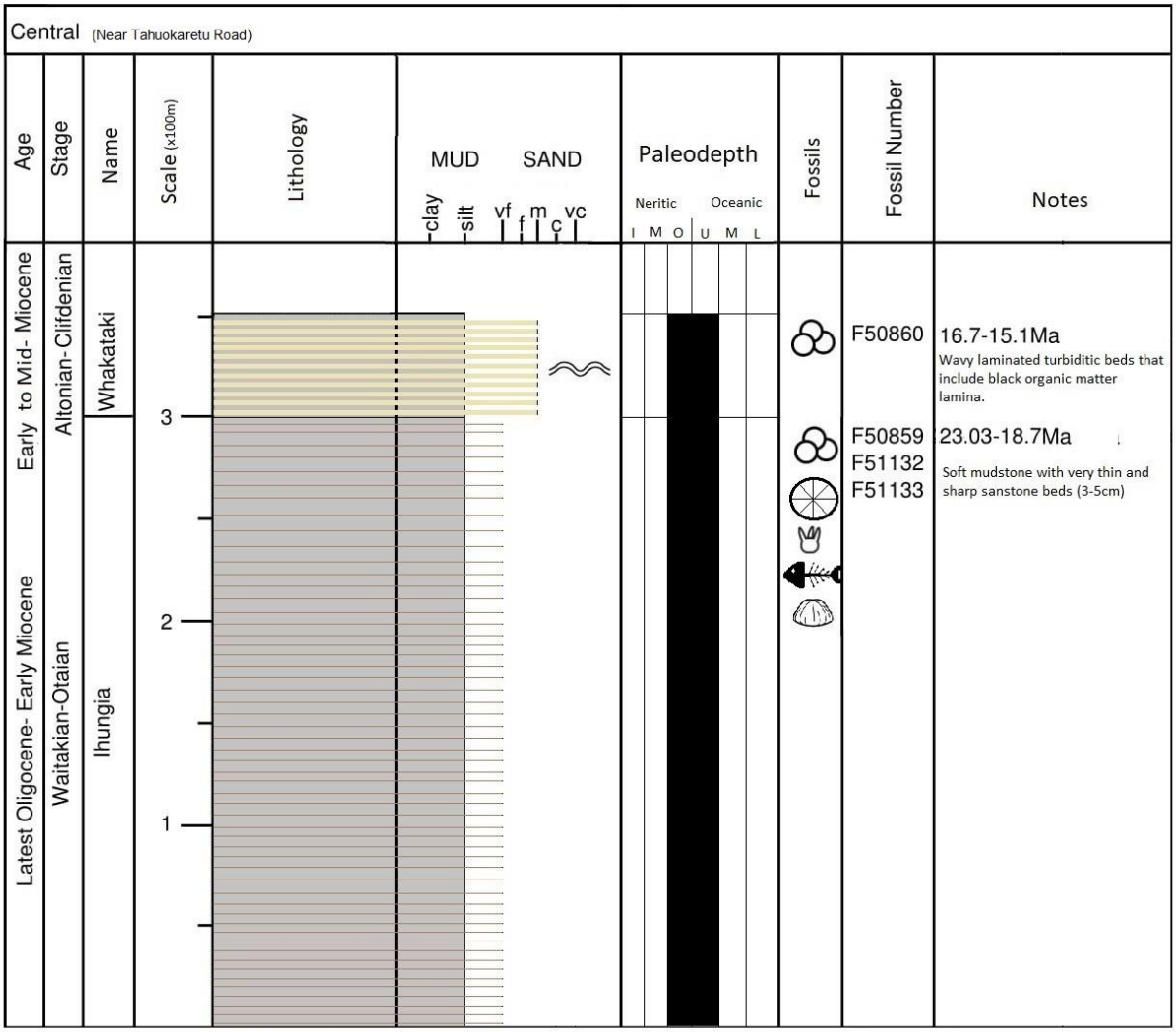
Central (Near Tahuokaretu Road)
Age
Stage
Name
Scale (x100m)
Lithology
MUD
SAND
clay
silt
vf
f
m
c
vc
Paleodepth
Neritic
Oceanic
I M O U M L
Fossils
Fossil Number
Notes
Early to Mid- Miocene
Latest Oligocene- Early Miocene
Altonian-Clifdenian
Waitakian-Otaian
Whakataki
Ihungia
3
2
1
F50860
16.7-15.1Ma
Wavy laminated turbiditic beds that include black organic matter lamina.
F50859
F51132
F51133
23.03-18.7Ma
Soft mudstone with very thin and sharp sanstone beds (3-5cm)

East (Mt McCartie towards Mangatoitoi - Tahuokaretu Stream)

Age	Stage	Name	Scale (x100m)	Lithology	MUD / SAND (clay, silt, vf, f, m, c, vc)	Paleodepth (Neritic: I M O; Oceanic: U M L)	Fossils	Fossil Number	Notes
Late Miocene	Tongaporutuan	McCartie							Biotite rich and friable orange sandstone.
		McCartie Mudstone	15					F51119 F51118 F51122	8.96-7.12Ma Mudstone with two sandstone beds of different thickness. Bottom contacts are sharp and mudstone contants very small (2-4mm) shell fragement lenses.Bioturbation evident and minor some lamina in bottom contact of mudstone
			14						
		Franklin Road						F50864	8.96-7.12Ma 30-50cm alternating sandstone and mudstone layers. Mudstone contains 1-3mm shell fragment lenses and has minor bioturbation
			13						
			12						
			11						
Mid Miocene	Lillburnian	Riddells Culvert						F50862	15.9-13.05Ma Sandstone that grades to mudstone and to siltstone. Wavey bedding and contains black organic matter particles. Either reowrked or turbiditic.
			10						
Early to Mid Miocene	Altonian - Clifdenian	Riddells Mud						F50861	16.7-15.1Ma Massive grey mudstone
			9						
			8						
Early Miocene	Late Altonian	Upper Tahuokaretu						F51126 F51127 F51136	15.9-11.04Ma Alternating mudstone and sandstone with sharp contacts. Sandstone shows minor lamina
	Mid to Late Altonian		7						
		Middle Tahuokaretu						F51128 F51129 F51130 F51134	18.2-11.04Ma Mudstone with sharp sand beds that show minor lamina
			6						
			5						
		Lower Tahuokaretu							Mudstone with moderate sandstone beds (4-5cm). Contacts are sharp
			4						
		Mangato Mudstone							Mudstone with thick laminated sandstone beds (50cm+). Contacts are sharp.
			3						
Latest Oligocene- Early Miocene	Waitakian-Otaian	Ihungia						F50859 F51132 F51133	18.7-23.03Ma Soft mudstone with very thin and sharp sanstone beds (3-5cm)
			2						
			1						

Appendix Three – Cross Section and Balanced Cross Section

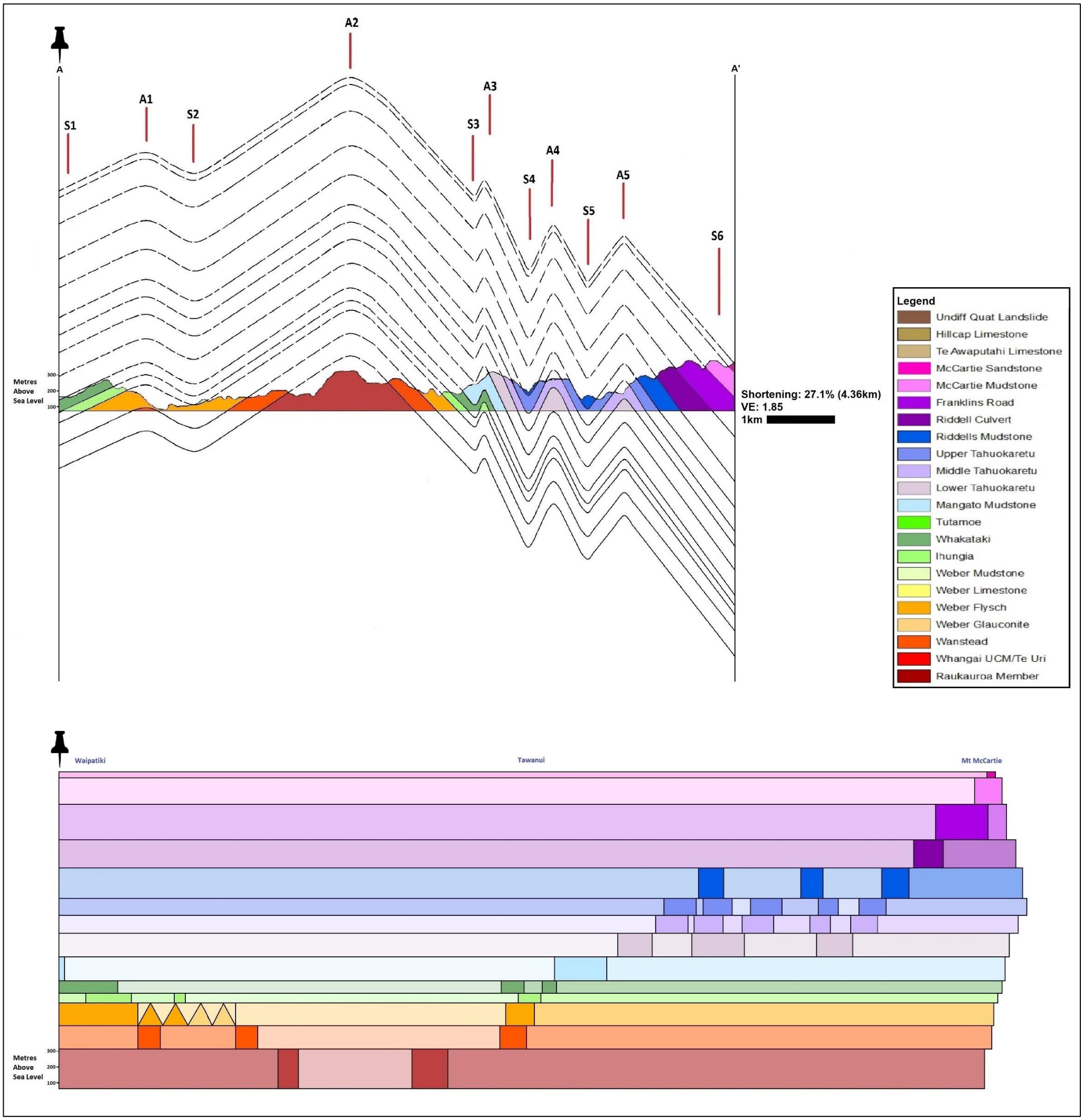

Foraminifera distribution chart (U24 samples) Hannah Harvey_2nd Suite January 2019																							
Fossil record number	U24/f1571	U24/f1572	U24/f1573	U24/f1574	U24/f1575	U24/f1576	U24/f1577	U24/f1578	U24/f1579	U24/f1580	U24/f1581	U24/f1582	U24/f1583	U24/f1584	U24/f1585	U24/f1586	U24/f1587	U24/f1588	U24/f1589	U24/f1590	U24/f1591	U24/f1592	U24/f1593
Field number	1.08	1.27	1.47 (2)	1.47 (gladwrap)	10.10 (1)	10.38 turb	10.56(1)	10.56(2)	11.24 mud	11.24 sand	12.52	2.3	2.39 mud	2.39 silt	2.52	3.12	3.34 mud	3.34 sand	3.5	3.50 (boundary)	Strat (mud)	Strat (sand)	2.34
Lab number	F51127	F51128	F51130	F51129	F51123	F51138	F51124	F51125	F51132	F51133	F51126	F51117	F51118	F51119	F51120	F51131	F51134	F51135	F51122	F51121	F51136	F51137	F51248
Age	Sw	Pl	Sc-Sl	Sl	nf.	Lw-Sl	nf	nf	late Po	Lw-Po	Sl	nd	late Tt	late Tt	nd	nd	Pl	nd	late Tt	nf	Sc	nd	e Po
Paleobathymetry	>800 m	>1500 m	700-1000 m	600-800 m		>1000 m			>700	400-600 m	>600		400-600 m	400-600 m	400-600 m		600-800 m				>1500 m		>1500 m
Agglutinated Foraminifera																							
Ammodiscus archimedis		x							x												x		
Ammodiscus finlayi											x						x				x		
Bathysiphon eocenica	x	x							x	x													
Bathysiphon sp.	x					x			x	x		bits				bits	x	x			x		x
Cyclammina incisa		x									x						x				x	x	
Cyclammina sp.																		x					
Dorothia sp.				x																			
Gaudryina kingi		x																					
Haeuslerella morgani																			x				
Haeuslerella hectori						x			x	x													x
Haplophragmoides sp.	x	x		x					x								x				x		
Hyperammina sp.				x																			
Karreriella bradyi		x							x								x						
Karreriella cushmani									x	x							x						x
Karreriella cylindrica				x		x					x		x	x	x				x				
Karrerulina obscura		x																					
Marinottiella communis		x	x			x			x	x							x		x				x
Schenckiella weymouthi	x																						
Sigmoilopsis schlumbergeri	x	x	x	x					x		x			x			x		x		x		
Spiroplectammina cubensis		x																					
Textularia miozea									x	x							x						
Tritaxilina zealandica		x																			x		x
Trochammina spp.		x																					
Calcareous Foraminifera																							
Amphicoryne hirsuta													x	x	x								
Amphicoryne scalaris				x					x												x		
Anomalina aotea				x																			
Anomalinoides macraglabra																							x
Anomalinoides orbiculus				x		x			x														x
Anomalinoides parvumbilia													x	x					x				
Anomalinoides sp.	x																						
Astacolus sp.									x														
Baggina ampla	x																				x		
Bolivina punctatostriata																	x						
Bolivina sp.		x	x	x		x							x										x
Bolivinita pliobliqua														x					x				
Bolivinita pliozea													x						x				
Bulimina pupula		x							x	x											x		x
Bulimina senta	x	x																			x		
Bulimina striata	x			x													x						x
Bulimina truncanella	x	x																					
Bulimina spp.	x			x																			x
Cancris sp.														x									
Cassidulina cuneata											x												
Cassidulina neocarinata														x									
Cassidulina sp.														x									x
Chilostomella ovoidea			x														x						x

Chilostomelloides sp.									x														x
Cibicides ihungia									x	x				x			x		x				x
Cibicides kullenbergi	x																						
Cibicides deliquatus													x	x									
Cibicides molestus						x			x	x			x	x	x		x		x				x
Cibicides novozelandicus										x													x
Cibicides robertsonianus	x																						
Cibicides spp.	x	x	x	x		x			x	x	x		x	x			x		x		x		x
Dentalina sp.										x													
Discorbinella sp.																							x
Ehrenbergina marwicki																							x
Eponides broeckhianus										x													
Euuvigerina mioshwaggeri				x																			
Euuvigerina miozea									x	x			x	x	x		x		x				x
Euuvigerina sp.			x	x		x					x		x	x								x	
Evolvocassidulina orientalis													x										
Globobulimina pacifica		x	x						x														x
Globocassidulina subglobosa		x		x																	x		
Gyroidina zelandica									x					x			x		x				x
Gyroidinoides neosoldanii	x	x	x	x		x			x	x	x						x				x		
Gyroidinoides spp.													x										
Guttulina sp.									x														
Hoeglundina elegans		x												x									x
Hopkinsina mioindex	x	x				x													x				
Lagena sp.	x								x				x	x			x		x		x		
Laticarinina pauperata	x												x	x									
Lenticulina calcar															x								
Lenticulina dorothiae																	x						
Lenticulina gyroscalprus									x														
Lenticulina mamilligera									x	x													
Lenticulina pusillus																	x						x
Lenticulina vortex										x													
Lenticulina sp.	x	x		x		x			x	x			x	x			x		x			x	x
Marginulina duracina									x														
Melonis sp.	x	x				x											x		x				x
Nodosaria acuminata									x										x		x		x
Nodosaria longiscata	x	x	x	x		x			x	x	x								x		x		x
Nodosaria sp.	x	x		x		x			x	x	x		x	x			x				x		x
Nonionella sp.			x						x														x
Notorotalia sp.				x																		x	
Notorotalia taranakia													x	x	x				x				
Oridorsalis umbonatus	x	x											x				x		x		x		x
Osangularia culter	x																x		x				x
Parafissurina sp.	x	x		x										x							x		
Parvicarinina altocamerata																							x
Planulina weullerstorfi	x			x																	x		
Plectofrondicularia parri									x														
Plectofrondicularia sp.		x												x					x				x
Pleurostomella alternans			x																				
Pleurostomella sp.	x																						
Pseudonodosaria symmetrica				x					x	x													
Pullenia bulloides	x			x		x			x				x	x	x		x		x		x		
Pullenia sp.			x																				
Quinqueloculina spp.	x	x																					x
Rectuvigerina rerensis						x											x						x
Saracenaria italica														x			x						x
Sigmoidella sp.		x																					

Siphouvigerina plebeja		x	x	x										x	x		x		x				x
Sphaeroidina bulloides	x			x					x	x			x	x	x		x		x		x		x
Spiroloculina novozealandicus									x														
Stilostomella pomuligera														x	x				x				
Stilostomella spp.				x						x			x	x			x		x		x		x
Trifarina sp.																	x						3 species
Vaginulina elegans																	x						x
Vaginulina vagina										x													x
Vaginulina spp.				x					x														
Planktic Foraminifera																							
Fohsella peripheronda				x																	x		
Globigerina bulloides										x													x
Globigerina connecta		x															x				x		
Globigerina praebulloides	x	x				x			x				x	x	x				x		x		
Globigerina woodi	x	x	x						x				x	x			x		x		x		
Globigerina spp.		x	x						x				x	x			x		x			x	x
Globigerinita glutinata		x	x														x		x		x		x
Globigerinoides bisphericus		x																					
Globigerinoides trilobus																	x				x		
Globoquadrina dehiscens	x	x	x	x		x			x	x	x						x				x		
Globorotalia miotumida	28s:2d										4s:0d		10s:0d	sinistral					sinistral				
Globorotalia miozea		25s:1d	2s:0d	sinistral													29s:23D				x		
Globorotalia praescitula		x															x						
Globorotalia scitula														x									
Globorotalia zealandica		x															small				cf.		
Neogloboquadrina pachyderma													x	x									
Orbulina suturalis			x								x												
Orbulina universa	x			x															x				
Paragloborotalia bella																	x				x		
Paragloborotalia continuosa																							x
Paragloborotalia incognita									x														
Paragloborotalia mayeri	>5%			x																	x		
Paragloborotalia nana			x																				
Paragloborotalia semivera																							x
Paragloborotalia sp.									x														
Praeorbulina sp.			x								x										x		
Other biogenic material																							
Otoliths																							x
Ostracods																	x						
Fisht teeth	x	x				x	abundant			x			x		x			x					x
Shell hash																		x					
Molluscs				x																			x
Diatoms		x	x														x	x			x		x
Echinoid spines				x		x			x		x			x		x							x
Echinoid plates																							x

Hannah Harvey samples (July 2018)																		
Paleontology list																		
Fossil record number	U24/f1535	U24/f1536	U24/f1537	U24/f1538	U24/f1539	U24/f1540	U24/f1541	U24/f1542	U24/f1543	U24/f1544	U24/f1545	U24/f1546	U24/f1547	U24/f1548	U24/f1549	U24/f1550	U24/f1551	
Field number	HH log (3)	HH 1.2	HH 1.48	HH 3.25 (1)	HH 3.25 (2)	HH 9.16 (sst)	HH 9.16 (mst)	HH 9.18	HH 10.05	HH 10.10	HH 10.23 (1)	HH 11.14	HH 11.20 (sst)	HH 11.2 (mst)	HH 11.33	HH 11.53	HH 12.39	
Sample type	hand specimen	hand specimen	hand specimen	hand specimen	hand specimen	hand specimen	hand specimen	hand specimen	hand specimen	hand specimen	hand specimen	hand specimen	hand specimen	hand specimen	hand specimen	hand specimen	hand specimen	
Identification date	24/07/2018	24/07/2018	24/07/2018	24/07/2018	24/07/2018	24/07/2018	24/07/2018	24/07/2018	24/07/2018	24/07/2018	24/07/2018	24/07/2018	24/07/2018	24/07/2018	24/07/2018	24/07/2018	24/07/2018	
Identifier	Morgans, H.E.G	Morgans, H.E.G	Morgans, H.E.G	Morgans, H.E.G	Morgans, H.E.G	Morgans, H.E.G	Morgans, H.E.G	Morgans, H.E.G	Morgans, H.E.G	Morgans, H.E.G	Morgans, H.E.G	Morgans, H.E.G	Morgans, H.E.G	Morgans, H.E.G	Morgans, H.E.G	Morgans, H.E.G	Morgans, H.E.G	
New Zealand Stage	late Po - early Pl	early Tt	Dt	late Mh	nf	?Sl (Lw-eTt	early Lw	nd	l Lw - e Po	Pl - Sc	early Lw	l Pl - Sc	Sw - Tt	Lw - e Tt	Sc - Sl	nf	early Lw	
Laboratory	GNS	GNS	GNS	GNS	GNS	GNS	GNS	GNS	GNS	GNS	GNS	GNS	GNS	GNS	GNS	GNS	GNS	
Laboratory number	F50856	F50864	F50867	F50854	F50855	F50866	F50870	F50857	F50859	F50860	F50858	F50861	F50868	F50865	F50862	F50863	F50869	
Agglutinated benthic foraminifera																		
Ammodiscus finlayi			x				x								x			
Arenodosaria antipoda									x									
Bathysiphon eocenica							x		x			x			x			
Bathysiphon sp.	x		x	x			x	x		x		x		x			x	
Cyclammina elegans			x															
Cyclammina incisa	x					x	x		x			x						
Cyclammina rotundata												x						
Dorothia elongata				x														
Eggerella columna			x															
Gaudryina healyi				x														
Gaudryina whangaia			x															
Gaudryina sp.												x						
Glomospira charoides			x															
Haeuslerella hectori	x						x		x									
Haeuslerella morgani		x																
Haeuslerella pukeuriensis						x												
Haeuslerella sp.													x	x				
Haplophragmoides sp.	x		x	x			x		x	x	x	x		x				
Hyperammina sp.			x															
Karreriella bradyi																	x	
Karreriella chilostoma																	x	
Karreriella cylindrica		x																
Karreriella cushmani							x		x									
Marinottiella communis	x	x				x	x		x		x	x						
Matanzia varians			x	x														
Rzehakina epigona				x														
Tritaxilina zealandica												x			x			
Schenckiella weymouthi											x						x	
Sigmoilopsis neocelata											x							
Sigmoilopsis schlumbergeri												x			x			
Siphotextularia sp.									x									
Spiroplectammina cubensis																	x	
Spiroplectammina piripaua				x														
Textularia sp.	x	x																
Textularia gladizea						x												
Textularia leuzingeri												x						
Textularia miozea													x					
Textularia plummerae			x															
Calcareous benthic foraminifera																		
Alabamina creta				x														
Allomorphina conica			x															
Amphicoryne scalaris											x							
Amphistegina sp.						x								x				
Anomalinoides parvumbilia	cf.	x											x	x				
Anomalinoides fasciatus									x									
Anomalinoides orbiculus									x									
Anomalinoides sp.		x																

Baggina sp.																	x
Baggina ampla							x										
Bolivina affiliata							x										
Bolivinita pliobliqua		x															
Bulimina aculeata		x															
Bulimina pupula							x		x		x	x					x
Bulimina truncanella							x								x		
Bulimina sp.		x	x	x					x					x			x
Cassidulina cuneata									cf.								
Chilostomella ovoidea									x					x			
Chrysalogonium striatissimum	x										x						
Cibicides deliquatus		x															
Cibicides spp.							x		x				x				
Cibicides ihungia		x					x		x								
Cibicides kullenbergi															x		
Cibicides molestus	x	x				x		contamination	x				x	x			
Cibicides novozelandicus									x								
Cibicides perforatus						x							x				x
Cibicides robertsonianus									x						x		x
Cibicides "teuriensis"			x														
Cibicides Tawanui sp. A			x														
Citharina plumoides			x														
Discorbinella sp.									x								
Elphidium crispum						x							x				
Eponides broeckhianus									x								
Euuvigerina miozea	x	x				x			x					x	x		
Euuvigerina pliozea		x															
Euuvigerina picki									x								x
Euuvigerina rodleyi														x			
Euuvigerina sp.												x	x				
Evolvocassidulina orientalis		x															
Ellipsoglandulina Tawanui sp. A			x														
Globobulimina pacifica	x									x				x			
Globocassidulina cuneata							x										
Globocassidulina subglobosa															x		
Gyroidina zelandica	x	x												x	x		
Gyroidinoides neosoldanii							x		x		x	x					x
Gyroidinoides globosa			x														
Guttulina sp.							x										
Hoeglundina elegans		x													x		
Lagena sp.	x	x										x			x		
Laticarinina pauperata		x					x				x						x
Lenticulina spp.	not on species card	x	x			x			x		x	x	x	x			x
Lenticulina calcar	x	x															
Lenticulina gyroscalprus									x								
Lenticulina mamilligera									x								
Lenticulina pusillus							x										
Lenticulina planula	x																
Lenticulina loculosus							x		x								
Lenticulina navarroensis			x	x													
Lenticulina vortex							x										
Lingulina avellanoides	x																
Melonis sp.	x						x						x				
Nodosarella sp.											x						
Nodosaria sp.							x		x		x	x			x		x
Nodosaria callosa							x		x								
Nodosaria longiscata	x						x				x	x					x
Nonionella magnalingua									x								
Notoplanulina rakauroana				x													
Notorotalia hurupiensis		x											x				
Notorotalia sp.	not on species card	x				x						x		x			

Oridorsalis umbonatus											x	x			x		
Osangularia culter																	x
Parafissurina sp.	x								x			x			x		
Planulina weullerstorfi																	x
Plectofrondicularia pellucida		x															
Plectofrondicularia whaingaroica							x										
Plectofrondicularia sp.									x								
Pleurostomella obtusa											x						x
Parvicarinina altocamerata															x		
Pseudonodosaria symmetrica							x		x								x
Pseudonodosaria sp.											x						
Pullenia bulloides	x						x		x			x			x		x
Pullenia sp.			x														
Quadrimorphina allomorphinoides			x														
Rectobolivina striatula		x															
Rectuvigerina rerensis									x								
Saracenaria sp.									x								
Sphaeroidina bulloides	x	x					x		x			x		x			
Siphonina australis																	x
Siphouvigerina sp.										x							
Siphouvigerina plebeja												x					
Stenioina beccariiformis			x														
Stilostomella pomuligera		x					x										
Stilostomella sp.														x			
Vaginulina elegans	x								x								
Vaginulina vagina							x										
Vaginulina sp.		x					x		x								
Zeaflorilus parri		x															
Planktics																	
Catapsydrax dissimilis							x		x		x						x
Globigerina spp.		x				x	x		x	x	x		x		x		x
Globigerina bulloides							x										
Globigerina connecta									x			x					
Globigerina euapertura							x				x						x
Globigerina praebulloides	x						x		x	x		x			x		x
Globigerina woodi	x	x							x	x		x					
Globigerinita glutinata															x		
Globigerinoides bisphericus												x					
Globigerinoides trilobus												x			x		
Globoquadrina dehiscens						x	x		x		x			x	x		x
Globorotalia miotumida		x													x		
Globorotalia miozea										x		x			x		
Globorotaloides suteri																	x
Globorotaloides testarugosa							x										
Gublerina sp.				x													
Orbulina universa		x															
Paragloborotalia continuosa															x		
Paragloborotalia semivera											x						
Paragloborotalia nana							x										
Paragloborotalia incognita	x																
Paragloborotalia sp.	x									x							
Praeorbulina circularis															x		
Sphaeroidinella grimsdalei												x			x		
Rugolobigerina rugosa				x													

Appendix Five - Macrofossils

Mollusca Bivalvia Glycymeriddidae (*Glycymerita rangatira*)

Age: Mid Miocene to Early Pliocene Sc-Wo (15.9-3.6Ma)

Rock Unit: Shallow-water (sand with decreasing amount of silt/mud) formations in the eastern North Island. Often light to medium grey colour.

Description: Height 85-115mm, thick shelled, higher than long, weakly triangular shape; sculptured with many fine radial grooves.

Habitat: Burrowing shallowly in soft sediments. All records of the genus are from shallow-water (inner or middle shelf) assemblages.

Notes: The largest NZ glycymeridid

Mollusca Bivalvia Crassatellidae (*Eucrassatella australis*)

Age: Early to Late Eocene Dm-Ak (53.3-36Ma)

Rock Unit: Common in shallow-water rocks throughout South Canterbury to North Otago

Description: Length 40-80mm, thick, subtriangular in shape; exterior smooth except for a few ridges near the beak.

Habitat: Burrowing shallowly in soft sediments. Not uncommon in shallow-water, sandy bottom assemblages

Notes: Likely to be reworked into younger geological unit.

Mollusca Scaphopoda*Dentaliidae (Fissidentalium solidum)*

Age: Late Oligocene to Late Miocene (27.3-7.2Ma)

Rock Unit: Common in shallow-water formations

Description: Length 25-30mm (broken), thick, tubular, open both ends; almost straight for most of its length, sculptured with about 45 low, rounded, closely spaced longitudinal ribs; narrow aperture with a long, narrow slit.

Habitat: Partially buried in soft sediments, with the narrow end protruding

Diet: A selective carnivore of foraminifera

Notes: Large ‘tusk shells’ are common in many New Zealand rocks, although the time ranges of most species are poorly understood.

Cnidaria Anthozoa Scleractinia (*Flabellum circulare*)

Age: Middle Eocene to Early Miocene Ab-Po (43-19Ma)

Rock Unit: A wide variety of deep to shallow-water formations

Description: Width 25-50mm, almost circular in side view, but thin and flat and only slightly expanding outwards in the other plane; septae curving outwards at 180°-250° to produce a coin shaped shell.

Habitat: Initially cemented to rocks, but old specimens became recurved to the point where they detached and lay on the seafloor

Notes: Specimens of this flat, almost circular coral usually occur in quite large numbers together on the one bedding plane, and many have the shell dissolved away. At this site specimens are quite large and intact.

Mollusca Gastrpoda Cassidae (*Echinophoria pollens*)

Age: Early to Middle Miocene (21.7-15.1Ma)

Rock Unit: Shallow-water sandstone

Description: Height 45-70mm, sub spherical, with a short spire, mostly enveloped by the last whorl; sculpture of three to five rows of large, pointed nodules on the last whorl, the uppermost also present on the spire; nodules variable in size and spacing, 7-12 per whorl; aperture large, oval, with strongly thickened lips.

Habitat: Epifaunal on soft substrates

Diet: A carnivore, mostly a predator of sea urchins

Notes: This is the most strongly sculptured species of New Zealand Cassidae, and a member of a warm-water genus.

Brachipoda Terebratellidae (*Pachymagas forbesi*)

Age: Early Miocene Pl (18.7-15.9Ma)

Rock Unit: ‘Pachymagas bed” in Otahu Formation (Clifden, Southland) (many East Coast South Island species are found in the Weber region, not confident on specific identification)

Description: Length 40-50mm, evenly oval vertically compressed; smooth apart from a shallowing at hinge, black dull brown colour, thin and fragile, no visual ribs.

Habitat: The small pedicle foramen suggests Pachymagas probably lived lying on the seabed and rolling in currents.

Notes: This large group of smoothed brachiopods with a shallow sulcus in the shell is common in limestone and shallow-water shell-beds throughout the Middle Cenozoic.

Amalda (Gemmuspira) platycephal or Amalda australis?

Age: fossil to recent

Rock unit: unknown

Description: Length 20-25mm (approx., could be broken. Looks olive shell like, pointed top. Wide banded (wrapped look).

Habitat: Shallow to shelf edge

Notes: more identification needed, unbroken samples may be needed.

Naticidae Poliniceinae undifferentiated (*Eunaticina fornicata*?)

Age: Early to Mid-Eocene (Mangaorapan — Bortonian)

Rock unit: unknown

Description: Width visible 20mm, length unknown (looks wider than long), clockwise swirl, top is mostly flat with small but clear centre. Thin ribbing on outer (growth lines).

Habitat: Outer shelf – bathyal.

Distribution: East Coast South Island, Otago.

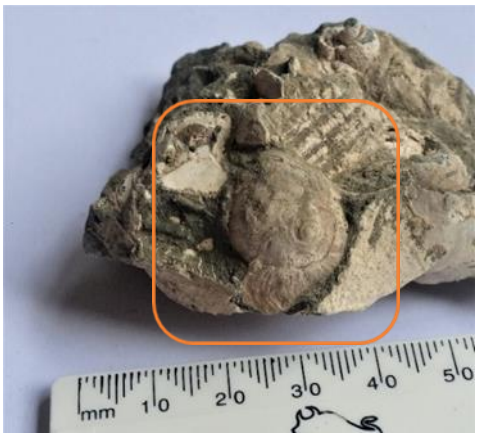

Mauicetus Mandible Bone

Site description: River left facing downstream. Mangapuku stream, just up from large waterfall. Close to where previous fossils were collected (underlying geological unit)

Age: Approximate 22-28Ma

Rock Unit: Reworked shell bed of upper Westcott sandstone

Description: Black 0.5-2cm bone outer, eye shape, linear striations on outer, cauliflower light grey inner with circular structures at corner interior. 35cm in length.

Notes: Ewan Fordyce has informally identified sample as a Mauicetus (undifferentiated) mandible bone.

Appendix Six - Point Counting

Sample Name	Sample Number	Mono Quartz	Poly Quartz	Plag Feldspar	Potass Feldspar	Glauconite	Mica (biotite)	Shell/fossil	Pyrite	Oxides/opaques	Fragments	Matrix	Calcium Carbonate/ Calcite	Organic Matter	total
Turb sand below	3	123	18	4		68	2		8	10	13		70		316
Weber Glauc	4	167				90	7			35		41			340
Waipawa Tawanui	5	82	50	8		168	10		14	17	42				391
Turb sand w black	6	178		38		57	10				30			75	388
Reid wf fossil	7	133	27	53		52		15		22	32	42			376
Weber flysch sand	8	148	80	31		50				22			64		395
Tutamoe Sand	9	178		26		91				29	23	42			389
Ossa Glauc	10	64		8		136				32	94				334
Reid Westcott	12	174		41		45				43	40		10		353
McCartie Sand	13	94	152	40	2	5	8			16	12				329
Waipawa T road	15	131		23		89	2		14	28	35				322
1.20 Sand	16 Sand	70	119	25		57	13	2		8	35				329
1.20 Sand	16 Mud	98		27		26	34	5		28	131		20		369
Waipatki wf Westcott	17	179	30	45		49		2		7			25		337
Waipatiki wf fossils	18	149	106	24		55	8	8		20	30	26	15		441
Millstream Glauc	20	79	6			127			9	17	98				336
Wanstead Glauc	21	78	8			131	5		6	21	71	5			325
Rc sand	b	125		56		75	6		12	36	45	22			377
Riddells mud	c	129		42		47				34	55	61			368
Above turb mud	f	163		45		44	4		6	22	54	28			366
Whangai Te Uri	g	152	68	52			14			24	52	19			381
Tutamoe mud	j	137		45		44	12		9	19	46	25			337
Weber flysch mud	k	85		22		42	8	30		18	74		73		352
Reid wf u mud	l	105		10		31		14		9	92	37		17	315

						Measured major elements (wt%)																				
Sample Name	**Age**	**Preparation name**	**Ignited mass**	**Additive mass**		**SiO2**	**TiO2**	**Al2O3**	**Fe2O3T**	**MnO**	**MgO**	**CaO**	**Na2O**	**K2O**	**P2O5**	**SO3**	**LOI_{550}**	**LOI_{900}**	**LOI_T**	**Measured total**	**$C_{inorganic}$**	**F1**	**F2**	**Carbonate-free total**	**$f_{carbonate-free}$**	**$CaO_{carbonate-free}$**
Scallop Limestone	Plio–Pleistocene	57-43 Bead	0.81	8.334		8.2	0.08	1.63	1.2	0.03	0.71	47.04	0.38	0.31	0.08	0.03	1.03	35.12	39.36	99.05	35.12	20.40	13.78	14.73	0.15	1.05
Hillcap Limestone	Plio–Pleistocene	57-43 Bead	0.804	8.046		2.81	0.03	0.65	0.82	0.02	0.34	51.39	0.12	0.11	0.05	0.02	0.57	25.94	42.41	98.77	25.94	22.95	15.45	7.09	0.07	1.55
Te Awaputahi Limestone	Plio–Pleistocene	57-43 Bead	0.805	8.012		28.83	0.18	4.37	1.28	0.02	0.96	33.96	1.18	0.75	0.15	0.03	1.06	25.54	28.34	100.05	25.54	13.38	9.79	39.85	0.40	1.04
McCartie Sand	Late Miocene	57-43 Bead	0.86	8.018		75.56	0.43	11.49	3.23	0.04	0.97	1.01	2.86	2	0.1	0	2.01	2.89	3.16	100.86	2.89	-2.25	-0.27	98.96	0.98	0.27
Franklin Road Sand	Miocene	57-43 Bead	0.818	8.018		74.36	0.46	12.15	3.2	0.04	1.17	1.35	2.9	2.15	0.1	0.02	1.84	2.70	3.09	100.98	2.70	-2.18	-0.01	98.78	0.98	0.39
Franklin Road Mud	Miocene	57-43 Bead	0.823	8.096		62.91	0.62	14.43	4.38	0.05	1.77	3.71	2.62	2.6	0.15	0.07	1.80	5.22	6.5	99.82	5.22	-0.32	0.51	91.96	0.92	0.56
Riddells mud	Miocene	57-43 Bead	0.804	8.011		57.34	0.6	13.99	4.68	0.05	1.62	4.98	1.96	2.44	0.1	0.06	3.10	7.71	10.07	97.89	7.71	0.54	-0.08	86.44	0.88	0.51
Riddells culvert flow banding	Miocene	57-43 Bead	0.805	8.021		68.9	0.53	14.23	3.72	0.03	1.18	1.65	3.32	2.57	0.11	0.05	2.10	3.34	4.06	100.34	3.34	-0.77	1.38	97.13	0.97	0.39
Riddells culvert mud	Miocene	57-43 Bead	0.81	8.014		61.65	0.64	15.11	5.05	0.05	1.65	3.34	2.74	2.66	0.13	0.1	3.01	5.65	6.88	99.98	5.65	0.51	0.63	93.25	0.93	0.46
Riddells culvert sand	Miocene	57-43 Bead	0.841	8.043		75.25	0.39	12.78	2.6	0.03	0.86	0.91	3.58	2.52	0.09	0.01	1.14	1.81	2.28	101.3	1.81	-2.04	1.85	99.65	0.98	0.39
Tutamoe Sand	Otaian/ Early Miocene	57-43 Bead	0.805	8.085		72.28	0.42	13.33	3.42	0.02	0.83	0.68	3.31	2.71	0.08	0.02	2.33	3.10	3.49	100.57	3.10	-1.60	1.50	98.92	0.98	0.17
Tutamoe mud	Otaian/ Early Miocene	57-43 Bead	0.835	8.014		68.65	0.55	14.1	4.03	0.03	1.3	1.23	3.11	2.73	0.1	0.06	2.78	3.55	4.19	100.06	3.55	-1.39	0.90	97.71	0.98	0.27
Waipatki waterfall Westcott	Otaian–Altonian/Early Miocene	57-43 Bead	0.805	8.021		68.93	0.35	9.75	1.86	0.03	0.6	6.57	2.56	2.25	0.05	0.01	1.19	6.42	6.82	99.79	6.42	-0.68	2.69	88.38	0.89	0.80
Waipatiki waterfall fossils	Otaian–Altonian/Early Miocene	57-43 Bead	0.807	8.036		66.45	0.13	2.55	9.1	0.03	0.97	1.92	0.46	1.55	0.06	0.28	1.72	14.73	15.28	98.77	14.73	-2.79	-6.28	83.40	0.84	0.10
Reid Westcott	Otaian–Altonian/Early Miocene	57-43 Bead	0.801	8.003		77.12	0.34	11.92	2.14	0.02	0.69	0.59	3.06	2.64	0.06	0	1.41	2.02	2.25	100.85	2.02	-3.18	1.34	99.63	0.99	0.23
Reid waterfall fossil base	Otaian–Altonian/Early Miocene	57-43 Bead	0.813	8.031		57.01	0.36	10.28	3.05	0.11	0.96	12.69	2.4	2.12	0.73	0.02	1.64	11.12	11.39	101.11	11.12	3.83	4.28	79.58	0.79	0.90
Whakataki mud	Early Miocene	57-43 Bead	0.805	8.121		63.44	0.66	14.52	5.02	0.03	1.75	2.17	2.44	2.49	0.11	0.07	3.75	5.44	6.88	99.59	5.44	-0.73	-0.70	94.59	0.95	0.31
Whakataki sand below	Early Miocene	57-43 Bead	0.832	8.143		72.42	0.48	12.5	3.2	0.02	1.13	1.91	2.73	2.28	0.11	0.09	2.59	3.74	4.44	101.3	3.74	-1.84	0.25	97.95	0.97	0.40
Whakataki sand with black	Early Miocene	57-43 Bead	0.831	8.009		68.45	0.46	11.4	3.88	0.02	1.03	2.45	2.4	2.12	0.11	0.15	4.61	5.83	7.5	99.98	5.83	-1.45	-0.37	94.96	0.95	0.33
Reid waterfall under mud	Altonian/ Early Miocene	57-43 Bead	0.814	8.129		67.58	0.59	15.03	4.33	0.03	1.42	1.27	3.11	2.7	0.13	0.02	2.79	3.77	4.35	100.55	3.77	-0.79	0.74	97.99	0.97	0.26
Waipatiki house under mud	Altonian/ Early Miocene	57-43 Bead	0.821	8.012		51.22	0.45	10.02	3.41	0.03	1.4	14.02	1.27	1.78	0.1	0.2	2.41	14.01	15.75	99.64	14.01	3.79	2.14	73.08	0.73	0.79
Ihungia	Altonian/ Early Miocene	57-43 Bead	0.81	8.02		61.51	0.65	15.69	4.75	0.03	2.03	3.07	2.67	2.53	0.13	0.14	2.72	5.91	6.95	100.16	5.91	0.00	-0.09	93.26	0.93	0.41
Weber flysch sand	Late Oligocene	57-43 Bead	0.816	8.169		60.05	0.29	7.81	3.49	0.03	0.7	13.05	1.73	1.84	0.1	0.18	1.78	12.02	11.36	100.65	12.02	3.41	3.03	78.85	0.78	0.85
Weber flysch mud	Late Oligocene	57-43 Bead	0.822	8.021		46.47	0.41	8.91	3.2	0.03	1.14	16.73	0.99	1.6	0.1	0.11	2.64	16.66	18.05	97.72	16.66	5.16	2.91	66.38	0.68	0.79
Weber Limestone	Late Eocene – Early Oligocene	57-43 Bead	0.816	8.06		48.68	0.38	7.57	2.68	0.02	0.87	18.66	0.65	1.13	0.12	0.15	2.50	17.53	19.16	100.08	17.53	6.01	2.92	65.59	0.66	0.84
Weber Glauconite	Late Eocene	12-22 Bead	0.809	8.064		53.92	0.27	6.24	3.75	0.01	0.98	15.71	0.87	1.52	0.35	0.02	1.91	14.53	16.27	99.91	14.53	3.86	1.97	70.68	0.71	0.85
Wanstead Glauconite	Early–mid Eocene	57-43 Bead	0.827	8.018		63.65	0.26	6.96	12.71	0.02	2	0.39	0.42	3.94	0.08	0.01	3.51	4.66	8.35	98.8	4.66	-3.04	-5.31	93.62	0.95	0.07

Wanstead	Early–mid Eocene	57-43 Bead	0.804	8.008		57.53	0.44	9.93	3.03	0.02	1.22	11.31	0.66	1.5	0.1	0.14	3.13	12.46	14.12	100.01	12.46	2.10	-0.05	78.41	0.78	0.71
Millstream Glauconite	Unknown	57-43 Bead	0.808	8.017		59.14	0.32	9.4	3.05	0.05	0.77	18.69	2.22	2.08	0.08	0.04	2.56	3.71	5.41	101.25	3.71	7.31	6.72	83.66	0.83	3.95
Ossa Glauconite	Early Paleocene	57-43 Bead	0.805	8.057		76.54	0.21	4.41	9.42	0.04	1.3	0.56	0.52	2.35	0.07	0.05	3.20	4.33	5.13	100.59	4.33	-3.84	-5.94	98.21	0.98	0.10
Waipawa T-road	Early Paleocene	57-43 Bead	0.82	8.02		67.53	0.3	7	5.39	0.02	1.13	7.67	1.41	1.95	0.52	0.23	1.58	7.22	7.31	100.46	7.22	0.08	-0.66	87.89	0.87	0.83
Waipawa Tawanui	Early Paleocene	57-43 Bead	0.807	8.008		65.34	0.27	6.85	12.16	0.01	2.08	0.97	0.54	3.88	0.08	0.12	3.17	4.92	6.94	99.24	4.92	-3.17	-4.92	94.66	0.95	0.15
Te Uri Member Whangai	Early Paleocene	57-43 Bead	0.805	8.025		79.78	0.32	7.09	3.9	0.01	1.01	0.68	1.17	1.73	0.27	0.1	2.18	3.33	4.44	100.51	3.33	-5.01	-3.86	97.72	0.97	0.16
Upper Calcareous Member Whangai	Late Cretaceous	57-43 Bead	0.807	8.024		66.99	0.32	7.53	1.92	0.02	1.12	8.61	0.59	1.24	0.12	0.11	2.33	9.45	11.04	99.6	9.45	-1.22	-1.54	83.01	0.83	0.72
Rakauroa Member Whangai	Late Cretaceous	57-43 Bead	0.804	8.006		84.7	0.3	6.65	1.89	0.01	0.62	0.07	0.37	1.11	0.05	0.01	2.67	3.63	4.41	100.18	3.63	-6.21	-5.28	98.39	0.98	0.02

	Trace elements (ppm), CORRECTED FOR CARBONATE																																		Trace element ratios			
Sample Name	**S**	**F**	**Cl**	**V**	**Mn**	**Co**	**Cu**	**Zn**	**Ga**	**As**	**Cs**	**Rb**	**Ba**	**Th**	**U**	**Nb**	**K**	**La**	**Ce**	**Pb**	**Nd**	**Sr**	**P**	**Zr**	**Ti**	**Sc**	**Y**	**Cr**	**Ni**	**Mo**	**Sn**	**Sb**	**Tl**		**La/Sc**	**Ti/Zr**	**Zr/Sc**	**Th/S**
Scallop Limestone	6925	3510	1728	195	1627	0	54	128	13	13	7	94	598	40	27	7	8651	34	108	20	54	5500	1174	222	3224	410	34	0	13	34	0	0	0		0.08	14.5	0.54	0.10
Hillcap Limestone	12756	5459	3607	251	2158	14	97	195	0	28	14	111	585	70	56	14	6358	70	0	70	111	6754	1519	251	2504	989	56	0	28	56	0	0	0		0.07	10.0	0.25	0.07
Te Awaputahi Limestone	3191	984	1664	83	495	18	18	63	10	8	3	73	459	15	10	5	7815	30	58	10	20	2116	822	161	2708	95	15	53	20	13	0	0	0		0.32	16.9	1.68	0.16
McCartie Sand	1861	501	17215	82	435	11	7	45	12	6	5	67	447	5	4	5	8460	9	43	9	20	206	222	111	2627	8	10	50	15	5	1	0	0		1.13	23.6	13.63	0.63
Franklin Road Sand	3347	596	459	80	366	10	9	50	13	5	7	78	515	6	4	6	9122	16	45	10	22	260	223	164	2818	9	14	51	14	5	2	2	0		1.78	17.2	17.78	0.67
Franklin Road Mud	6810	426	378	112	471	15	15	81	18	5	8	117	519	10	4	10	11714	25	65	14	27	304	355	208	4034	14	21	64	25	5	5	5	0		1.77	19.4	14.77	0.69
Riddells mud	3116	444	177	131	470	9	25	87	20	6	5	135	617	10	5	11	11468	23	61	18	26	391	247	213	4072	16	23	57	15	6	3	3	0		1.43	19.1	13.43	0.64
Riddells culvert flow banding	3988	571	333	87	291	8	10	60	15	6	6	95	532	7	4	7	11019	17	51	12	23	253	248	228	3281	11	15	89	12	5	3	3	0		1.45	14.4	20.09	0.64
Riddells culvert mud	7369	756	1621	116	416	12	18	77	19	6	9	116	502	11	4	9	11837	18	56	15	25	284	304	183	4112	15	19	53	14	5	3	3	0		1.21	22.4	12.21	0.71
Riddells culvert sand	4793	482	2612	59	221	9	7	44	12	10	7	77	561	5	4	5	10633	11	42	11	17	238	200	179	2376	8	12	114	12	5	1	2	0		1.38	13.3	22.00	0.63
Tutamoe Sand	10294	639	462	99	258	12	11	61	15	7	7	89	476	8	4	6	11435	17	54	14	25	233	177	188	2559	12	14	38	12	5	1	0	0		1.42	13.6	15.42	0.67
Tutamoe mud	10315	461	456	100	262	12	12	65	16	7	7	97	484	8	4	7	11603	20	48	17	29	252	223	209	3376	12	16	41	13	5	1	1	0		1.67	16.2	17.00	0.67
Waipatki waterfall Westcott	620	495	371	61	252	9	7	38	9	7	3	77	495	6	5	6	10544	16	52	14	23	270	123	491	2368	11	16	36	9	7	3	5	0		1.40	4.8	43.50	0.50
Waipatiki waterfall fossils	1595	657	557	49	371	5	8	44	11	9	7	73	311	5	5	6	7619	19	41	13	25	578	155	351	923	15	15	109	8	6	5	5	0		1.23	2.6	22.77	0.31
Reid Westcott	438	674	990	62	180	7	7	40	12	8	8	78	555	5	4	5	11091	13	44	14	21	198	133	192	2063	8	10	40	7	5	2	2	0		1.63	10.7	23.75	0.63
Reid waterfall fossil base	985	1750	792	95	1141	11	10	57	14	17	3	89	501	5	5	6	11180	29	72	17	34	479	2024	274	2741	14	29	42	13	6	0	0	0		2.09	10.0	19.64	0.36
Whakataki mud	9779	413	94	123	300	12	19	82	17	6	7	101	422	8	4	7	10881	17	41	17	22	288	253	187	4165	16	17	56	16	5	2	3	0		1.07	22.2	11.87	0.53
Whakataki sand below	8967	489	150	85	200	8	12	56	12	7	4	73	419	4	4	5	9787	11	42	10	23	263	248	177	2975	11	12	85	16	5	1	2	0		1.00	16.8	15.55	0.36
Whakataki sand with black	28129	466	139	98	181	8	14	61	14	11	6	69	440	4	4	4	9264	13	46	12	22	254	253	160	2903	11	12	51	17	5	0	0	0		1.20	18.1	15.20	0.40
Reid waterfall under mud	2123	824	490	108	297	11	14	71	16	7	7	96	472	8	4	7	11499	19	48	15	24	217	291	211	3628	14	17	44	12	5	2	3	0		1.36	17.2	14.71	0.57
Waipatiki house under mud	9868	758	564	110	292	5	18	101	16	5	7	112	410	7	5	8	10073	12	42	12	22	679	298	241	3677	16	16	67	19	7	1	4	0		0.75	15.2	14.75	0.42
Ihungia	7589	421	191	107	285	10	15	92	19	4	4	98	409	11	4	9	11278	24	61	15	28	345	305	206	4184	15	21	43	15	5	3	3	0		1.57	20.3	13.71	0.71
Weber flysch sand	14434	540	6999	59	348	10	9	115	11	8	1	69	540	4	5	4	9748	15	43	13	19	340	279	204	2219	18	14	97	27	6	0	0	0		0.86	10.9	11.43	0.21
Weber flysch mud	7148	577	237	125	328	6	35	107	18	6	3	113	630	7	6	9	9776	16	50	13	21	955	321	221	3617	21	21	71	21	7	6	7	0		0.79	16.4	10.71	0.36
Weber Limestone	5752	598	125	90	223	3	29	87	12	8	3	78	809	8	6	8	7156	12	27	8	17	1019	400	204	3475	26	17	52	24	8	2	5	0		0.47	17.0	7.88	0.29
Weber Glauconite	1307	1519	455	103	151	7	21	95	13	4	1	92	944	6	6	6	8917	21	47	6	30	725	1080	188	2287	24	31	127	11	7	1	1	0		0.88	12.2	7.82	0.24
Wanstead Glauconite	229	414	168	149	265	9	24	106	22	2	8	198	786	4	4	5	17258	5	19	8	14	63	184	115	1644	12	8	331	0	5	2	1	0		0.45	14.3	9.91	0.36
Wanstead	9938	500	342	94	219	18	20	89	15	4	3	91	718	6	5	8	7941	18	41	13	18	490	278	181	3363	17	17	59	33	6	1	3	0		1.08	18.6	10.92	0.38
Millstream Glauconite	6111	1011	373067	81	272	17	13	191	10	5	1	25	232	4	5	0	10449	6	18	0	10	16	211	0	2321	10	0	420	7	5	0	0	0		0.63			0.38
Ossa Glauconite	4626	768	94163	131	323	13	10	207	15	5	2	84	1069	3	4	1	9990	5	17	1	8	78	156	48	1289	16	5	326	9	4	0	0	0		0.31	26.8	2.94	0.19
Waipawa T-road	11965	1242	505	93	239	17	6	114	15	7	2	89	467	5	5	5	9251	33	75	9	31	200	1297	161	2055	18	48	248	23	6	2	3	0		1.81	12.8	8.81	0.25
Waipawa Tawanui	19389	831	205	127	131	13	10	122	21	7	6	180	366	3	4	4	16884	5	18	5	12	73	183	102	1697	15	10	427	6	9	2	1	0		0.36	16.7	6.93	0.21
Te Uri Member Whangai	20812	403	133	80	105	15	8	73	10	6	9	70	425	3	4	4	7386	22	49	5	28	105	606	112	1973	12	16	146	13	5	1	1	0		1.75	17.6	9.08	0.25
Upper Calcareous Member Whangai	5897	470	4486	70	184	6	16	79	12	5	5	68	506	4	5	5	6175	13	40	8	18	335	314	109	2301	11	24	34	18	6	6	4	0		1.22	21.1	10.11	0.33
Rakauroa Member Whangai	2138	399	208	55	57	9	17	43	9	3	2	52	403	5	4	5	4691	5	18	6	14	43	111	74	1831	6	7	39	9	5	3	4	0		0.83	24.6	12.17	0.83

	Major elements (wt%), CORRECTED FOR CARBONATE																
Sample Name	**SiO2**	**TiO2**	**Al2O3**	**Fe2O3T**	**MnO**	**MgO**	**CaO**	**Na2O**	**K2O**	**P2O5**	**SO3**	**LOI_{550}**	**Total**	**F1**	**F2**	**Anhydrous total**	**$f_{anhydrous}$**
Scallop Limestone	55.13	0.54	10.96	8.07	0.20	4.77	7.07	2.55	2.08	0.54	0.20	6.93	99.05	-1.32	-3.49	91.91	0.92
Hillcap Limestone	39.13	0.42	9.05	11.42	0.28	4.73	21.65	1.67	1.53	0.70	0.28	7.91	98.77	9.55	-0.17	90.58	0.91
Te Awaputahi Limestone	72.38	0.45	10.97	3.21	0.05	2.41	2.62	2.96	1.88	0.38	0.08	2.66	100.05	-3.59	-1.25	97.32	0.97
McCartie Sand	77.01	0.44	11.71	3.29	0.04	0.99	0.28	2.91	2.04	0.10	0.00	2.05	100.86	-2.58	-0.47	98.81	0.99
Franklin Road Sand	76.02	0.47	12.42	3.27	0.04	1.20	0.40	2.96	2.20	0.10	0.02	1.88	100.98	-2.63	-0.28	99.08	0.99
Franklin Road Mud	68.29	0.67	15.66	4.75	0.05	1.92	0.61	2.84	2.82	0.16	0.08	1.96	99.82	-1.68	-0.36	97.79	0.98
Riddells mud	64.93	0.68	15.84	5.30	0.06	1.83	0.57	2.22	2.76	0.11	0.07	3.51	97.89	-1.30	-1.40	94.31	0.94
Riddells culvert flow banding	71.18	0.55	14.70	3.84	0.03	1.22	0.40	3.43	2.65	0.11	0.05	2.17	100.34	-1.30	1.08	98.12	0.98
Riddells culvert mud	66.10	0.69	16.20	5.41	0.05	1.77	0.50	2.94	2.85	0.14	0.11	3.23	99.98	-0.70	-0.18	96.65	0.97
Riddells culvert sand	76.50	0.40	12.99	2.64	0.03	0.87	0.40	3.64	2.56	0.09	0.01	1.16	101.30	-2.25	1.76	100.13	1.00
Tutamoe Sand	73.48	0.43	13.55	3.48	0.02	0.84	0.18	3.37	2.76	0.08	0.02	2.37	100.57	-1.80	1.41	98.18	0.98
Tutamoe mud	70.30	0.56	14.44	4.13	0.03	1.33	0.28	3.18	2.80	0.10	0.06	2.85	100.06	-1.81	0.65	97.15	0.97
Waipatki waterfall Westcott	77.83	0.40	11.01	2.10	0.03	0.68	0.91	2.89	2.54	0.06	0.01	1.34	99.79	-3.61	1.07	98.44	0.98
Waipatiki waterfall fossils	78.70	0.15	3.02	10.78	0.04	1.15	0.12	0.54	1.84	0.07	0.33	2.04	98.77	-2.96	-7.11	96.40	0.96
Reid Westcott	78.06	0.34	12.07	2.17	0.02	0.70	0.23	3.10	2.67	0.06	0.00	1.43	100.85	-3.33	1.28	99.42	0.99
Reid waterfall fossil base	72.44	0.46	13.06	3.88	0.14	1.22	1.14	3.05	2.69	0.93	0.03	2.09	101.11	-1.90	0.73	99.00	0.99
Whakataki mud	66.79	0.69	15.29	5.29	0.03	1.84	0.33	2.57	2.62	0.12	0.07	3.94	99.59	-1.49	-1.23	95.57	0.96
Whakataki sand below	74.90	0.50	12.93	3.31	0.02	1.17	0.41	2.82	2.36	0.11	0.09	2.68	101.30	-2.55	-0.19	98.53	0.99
Whakataki sand with black	72.07	0.48	12.00	4.09	0.02	1.08	0.35	2.53	2.23	0.12	0.16	4.85	99.98	-2.42	-1.00	94.97	0.95
Reid waterfall under mud	69.34	0.61	15.42	4.44	0.03	1.46	0.27	3.19	2.77	0.13	0.02	2.86	100.55	-1.21	0.49	97.67	0.98
Waipatiki house under mud	69.84	0.61	13.66	4.65	0.04	1.91	1.07	1.73	2.43	0.14	0.27	3.29	99.64	-2.64	-2.49	96.08	0.96
Ihungia	66.06	0.70	16.85	5.10	0.03	2.18	0.44	2.87	2.72	0.14	0.15	2.92	100.16	-1.09	-0.84	97.09	0.97
Weber flysch sand	76.65	0.37	9.97	4.45	0.04	0.89	1.09	2.21	2.35	0.13	0.23	2.27	100.65	-2.73	-1.05	98.15	0.98
Weber flysch mud	68.41	0.60	13.12	4.71	0.04	1.68	1.16	1.46	2.36	0.15	0.16	3.88	97.72	-2.56	-2.75	93.68	0.94
Weber Limestone	74.28	0.58	11.55	4.09	0.03	1.33	1.27	0.99	1.72	0.18	0.23	3.82	100.08	-2.81	-3.85	96.03	0.96
Weber Glauconite	76.21	0.38	8.82	5.30	0.01	1.39	1.20	1.23	2.15	0.49	0.03	2.69	99.91	-3.73	-3.58	97.19	0.97
Wanstead Glauconite	67.17	0.27	7.34	13.41	0.02	2.11	0.07	0.44	4.16	0.08	0.01	3.70	98.80	-2.91	-5.38	95.09	0.95
Wanstead	73.38	0.56	12.66	3.86	0.03	1.56	0.91	0.84	1.91	0.13	0.18	3.99	100.01	-3.15	-4.10	95.84	0.96
Millstream Glauconite	71.58	0.39	11.38	3.69	0.06	0.93	4.78	2.69	2.52	0.10	0.05	3.10	101.25	-0.23	1.77	98.11	0.98
Ossa Glauconite	78.39	0.22	4.52	9.65	0.04	1.33	0.10	0.53	2.41	0.07	0.05	3.28	100.59	-4.01	-6.12	97.26	0.97
Waipawa T-road	77.18	0.34	8.00	6.16	0.02	1.29	0.95	1.61	2.23	0.59	0.26	1.81	100.46	-3.42	-3.19	98.39	0.98
Waipawa Tawanui	68.50	0.28	7.18	12.75	0.01	2.18	0.16	0.57	4.07	0.08	0.13	3.32	99.24	-3.41	-5.20	95.79	0.96
Te Uri Member Whangai	82.06	0.33	7.29	4.01	0.01	1.04	0.16	1.20	1.78	0.28	0.10	2.24	100.51	-5.22	-4.01	98.17	0.98
Upper Calcareous Member Whangai	80.38	0.38	9.04	2.30	0.02	1.34	0.86	0.71	1.49	0.14	0.13	2.80	99.60	-5.48	-4.63	96.67	0.97
Rakauroa Member Whangai	86.24	0.31	6.77	1.92	0.01	0.63	0.02	0.38	1.13	0.05	0.01	2.71	100.18	-6.19	-5.28	97.46	0.97

	UCC-normalised trace elements, CORRECTED FOR CARBONATE																				Major elements (wt%), CORRECTED FOR CARBONATE and NORMALISED TO 100 WT% ANHYDROUS												
Sample Name	**Cs**	**Rb**	**Ba**	**Th**	**U**	**Nb**	**K**	**La**	**Ce**	**Pb**	**Nd**	**Sr**	**P**	**Zr**	**Ti**	**Sc**	**Y**	**Cr**	**Ni**		**SiO2**	**TiO2**	**Al2O3**	**Fe2O3**	**MnO**	**MgO**	**CaO**	**Na2O**	**K2O**	**P2O5**	**Total**	**F1**	**F2**
Scallop Limestone	1.37	1.12	0.95	3.84	9.96	0.56	0.74	1.08	1.71	1.19	1.99	17.19	3.59	1.15	0.84	29.29	1.60		0.29		59.98	0.59	11.92	8.78	0.22	5.19	7.69	2.78	2.27	0.59	100.00	-0.63	-3.19
Hillcap Limestone	2.84	1.33	0.93	6.63	20.63	1.16	0.55	2.25		4.10	4.13	21.11	4.64	1.30	0.65	70.62	2.65		0.59		43.20	0.46	9.99	12.61	0.31	5.23	23.90	1.84	1.69	0.77	100.00	11.49	0.52
Te Awaputahi Limestone	0.51	0.87	0.73	1.43	3.72	0.42	0.67	0.97	0.92	0.59	0.74	6.61	2.51	0.83	0.71	6.81	0.72	0.57	0.43		74.37	0.46	11.27	3.30	0.05	2.48	2.69	3.04	1.93	0.39	100.00	-3.44	-1.09
McCartie Sand	1.04	0.80	0.71	0.49	1.51	0.42	0.73	0.30	0.68	0.54	0.75	0.64	0.68	0.58	0.68	0.58	0.49	0.54	0.33		77.93	0.44	11.85	3.33	0.04	1.00	0.28	2.95	2.06	0.10	100.00	-2.50	-0.39
Franklin Road Sand	1.46	0.92	0.82	0.58	1.51	0.51	0.78	0.53	0.71	0.60	0.83	0.81	0.68	0.85	0.73	0.66	0.68	0.56	0.30		76.72	0.47	12.54	3.30	0.04	1.21	0.40	2.99	2.22	0.10	100.00	-2.57	-0.22
Franklin Road Mud	1.55	1.40	0.83	0.93	1.61	0.81	1.01	0.81	1.03	0.83	1.01	0.95	1.09	1.08	1.05	1.01	0.98	0.70	0.53		69.83	0.69	16.02	4.86	0.06	1.96	0.62	2.91	2.89	0.17	100.00	-1.51	-0.22
Riddells mud	0.92	1.60	0.98	0.97	1.68	0.94	0.99	0.73	0.97	1.07	0.96	1.22	0.75	1.10	1.06	1.13	1.08	0.62	0.31		68.85	0.72	16.80	5.62	0.06	1.95	0.61	2.35	2.93	0.12	100.00	-0.83	-1.08
Riddells culvert flow banding	1.26	1.13	0.85	0.69	1.53	0.60	0.95	0.53	0.80	0.73	0.84	0.79	0.76	1.18	0.86	0.81	0.74	0.97	0.26		72.54	0.56	14.98	3.92	0.03	1.24	0.41	3.50	2.71	0.12	100.00	-1.15	1.23
Riddells culvert mud	1.75	1.38	0.80	1.02	1.59	0.71	1.02	0.59	0.88	0.88	0.91	0.89	0.93	0.95	1.07	1.07	0.92	0.57	0.30		68.39	0.71	16.76	5.60	0.06	1.83	0.51	3.04	2.95	0.14	100.00	-0.41	0.05
Riddells culvert sand	1.45	0.92	0.89	0.48	1.51	0.42	0.91	0.36	0.66	0.66	0.64	0.74	0.61	0.93	0.62	0.58	0.58	1.24	0.26		76.40	0.40	12.98	2.64	0.03	0.87	0.40	3.63	2.56	0.09	100.00	-2.25	1.75
Tutamoe Sand	1.45	1.07	0.76	0.77	1.51	0.51	0.98	0.56	0.86	0.84	0.94	0.73	0.54	0.97	0.67	0.87	0.68	0.41	0.26		74.85	0.43	13.80	3.54	0.02	0.86	0.18	3.43	2.81	0.08	100.00	-1.66	1.57
Tutamoe mud	1.46	1.16	0.77	0.78	1.52	0.60	1.00	0.66	0.76	1.02	1.06	0.79	0.68	1.08	0.88	0.88	0.78	0.45	0.28		72.36	0.58	14.86	4.25	0.03	1.37	0.29	3.28	2.88	0.11	100.00	-1.60	0.87
Waipatki waterfall Westcott	0.69	0.91	0.79	0.54	1.67	0.47	0.91	0.51	0.82	0.80	0.84	0.84	0.38	2.54	0.62	0.81	0.75	0.39	0.19		79.06	0.40	11.18	2.13	0.03	0.69	0.92	2.94	2.58	0.06	100.00	-3.52	1.20
Waipatiki waterfall fossils	1.45	0.87	0.50	0.45	1.75	0.49	0.66	0.61	0.66	0.77	0.92	1.81	0.47	1.82	0.24	1.10	0.73	1.18	0.18		81.63	0.16	3.13	11.18	0.04	1.19	0.13	0.57	1.90	0.07	100.00	-2.73	-7.12
Reid Westcott	1.65	0.93	0.88	0.48	1.50	0.42	0.95	0.42	0.69	0.83	0.79	0.62	0.40	1.00	0.54	0.58	0.48	0.44	0.15		78.52	0.35	12.14	2.18	0.02	0.70	0.23	3.12	2.69	0.06	100.00	-3.30	1.33
Reid waterfall fossil base	0.52	1.06	0.80	0.48	1.88	0.53	0.96	0.94	1.15	0.97	1.27	1.50	6.18	1.42	0.71	1.00	1.39	0.46	0.27		73.17	0.46	13.19	3.91	0.14	1.23	1.15	3.08	2.72	0.94	100.00	-1.83	0.81
Whakataki mud	1.50	1.20	0.67	0.80	1.56	0.61	0.94	0.54	0.65	0.99	0.82	0.90	0.77	0.97	1.09	1.13	0.80	0.61	0.34		69.89	0.73	16.00	5.53	0.03	1.93	0.35	2.69	2.74	0.12	100.00	-1.14	-0.97
Whakataki sand below	0.84	0.87	0.67	0.39	1.53	0.43	0.84	0.37	0.67	0.61	0.84	0.82	0.76	0.92	0.78	0.81	0.59	0.92	0.33		76.01	0.50	13.12	3.36	0.02	1.19	0.42	2.87	2.39	0.12	100.00	-2.46	-0.09
Whakataki sand with black	1.29	0.83	0.70	0.40	1.56	0.35	0.80	0.41	0.74	0.68	0.82	0.79	0.77	0.83	0.76	0.75	0.55	0.55	0.36		75.89	0.51	12.64	4.30	0.02	1.14	0.37	2.66	2.35	0.12	100.00	-2.06	-0.69
Reid waterfall under mud	1.47	1.15	0.75	0.78	1.52	0.60	0.99	0.63	0.77	0.91	0.87	0.68	0.89	1.10	0.95	1.03	0.83	0.48	0.26		71.00	0.62	15.79	4.55	0.03	1.49	0.28	3.27	2.84	0.14	100.00	-1.02	0.67
Waipatiki house under mud	1.39	1.33	0.65	0.65	2.02	0.68	0.87	0.40	0.67	0.72	0.81	2.12	0.91	1.25	0.96	1.17	0.78	0.73	0.41		72.69	0.64	14.22	4.84	0.04	1.99	1.11	1.80	2.53	0.14	100.00	-2.38	-2.31
Ihungia	0.88	1.16	0.65	1.02	1.59	0.72	0.97	0.76	0.97	0.88	1.03	1.08	0.93	1.07	1.09	1.07	1.02	0.47	0.32		68.04	0.72	17.36	5.25	0.03	2.25	0.45	2.95	2.80	0.14	100.00	-0.85	-0.66
Weber flysch sand	0.26	0.82	0.86	0.36	1.89	0.32	0.84	0.49	0.69	0.75	0.71	1.06	0.85	1.06	0.58	1.28	0.67	1.05	0.57		78.10	0.38	10.16	4.54	0.04	0.91	1.11	2.25	2.39	0.13	100.00	-2.61	-0.94
Weber flysch mud	0.60	1.35	1.00	0.70	2.18	0.74	0.84	0.52	0.79	0.78	0.76	2.99	0.98	1.14	0.94	1.47	0.98	0.77	0.44		73.02	0.64	14.00	5.03	0.05	1.79	1.24	1.56	2.51	0.16	100.00	-2.12	-2.47
Weber Limestone	0.62	0.93	1.29	0.73	2.26	0.64	0.62	0.39	0.44	0.45	0.62	3.19	1.22	1.06	0.91	1.85	0.80	0.56	0.52		77.35	0.60	12.03	4.26	0.03	1.38	1.33	1.03	1.80	0.19	100.00	-2.55	-3.73
Weber Glauconite	0.29	1.09	1.50	0.54	2.09	0.47	0.77	0.68	0.74	0.33	1.10	2.27	3.30	0.97	0.60	1.72	1.48	1.38	0.24		78.42	0.39	9.08	5.45	0.01	1.43	1.23	1.27	2.21	0.51	100.00	-3.57	-3.48
Wanstead Glauconite	1.72	2.36	1.25	0.40	1.56	0.44	1.48	0.17	0.30	0.50	0.51	0.20	0.56	0.60	0.43	0.83	0.40	3.60			70.64	0.29	7.72	14.11	0.02	2.22	0.07	0.47	4.37	0.09	100.00	-2.59	-5.30
Wanstead	0.52	1.08	1.14	0.61	1.89	0.64	0.68	0.58	0.65	0.75	0.66	1.53	0.85	0.94	0.88	1.18	0.79	0.64	0.71		76.56	0.59	13.21	4.03	0.03	1.62	0.95	0.88	2.00	0.13	100.00	-2.89	-3.98
Millstream Glauconite	0.25	0.30	0.37	0.35	1.79		0.90	0.20	0.29		0.36	0.05	0.65		0.61	0.69		4.56	0.15		72.96	0.39	11.60	3.76	0.06	0.95	4.87	2.74	2.57	0.10	100.00	-0.06	1.93
Ossa Glauconite	0.42	1.00	1.70	0.29	1.52	0.09	0.86	0.17	0.28	0.06	0.30	0.24	0.48	0.25	0.34	1.17	0.24	3.54	0.20		80.60	0.22	4.64	9.92	0.04	1.37	0.11	0.55	2.47	0.07	100.00	-3.86	-6.10
Waipawa T-road	0.47	1.06	0.74	0.44	1.69	0.38	0.80	1.07	1.20	0.54	1.14	0.63	3.96	0.84	0.54	1.31	2.29	2.70	0.49		78.45	0.35	8.13	6.26	0.02	1.31	0.97	1.64	2.27	0.60	100.00	-3.32	-3.13
Waipawa Tawanui	1.28	2.15	0.58	0.30	1.55	0.35	1.45	0.17	0.28	0.31	0.43	0.23	0.56	0.53	0.44	1.05	0.50	4.64	0.13		71.52	0.30	7.50	13.31	0.01	2.28	0.17	0.59	4.25	0.09	100.00	-3.16	-5.13
Te Uri Member Whangai	1.89	0.83	0.68	0.29	1.52	0.34	0.64	0.70	0.78	0.30	1.03	0.33	1.85	0.58	0.51	0.88	0.78	1.59	0.28		83.59	0.34	7.43	4.09	0.01	1.06	0.17	1.23	1.81	0.28	100.00	-5.15	-3.96
Upper Calcareous Member Whangai	0.98	0.81	0.81	0.34	1.78	0.40	0.53	0.43	0.63	0.49	0.67	1.05	0.96	0.57	0.60	0.77	1.14	0.37	0.38		83.15	0.40	9.35	2.38	0.02	1.39	0.89	0.73	1.54	0.15	100.00	-5.36	-4.55
Rakauroa Member Whangai	0.42	0.62	0.64	0.48	1.51	0.42	0.40	0.16	0.29	0.36	0.53	0.13	0.34	0.39	0.48	0.44	0.34	0.42	0.19		88.49	0.31	6.95	1.97	0.01	0.65	0.02	0.39	1.16	0.05	100.00	-6.11	-5.24

	Major element molecular proportions, CORRECTED FOR CARBONATE and NORMALISED TO 100 WT% ANHYDROUS											ACNK, CORRECTED FOR CARBONATE and NORMALISED TO 100 WT% ANHYDROUS						
Sample Name	**SiO2**	**TiO2**	**Al2O3**	**Fe2O3**	**MnO**	**MgO**	**CaO**	**Na2O**	**K2O**	**P2O5**		**ACNK**	**A**	**CN**	**K**	**X-ACNK**	**Y-ACNK**	**CIA**
Scallop Limestone	0.998	0.007	0.117	0.055	0.003	0.129	0.137	0.045	0.024	0.004		0.32	40.25	60.26	8.29	28.41	40.25	37.00
Hillcap Limestone	0.719	0.006	0.098	0.079	0.004	0.130	0.426	0.030	0.018	0.005		0.56	19.22	87.65	3.52	13.13	19.22	17.41
Te Awaputahi Limestone	1.238	0.006	0.111	0.021	0.001	0.061	0.048	0.049	0.021	0.003		0.22	50.80	42.52	9.44	34.84	50.80	49.43
McCartie Sand	1.297	0.006	0.116	0.021	0.001	0.025	0.005	0.048	0.022	0.001		0.19	62.06	27.45	11.69	42.72	62.06	61.32
Franklin Road Sand	1.277	0.006	0.123	0.021	0.001	0.030	0.007	0.048	0.024	0.001		0.20	61.80	27.29	11.84	42.74	61.80	61.24
Franklin Road Mud	1.162	0.009	0.157	0.030	0.001	0.049	0.011	0.047	0.031	0.001		0.24	65.91	23.50	12.85	45.81	65.91	64.45
Riddells mud	1.146	0.009	0.165	0.035	0.001	0.048	0.011	0.038	0.031	0.001		0.24	71.81	20.66	13.56	49.46	71.81	67.73
Riddells culvert flow banding	1.207	0.007	0.147	0.025	0.000	0.031	0.007	0.056	0.029	0.001		0.24	62.93	26.69	12.30	43.77	62.93	61.75
Riddells culvert mud	1.138	0.009	0.164	0.035	0.001	0.045	0.009	0.049	0.031	0.001		0.25	67.44	23.18	12.85	46.57	67.44	65.18
Riddells culvert sand	1.272	0.005	0.127	0.017	0.000	0.022	0.007	0.059	0.027	0.001		0.22	58.01	29.49	12.38	41.38	58.01	58.08
Tutamoe Sand	1.246	0.005	0.135	0.022	0.000	0.021	0.003	0.055	0.030	0.001		0.22	61.92	26.30	13.63	44.59	61.92	60.80
Tutamoe mud	1.204	0.007	0.146	0.027	0.000	0.034	0.005	0.053	0.031	0.001		0.23	64.38	25.07	13.49	45.68	64.38	62.54
Waipatki waterfall Westcott	1.316	0.005	0.110	0.013	0.000	0.017	0.016	0.047	0.027	0.000		0.20	55.65	32.04	13.90	41.73	55.65	54.78
Waipatiki waterfall fossils	1.359	0.002	0.031	0.070	0.001	0.030	0.002	0.009	0.020	0.001		0.06	51.88	17.72	34.13	60.07	51.88	50.02
Reid Westcott	1.307	0.004	0.119	0.014	0.000	0.017	0.004	0.050	0.029	0.000		0.20	59.48	26.84	14.26	44.00	59.48	59.14
Reid waterfall fossil base	1.218	0.006	0.129	0.025	0.002	0.031	0.020	0.050	0.029	0.007		0.22	60.11	27.48	13.42	43.47	60.11	59.51
Whakataki mud	1.163	0.009	0.157	0.035	0.000	0.048	0.006	0.043	0.029	0.001		0.23	70.12	21.50	13.02	48.08	70.12	67.02
Whakataki sand below	1.265	0.006	0.129	0.021	0.000	0.029	0.008	0.046	0.025	0.001		0.21	63.26	25.75	12.49	44.12	63.26	62.33
Whakataki sand with black	1.263	0.006	0.124	0.027	0.000	0.028	0.007	0.043	0.025	0.001		0.20	66.28	25.67	13.34	46.48	66.28	62.95
Reid waterfall under mud	1.182	0.008	0.155	0.028	0.000	0.037	0.005	0.053	0.030	0.001		0.24	65.78	23.81	12.79	45.68	65.78	64.25
Waipatiki house under mud	1.210	0.008	0.139	0.030	0.001	0.049	0.020	0.029	0.027	0.001		0.21	67.97	23.04	13.07	47.05	67.97	65.30
Ihungia	1.132	0.009	0.170	0.033	0.000	0.056	0.008	0.048	0.030	0.001		0.25	69.05	21.90	12.05	46.57	69.05	67.04
Weber flysch sand	1.300	0.005	0.100	0.028	0.001	0.023	0.020	0.036	0.025	0.001		0.18	56.53	30.94	14.41	42.68	56.53	55.48
Weber flysch mud	1.215	0.008	0.137	0.031	0.001	0.044	0.022	0.025	0.027	0.001		0.21	70.02	23.12	13.61	48.62	70.02	65.59
Weber Limestone	1.287	0.008	0.118	0.027	0.000	0.034	0.024	0.017	0.019	0.001		0.18	70.15	22.65	11.33	46.41	70.15	67.37
Weber Glauconite	1.305	0.005	0.089	0.034	0.000	0.035	0.022	0.020	0.023	0.004		0.15	61.50	25.17	16.22	46.97	61.50	59.77
Wanstead Glauconite	1.176	0.004	0.076	0.088	0.000	0.055	0.001	0.008	0.046	0.001		0.13	61.31	6.29	37.56	68.22	61.31	58.30
Wanstead	1.274	0.007	0.130	0.025	0.000	0.040	0.017	0.014	0.021	0.001		0.18	75.00	17.08	12.26	49.77	75.00	71.88
Millstream Glauconite	1.214	0.005	0.114	0.024	0.001	0.024	0.087	0.044	0.027	0.001		0.27	42.80	48.88	10.25	31.65	42.80	41.99
Ossa Glauconite	1.341	0.003	0.046	0.062	0.001	0.034	0.002	0.009	0.026	0.001		0.08	57.33	12.43	33.06	61.73	57.33	55.76
Waipawa T-road	1.306	0.004	0.080	0.039	0.000	0.033	0.017	0.026	0.024	0.004		0.14	57.74	26.49	17.41	46.28	57.74	56.81
Waipawa Tawanui	1.190	0.004	0.074	0.083	0.000	0.056	0.003	0.010	0.045	0.001		0.13	58.99	9.25	36.16	65.66	58.99	56.50
Te Uri Member Whangai	1.391	0.004	0.073	0.026	0.000	0.026	0.003	0.020	0.019	0.002		0.11	66.54	17.76	17.57	50.84	66.54	65.32
Upper Calcareous Member Whangai	1.384	0.005	0.092	0.015	0.000	0.034	0.016	0.012	0.016	0.001		0.13	70.82	20.01	12.62	48.03	70.82	68.46
Rakauroa Member Whangai	1.473	0.004	0.068	0.012	0.000	0.016	0.000	0.006	0.012	0.000		0.09	80.97	7.02	14.63	55.11	80.97	78.91

	Trace elements (ppm), CORRECTED FOR CARBONATE and NORMALISED TO 100 WT% ANHYDROUS																														
Sample Name	**S**	**F**	**Cl**	**V**	**Mn**	**Co**	**Cu**	**Zn**	**Ga**	**As**	**Cs**	**Rb**	**Ba**	**Th**	**U**	**Nb**	**K**	**La**	**Ce**	**Pb**	**Nd**	**Sr**	**P**	**Zr**	**Ti**	**Sc**	**Y**	**Cr**	**Ni**	**Mo**	**Sn**	**Sb**	**Tl**
Scallop Limestone	7534	3818	1880	212	1770	0.00	58.5	139.0	14.63	14.63	7.31	102.4	651.0	43.89	29.26	7.31	9411.59	36.57	117.03	21.94	58.52	5983	1276.91	241.38	3507.18	446.19	36.57	0.00	14.63	36.57	0.00	0.00	0.00
Hillcap Limestone	14082	6026	3982	277	2383	15.37	107.6	215.2	0.00	30.75	15.37	123.0	645.7	76.87	61.49	15.37	7018.97	76.87	0.00	76.87	122.99	7456	1677.33	276.72	2764.20	1091.52	61.49	0.00	30.75	61.49	0.00	0.00	0.00
Te Awaputahi Limestone	3279	1011	1710	85	508	18.06	18.1	64.5	10.32	7.74	2.58	74.8	472.1	15.48	10.32	5.16	8030.58	30.96	59.33	10.32	20.64	2175	844.39	165.10	2783.08	98.03	15.48	54.17	20.64	12.90	0.00	0.00	0.00
McCartie Sand	1883	507	17422	83	440	11.35	7.2	45.4	12.38	6.19	5.16	68.1	452.8	5.16	4.13	5.16	8561.93	9.28	43.32	9.28	20.63	208	225.07	112.42	2658.14	8.25	10.31	50.54	15.47	5.16	1.03	0.00	0.00
Franklin Road Sand	3378	602	463	80	369	10.32	9.3	50.6	13.41	5.16	7.22	78.4	520.0	6.19	4.13	6.19	9207.07	16.51	45.40	10.32	22.70	262	225.14	165.08	2844.51	9.29	14.44	51.59	14.44	5.16	2.06	2.06	0.00
Franklin Road Mud	6964	435	386	114	482	15.54	15.5	83.3	18.87	5.55	7.77	119.9	530.6	9.99	4.44	9.99	11978.79	25.53	66.60	14.43	27.75	311	363.33	213.12	4124.76	14.43	21.09	65.49	25.53	5.55	5.55	5.55	0.00
Riddells mud	3304	471	187	139	498	9.61	26.4	92.5	21.61	6.00	4.80	142.9	654.4	10.81	4.80	12.01	12159.67	24.01	64.84	19.21	27.62	414	262.00	225.73	4317.68	16.81	24.01	60.03	15.61	6.00	3.60	3.60	0.00
Riddells culvert flow banding	4064	582	339	88	297	8.42	10.5	61.1	15.79	6.32	6.32	96.9	542.2	7.37	4.21	7.37	11231.04	16.85	51.59	12.63	23.16	258	252.72	232.69	3344.49	11.58	15.79	90.55	12.63	5.26	3.16	3.16	0.00
Riddells culvert mud	7624	782	1677	120	430	12.20	18.9	79.9	19.97	6.66	8.87	119.8	519.2	11.09	4.44	8.87	12247.66	18.86	57.69	15.53	25.51	294	314.69	189.70	4255.19	15.53	19.97	54.36	14.42	5.55	3.33	3.33	0.00
Riddells culvert sand	4787	481	2608	59	220	9.14	7.1	43.7	12.18	10.15	7.11	77.2	560.4	5.08	4.06	5.08	10619.39	11.17	41.63	11.17	17.26	238	199.39	178.69	2373.18	8.12	12.18	113.71	12.18	5.08	1.02	2.03	0.00
Tutamoe Sand	10484	651	470	100	263	12.43	11.4	62.1	15.53	7.25	7.25	91.1	484.6	8.28	4.14	6.21	11647.26	17.60	54.88	14.50	25.89	237	180.76	191.57	2606.58	12.43	14.50	38.31	12.43	5.18	1.04	0.00	0.00
Tutamoe mud	10617	474	469	103	270	12.65	12.6	66.4	16.86	7.38	7.38	100.1	498.6	8.43	4.22	7.38	11943.53	21.08	49.54	17.92	29.51	259	230.01	215.03	3474.56	12.65	16.86	42.16	13.70	5.27	1.05	1.05	0.00
Waipatki waterfall Westcott	630	502	377	62	256	9.18	6.9	39.0	9.18	6.88	3.44	78.0	502.4	5.74	4.59	5.74	10711.60	16.06	52.76	13.76	22.94	274	125.14	498.95	2406.06	11.47	16.06	36.70	9.18	6.88	3.44	4.59	0.00
Waipatiki waterfall fossils	1655	682	577	50	385	4.91	8.6	45.5	11.06	9.83	7.37	76.2	323.1	4.91	4.91	6.14	7903.18	19.66	43.00	13.51	25.80	599	160.84	363.63	957.15	15.97	15.97	113.02	8.60	6.14	4.91	4.91	0.00
Reid Westcott	441	678	996	62	181	7.13	7.1	40.7	12.22	8.15	8.15	78.4	557.9	5.09	4.07	5.09	11156.09	13.24	43.78	14.25	21.38	200	133.30	193.44	2074.70	8.15	10.18	40.73	7.13	5.09	2.04	2.04	0.00
Reid waterfall fossil base	995	1767	800	96	1153	11.55	10.3	57.8	14.12	16.68	2.57	89.8	505.7	5.13	5.13	6.42	11293.26	29.52	73.16	16.68	34.65	484	2044.44	277.22	2769.19	14.12	29.52	42.35	12.83	6.42	0.00	0.00	0.00
Whakataki mud	10232	432	98	129	314	12.12	19.8	85.9	17.63	6.61	7.71	105.8	441.8	8.81	4.41	7.71	11385.41	17.63	42.96	17.63	23.13	302	264.43	196.09	4357.73	16.52	17.63	58.39	16.52	5.51	2.20	3.30	0.00
Whakataki sand below	9100	496	152	86	203	8.40	12.6	56.7	12.60	7.35	4.20	74.5	425.1	4.20	4.20	5.25	9933.02	11.55	43.04	10.50	23.09	267	251.95	179.49	3019.64	11.55	12.60	86.07	15.74	5.25	1.05	2.10	0.00
Whakataki sand with black	29620	491	146	103	191	8.87	14.4	64.3	14.41	11.09	6.65	73.2	463.4	4.43	4.43	4.43	9755.26	13.30	48.78	12.20	23.28	267	266.11	168.52	3056.53	11.09	12.20	53.22	17.74	5.54	0.00	0.00	0.00
Reid waterfall under mud	2174	844	502	110	304	11.56	14.7	72.5	16.81	7.35	7.35	98.8	483.3	8.40	4.20	7.35	11773.47	19.96	49.38	15.76	24.16	222	298.02	216.42	3715.01	14.71	17.86	45.18	12.61	5.25	2.10	3.15	0.00
Waipatiki house under mud	10270	789	588	115	304	5.68	18.4	105.0	17.03	5.68	7.10	116.4	427.2	7.10	5.68	8.51	10484.58	12.77	43.99	12.77	22.71	707	309.67	251.19	3827.46	17.03	17.03	69.54	19.87	7.10	1.42	4.26	0.00
Ihungia	7817	434	197	111	293	9.96	15.5	95.1	19.91	4.42	4.42	100.7	421.5	11.06	4.42	8.85	11616.41	24.34	63.05	15.49	28.76	355	313.81	212.40	4309.55	15.49	22.12	44.25	15.49	5.53	3.32	3.32	0.00
Weber flysch sand	14706	550	7131	60	355	10.40	9.1	117.0	11.70	7.80	1.30	70.2	550.1	3.90	5.20	3.90	9932.14	15.61	44.22	13.01	19.51	346	283.79	208.08	2260.43	18.21	14.31	98.84	27.31	6.50	0.00	0.00	0.00
Weber flysch mud	7631	616	253	134	350	6.29	37.7	114.7	18.86	6.29	3.14	121.0	672.6	7.86	6.29	9.43	10435.39	17.29	53.43	14.14	22.00	1020	342.89	235.71	3861.36	22.00	22.00	75.43	22.00	7.86	6.29	7.86	0.00
Weber Limestone	5990	623	130	94	232	3.18	30.2	90.6	12.71	7.94	3.18	81.0	842.1	7.94	6.36	7.94	7452.30	12.71	28.60	7.94	17.48	1061	416.07	212.92	3618.79	27.01	17.48	54.02	25.42	7.94	1.59	4.77	0.00

Weber Glauconite	1345	1563	468	106	156	7.27	21.8	97.4	13.09	4.36	1.45	94.5	971.5	5.82	5.82	5.82	9175.38	21.82	47.99	5.82	30.54	746	1110.75	193.43	2353.48	24.72	32.00	130.89	11.63	7.27	1.45	1.45	0.00
Wanstead Glauconite	241	435	176	156	279	9.99	25.5	111.0	23.31	2.22	8.88	208.6	826.8	4.44	4.44	5.55	18148.93	5.55	19.98	8.88	14.43	67	193.74	120.97	1729.40	12.21	8.88	348.48	0.00	5.55	2.22	1.11	0.00
Wanstead	10370	522	357	98	229	18.63	21.3	93.2	15.97	3.99	2.66	94.5	749.2	6.65	5.32	7.98	8285.42	18.63	42.59	13.31	18.63	511	290.40	188.98	3509.48	17.30	17.30	61.22	34.60	6.65	1.33	2.66	0.00
Millstream Glauconite	6229	1030	380271	83	278	17.27	13.6	194.9	9.87	4.93	1.23	25.9	236.9	3.70	4.93	0.00	10650.38	6.17	18.50	0.00	9.87	16	215.36	0.00	2366.02	9.87	0.00	428.08	7.40	4.93	0.00	0.00	0.00
Ossa Glauconite	4757	790	96816	135	332	13.69	10.5	212.7	15.80	5.27	2.11	86.4	1099.4	3.16	4.21	1.05	10271.35	5.27	17.90	1.05	8.42	80	160.85	49.49	1325.40	16.85	5.27	334.87	9.48	4.21	0.00	0.00	0.00
Waipawa T-road	12160	1263	513	94	243	17.42	5.8	116.2	15.10	6.97	2.32	90.6	475.1	4.65	4.65	4.65	9401.99	33.69	76.67	9.29	31.36	203	1318.13	163.79	2088.69	18.59	48.79	252.08	23.23	5.81	2.32	3.48	0.00
Waipawa Tawanui	20241	868	215	132	137	13.13	10.9	127.0	21.89	7.66	6.57	188.3	382.0	3.28	4.38	4.38	17626.27	5.47	18.61	5.47	12.04	77	191.07	106.17	1771.17	15.32	10.95	445.47	6.57	9.85	2.19	1.09	0.00
Te Uri Member Whangai	21201	411	135	82	107	15.72	8.4	74.4	10.48	6.29	9.43	71.2	432.7	3.14	4.19	4.19	7523.52	22.00	50.29	5.24	28.29	107	617.32	114.21	2009.52	12.57	16.76	148.78	13.62	5.24	1.05	1.05	0.00
Upper Calcareous Member Whangai	6101	487	4641	72	190	6.21	16.1	81.9	12.41	4.96	4.96	70.8	523.8	3.72	4.96	4.96	6388.23	13.65	40.96	8.69	18.62	346	325.02	112.95	2380.54	11.17	24.82	34.75	18.62	6.21	6.21	3.72	0.00
Rakauroa Member Whangai	2194	410	213	56	59	9.40	17.8	43.9	9.40	3.13	2.09	53.3	413.7	5.22	4.18	5.22	4813.37	5.22	18.81	6.27	14.63	44	113.99	76.27	1878.52	6.27	7.31	39.70	9.40	5.22	3.13	4.18	0.00

	UCC-normalised trace elements, CORRECTED FOR CARBONATE and NORMALISED TO 100 WT% ANHYDROUS																		
	Cs	Rb	Ba	Th	U	Nb	K	La	Ce	Pb	Nd	Sr	P	Zr	Ti	Sc	Y	Cr	Ni
Sample Name	7.96	111.41	708.27	47.75	31.83	7.96	10239.51	39.79	127.33	23.87	63.66	6509.74	1389.24	262.62	3815.70	485.45	39.79	0.00	15.92
Scallop Limestone	16.97	135.77	712.82	84.86	67.89	16.97	7748.70	84.86	0.00	84.86	135.77	8231.35	1851.72	305.49	3051.58	1205.00	67.89	0.00	33.94
Hillcap Limestone	2.65	76.88	485.11	15.91	10.60	5.30	8252.00	31.81	60.97	10.60	21.21	2234.70	867.68	169.66	2859.81	100.73	15.91	55.67	21.21
Te Awaputahi Limestone	5.22	68.89	458.24	5.22	4.18	5.22	8664.95	9.39	43.84	9.39	20.88	210.85	227.77	113.78	2690.12	8.35	10.44	51.15	15.66
McCartie Sand	7.29	79.14	524.83	6.25	4.17	6.25	9292.47	16.66	45.82	10.41	22.91	264.50	227.23	166.61	2870.90	9.37	14.58	52.07	14.58
Franklin Road Sand	7.95	122.59	542.59	10.22	4.54	10.22	12249.65	26.11	68.11	14.76	28.38	317.83	371.54	217.94	4218.03	14.76	21.57	66.97	26.11
Franklin Road Mud	5.09	151.49	693.82	11.46	5.09	12.73	12892.72	25.46	68.75	20.37	29.28	439.20	277.79	239.33	4577.98	17.82	25.46	63.65	16.55
Riddells mud	6.44	98.73	552.65	7.51	4.29	7.51	11446.78	17.17	52.58	12.88	23.61	262.91	257.58	237.16	3408.74	11.80	16.10	92.29	12.88
Riddells culvert flow banding	9.18	123.97	537.19	11.48	4.59	9.18	12672.76	19.51	59.69	16.07	26.40	304.18	325.61	196.28	4402.88	16.07	20.66	56.24	14.92
Riddells culvert mud	7.10	77.06	559.73	5.07	4.06	5.07	10605.97	11.15	41.57	11.15	17.24	237.28	199.14	178.47	2370.18	8.11	12.17	113.57	12.17
Riddells culvert sand	7.38	92.81	493.59	8.44	4.22	6.33	11863.07	17.93	55.90	14.77	26.37	241.52	184.11	195.12	2654.88	12.66	14.77	39.02	12.66
Tutamoe Sand	7.59	103.07	513.20	8.68	4.34	7.59	12293.96	21.70	50.99	18.44	30.38	266.91	236.75	221.34	3576.51	13.02	17.36	43.40	14.10
Tutamoe mud	3.50	79.23	510.36	5.83	4.66	5.83	10881.62	16.31	53.60	13.98	23.30	278.49	127.13	506.87	2444.25	11.65	16.31	37.29	9.32
Waipatki waterfall Westcott	7.65	79.01	335.14	5.10	5.10	6.37	8198.09	20.39	44.60	14.02	26.76	621.86	166.84	377.19	992.87	16.57	16.57	117.24	8.92
Waipatiki waterfall fossils	8.19	78.85	561.19	5.12	4.10	5.12	11221.13	13.31	44.03	14.34	21.51	200.72	134.08	194.57	2086.79	8.19	10.24	40.96	7.17
Reid Westcott	2.59	90.75	510.79	5.19	5.19	6.48	11407.39	29.82	73.90	16.85	35.00	488.75	2065.10	280.03	2797.18	14.26	29.82	42.78	12.96
Reid waterfall fossil base	8.07	110.66	462.23	9.22	4.61	8.07	11912.89	18.44	44.95	18.44	24.21	315.84	276.68	205.18	4559.62	17.29	18.44	61.09	17.29
Whakataki mud	4.26	75.64	431.45	4.26	4.26	5.33	10081.25	11.72	43.68	10.65	23.44	270.59	255.71	182.17	3064.70	11.72	12.78	87.35	15.98
Whakataki sand below	7.00	77.05	487.97	4.67	4.67	4.67	10272.19	14.01	51.37	12.84	24.52	281.34	280.21	177.45	3218.49	11.67	12.84	56.04	18.68
Whakataki sand with black	7.53	101.11	494.80	8.61	4.30	7.53	12054.33	20.44	50.56	16.13	24.74	226.96	305.13	221.58	3803.63	15.06	18.29	46.25	12.91
Reid waterfall under mud	7.39	121.12	444.60	7.39	5.91	8.86	10912.53	13.29	45.79	13.29	23.63	735.58	322.31	261.44	3983.69	17.72	17.72	72.38	20.68
Waipatiki house under mud	4.56	103.69	434.11	11.39	4.56	9.12	11964.81	25.07	64.95	15.95	29.62	365.75	323.22	218.77	4438.80	15.95	22.79	45.58	15.95
Ihungia	1.33	71.55	560.50	3.98	5.30	3.98	10119.48	15.90	45.05	13.25	19.88	352.46	289.14	212.01	2303.06	18.55	14.58	100.70	27.83
Weber flysch sand	3.35	129.16	717.94	8.39	6.71	10.06	11139.65	18.45	57.03	15.10	23.48	1088.65	366.03	251.61	4121.95	23.48	23.48	80.52	23.48
Weber flysch mud	3.31	84.39	876.95	8.27	6.62	8.27	7760.38	13.24	29.78	8.27	18.20	1105.28	433.27	221.72	3768.39	28.13	18.20	56.26	26.47
Weber Limestone	1.50	97.27	999.63	5.99	5.99	5.99	9440.90	22.45	49.38	5.99	31.43	767.68	1142.89	199.03	2421.59	25.44	32.92	134.68	11.97
Weber Glauconite	9.34	219.42	869.51	4.67	4.67	5.84	19086.36	5.84	21.01	9.34	15.17	70.03	203.74	127.22	1818.73	12.84	9.34	366.48	0.00
Wanstead Glauconite	2.78	98.59	781.78	6.94	5.55	8.33	8645.21	19.44	44.44	13.89	19.44	533.22	303.01	197.18	3661.88	18.05	18.05	63.88	36.10
Wanstead	1.26	26.41	241.44	3.77	5.03	0.00	10856.04	6.29	18.86	0.00	10.06	16.35	219.52	0.00	2411.71	10.06	0.00	436.35	7.54
Millstream Glauconite	2.17	88.78	1130.37	3.25	4.33	1.08	10560.72	5.41	18.41	1.08	8.66	82.29	165.38	50.89	1362.74	17.32	5.41	344.31	9.74
Ossa Glauconite	2.36	92.09	482.89	4.72	4.72	4.72	9555.71	34.24	77.92	9.45	31.88	206.61	1339.68	166.47	2122.84	18.89	49.59	256.20	23.61
Waipawa T-road	6.86	196.53	398.77	3.43	4.57	4.57	18400.98	5.71	19.42	5.71	12.57	79.98	199.47	110.83	1849.01	16.00	11.43	465.05	6.86
Waipawa Tawanui	9.61	72.58	440.82	3.20	4.27	4.27	7664.08	22.41	51.23	5.34	28.82	108.87	628.85	116.34	2047.06	12.81	17.08	151.56	13.88
Te Uri Member Whangai	5.14	73.19	541.85	3.85	5.14	5.14	6608.43	14.12	42.37	8.99	19.26	358.24	336.22	116.85	2462.60	11.56	25.68	35.95	19.26
Upper Calcareous Member Whangai	2.14	54.67	424.53	5.36	4.29	5.36	4939.06	5.36	19.30	6.43	15.01	45.03	116.97	78.26	1927.57	6.43	7.50	40.74	9.65
Rakauroa Member Whangai	5.14	73.19	541.85	3.85	5.14	5.14	6608.43	14.12	42.37	8.99	19.26	358.24	336.22	116.85	2462.60	11.56	25.68	35.95	19.26